Some recent Insertion Device innovations on operating third and fourth generation light sources

M. E. Couprie,
C. Benabderrahmane, F. Briquez, O. Marcouillé, F. Marteau, M. Valleau, P. Berteaud, L. Chapuis, M. Massal, J.Vétéran, H.Abualrob, P. Brunelle, L. Nadolski, R. Nagaoka, A. Nadji (Synchrotron SOLEIL), O. Chubar, C. Kitegi (BNL), J. M. Filhol (Fusion to Energy)

Talk dedicated to P. Elleaume († 2011, March 19)

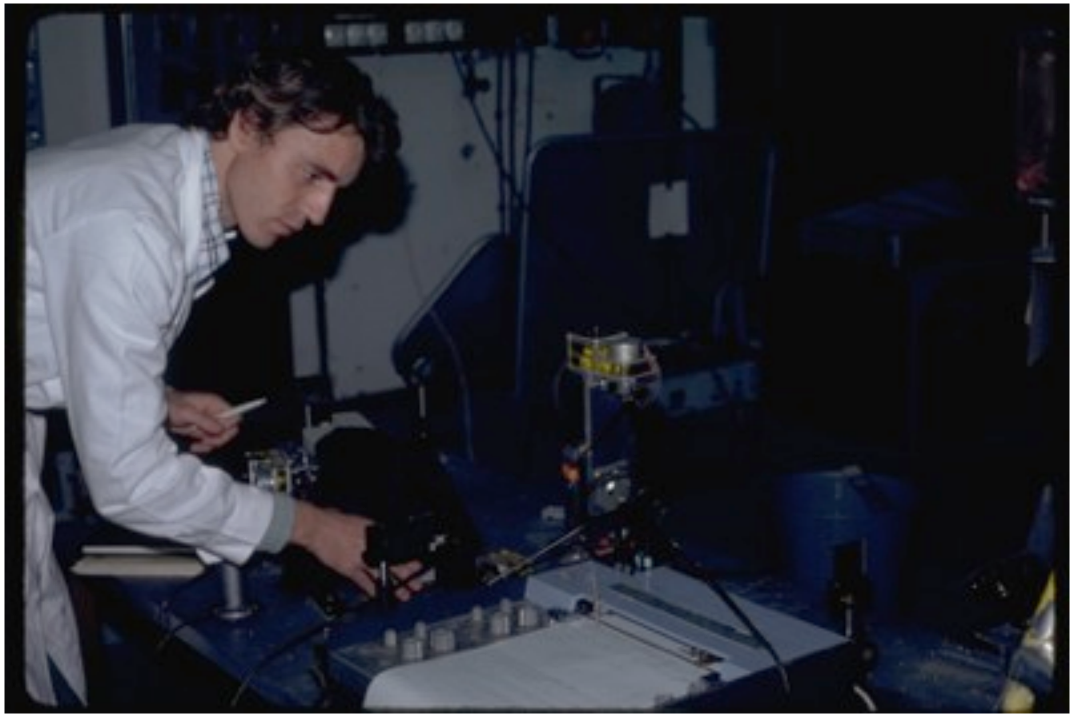

Outline

1- In vacuum undulators and wigglers

issues (transitions, direct in vacuum measurements..)
quest for short period high field, cryogenic systems
in vacuum wigglers as an alternative to superconducting wigglers

2- EPU and fast polarization switching

electromganetic system
Permanent magnet approach
Combined electromagnetic- permanent magnet approach : EMPHU

3- Effect of IDs on the light source operation

strategies to compenstate unwanted effects
desired effects : A Robinson wiggler as an alternative to the damping wiggler
canted undulators

Accelerator type issues for insertion devices

	storage ring	linac / ERL	LWFA
Emittance	E^2	1/E	
Beamsize (μm)	100 (H)-10 (V)	50-10	10-3
vacuum chamber H /V aperture	flat min gap: 5 mm	round (ex : bore 5 mm), min gap : 3 mm	round
charge	high	1 nC	10 pC
Pulse duration	10 ps	100 fs	10 fs
impedance	very critical	critical	critical
field integrals	very critical	very critical	very critical
double field integrals	very critical	very critical	very critical
phase error	very critical for high harmonics operation	critical	critical
multipoles	for beam lifetime and injection efficiency	less critical	not critical

In vacuum undulators

Motivation : reach a higher field by placing directly the magnets inside the vacuum chamber

Sm_2Co_{17} : Br $\leq$ 1.05T; μHcj = 2.8 T; $Nd_2Fe_{14}B$: Br $\leq$ 1.4T (1.26T); μ_oHc = 1.4-1.6 (resp. 2.4T)

Coercivity to avoid demagnetisation when baking and to resist against irradiation (GeV electrons, high energy photons and gamma-rays, neutrons) => Br<1.26T

Machine protection for the IVU to avoid magnet degradation, cases ESRF, APS

Historical steps :

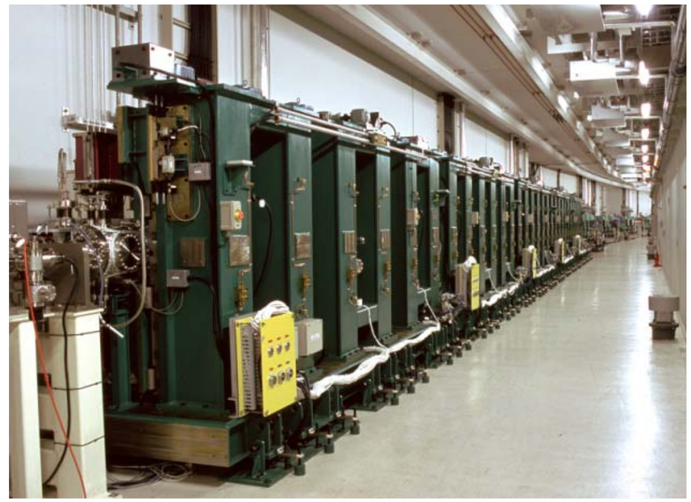

- First prototype at BESSY
W. Gudat et al. NIMA 246, 1986 50

- First In vac. undulator Installed on TRISTAN AR, Period : 40 mmX90, NdFeB (Br=1.2 T, iHc=21kOe), min gap 10 mm, B=0.82-0.36 T, NEG and sputter ion pumps, magnet stabilization at 125°C and vacuum commissioning at 115°C, *S. Yamamoto et al. Rev. Sci. Instr 63, 400 (1992)*

- 30 m long in-vacuum undulator at SPring-8 (SLUS-1) :
32 mm x 780, min gap = 12 mm (betaV = 15 m) B=0.59 T
5 segments without gaps, very fine adjustments of the gap segments for phase error (11°=> 3.6°)
H. Kitamura et al., NIMA 467 (2001) 110; T.Tanaka et al. NIMA 467, (2001) 149

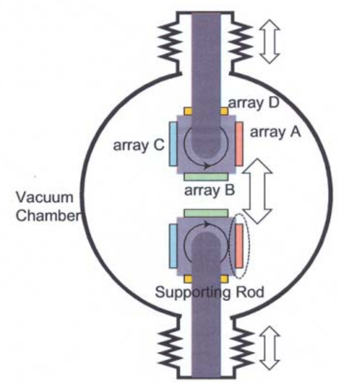

- Revolver in-vacuum undulator (INVRUM) :
6 mm x 133, 10 mmx100, 15 mmX66, 20mmx50; min gap = 3.2 mm, B=0.74, 1.07, 1.32, 1.44 T
T. Bizen et al. AIP 705, (2004), 175, 18th International Conference on Synchrotron Radiation Instrumentation, San Franscisco, 2003 417, H.S. Kang et al., EPAC 2006, 2771

I- In vacuum undulators and wigglers

Impedance issues : RF transitions

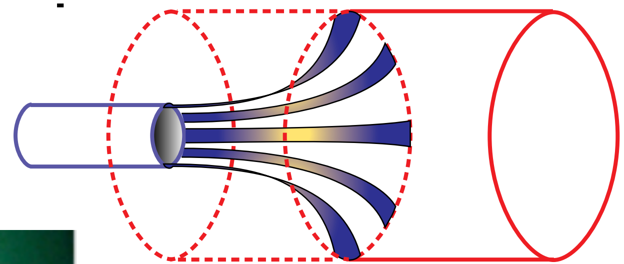

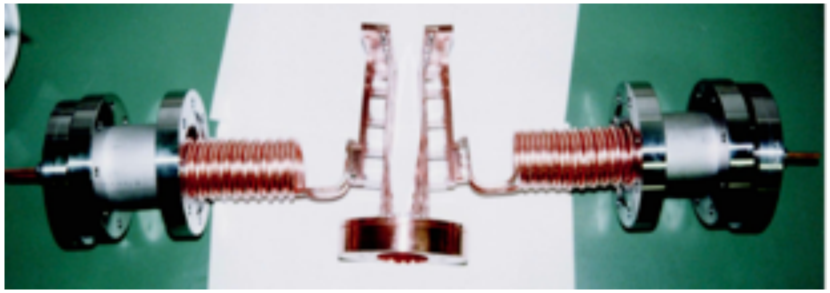

SPring-8 design, first adopted by SLS
(images : courtesy T. Hara)

T. Nakamura et al. PAC 2001, 1969

ALS design

A. Madur et al., PAC 2009; 333

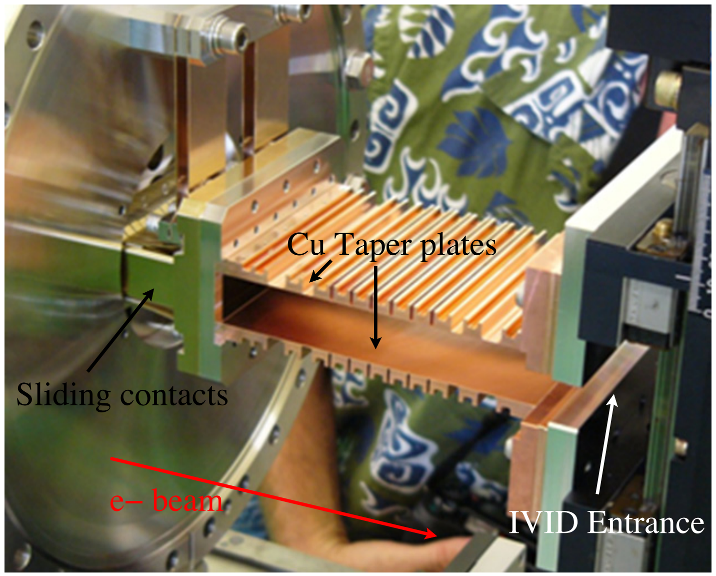

I- In vacuum undulators and wigglers

Impedance issues : RF transitions

Change of the design at SOLEIL : for SOLEIL
storage ring operation at 500 mA

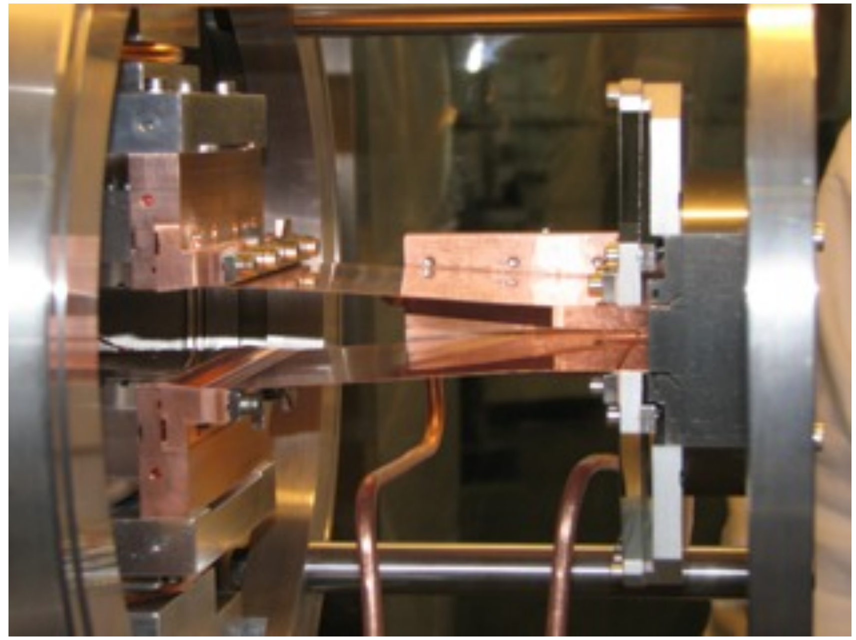

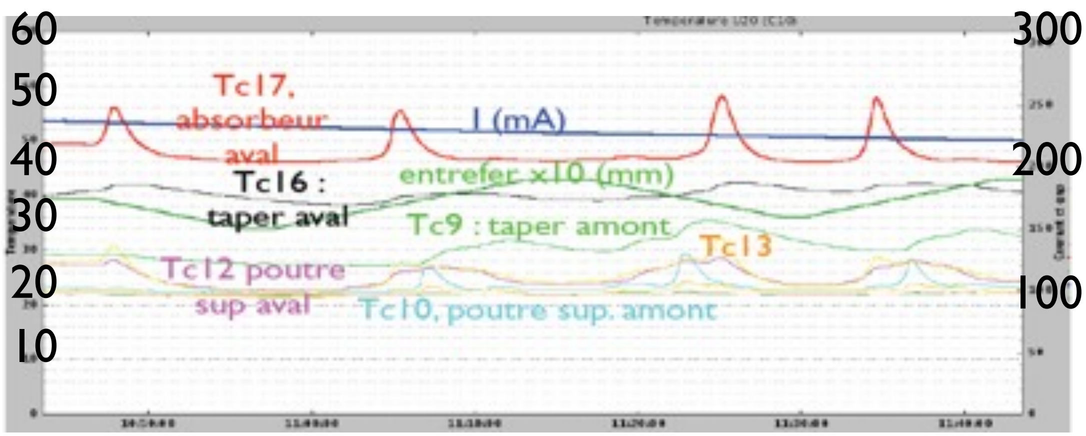

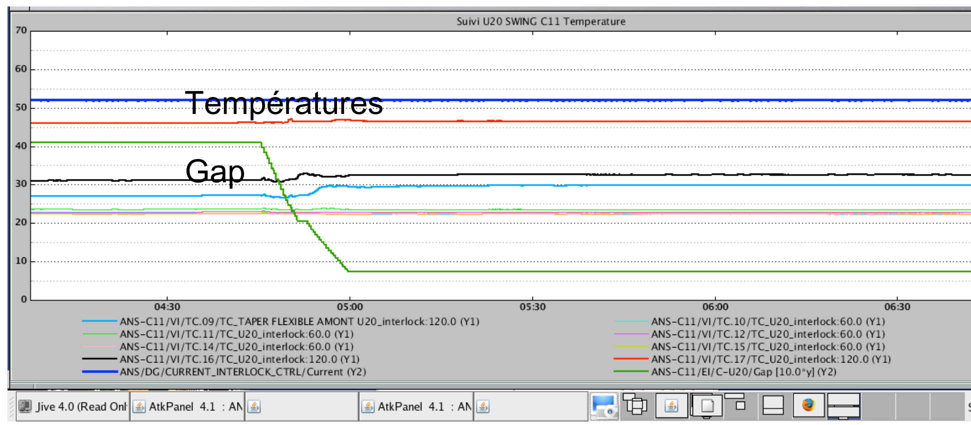

I- In vacuum undulators and wigglers

Impedance issues : RF transitions

R. Nagaoka, SOLEIL case (GdfidL)

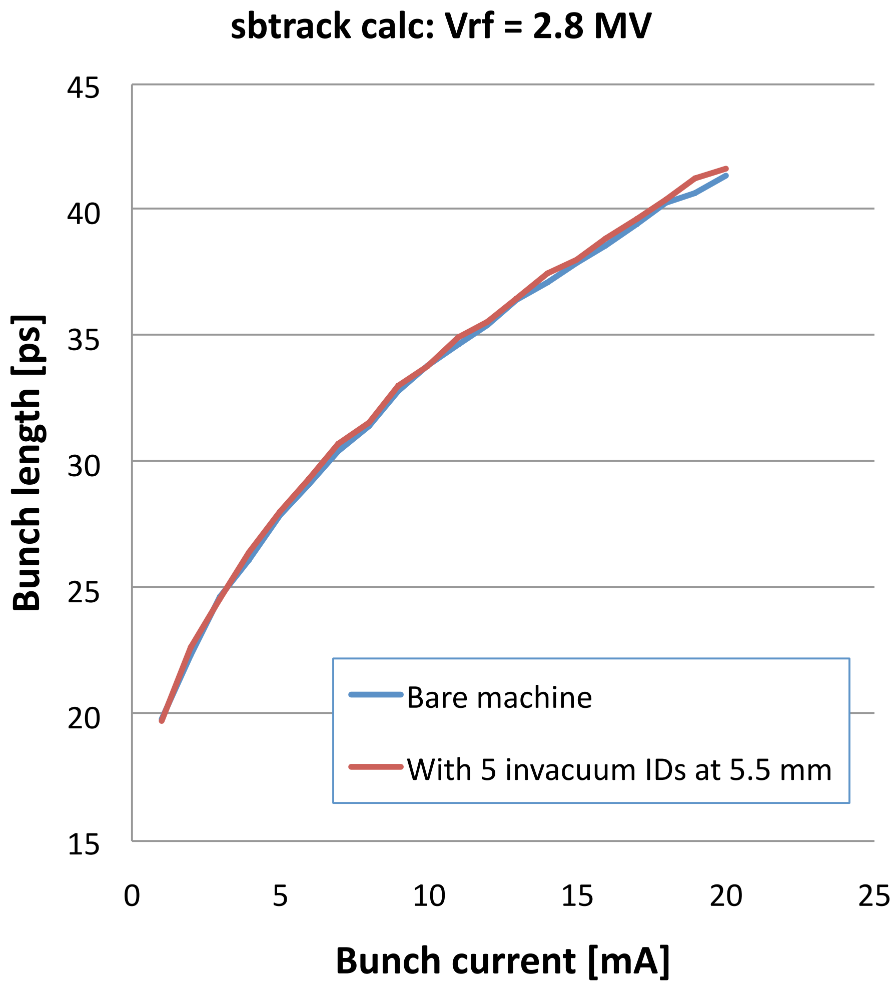

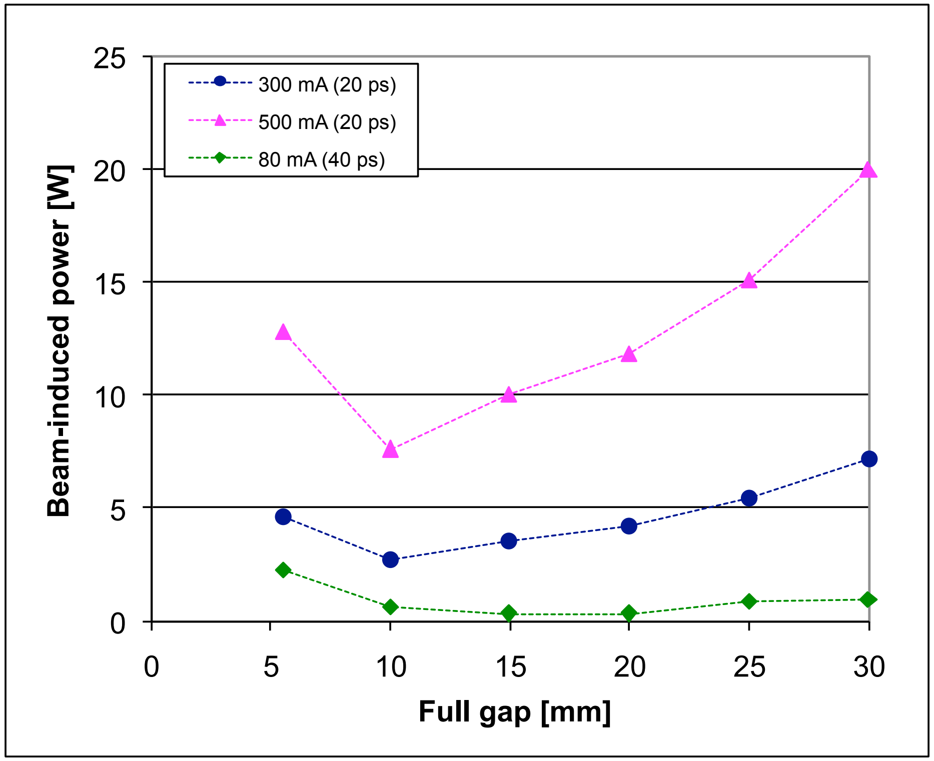

$|Z/n|_{eff}$ = 0.45 Ω, 5 in vacuum ID contribution : 11.6 mΩ

10 taper of middle SS contribution : 9.3 mΩ

Impedance issues : liner

Liner : Conductive foil

image current, heat load due to wakefields or up stream synchrotron radiation

Some observations of liner degradation

beam measurements
- obstacles with bumps
- outgassing
- partial loss

ESRF/SPring-8 : burned 50 µm stainless steel foil
=> demagnetisation of 0.5 % between poles 70-120
=> Cu(10 µm)-Ni(50 µm) foil with better thermal and electric conductivity

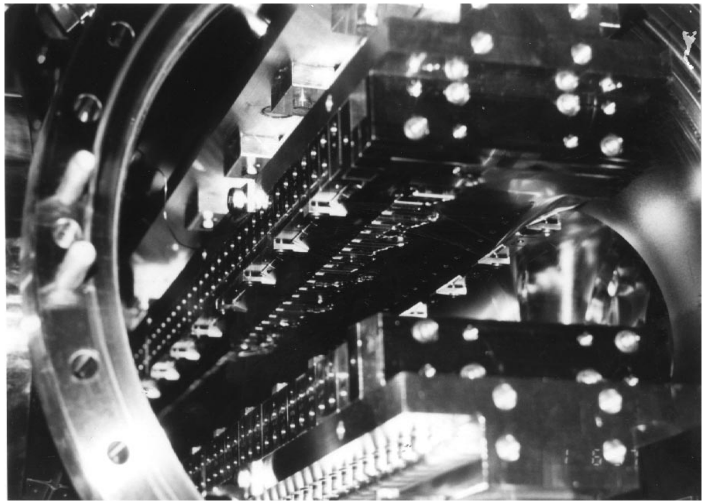

T. Hara et al., SPring-8 in-vacuum undulator beam test at the ESRF, J. Synchrotron Rad. (1998), 5, 406-408

Table 2
Power of the resistive wall heating calculated for the 1.5 m in-vacuum undulator at ESRF.

	Beam mode	Average current (mA)	Bunch length, σ_t (ps)	Material	Power (W m^{-1})
Magnet sheet gap 5 mm	1/3 filling (300 bunches)	140	15	SUS	28
				Ni + Cu	4.4
	16 bunches	90	35	SUS	61
				Ni + Cu	9.6
RF finger gap 5 mm	1/3 filling (300 bunches)	140	15	BeCu	2.2
	16 bunches	90	35	BeCu	4.8

Liner : conductive Ni-Cu foil

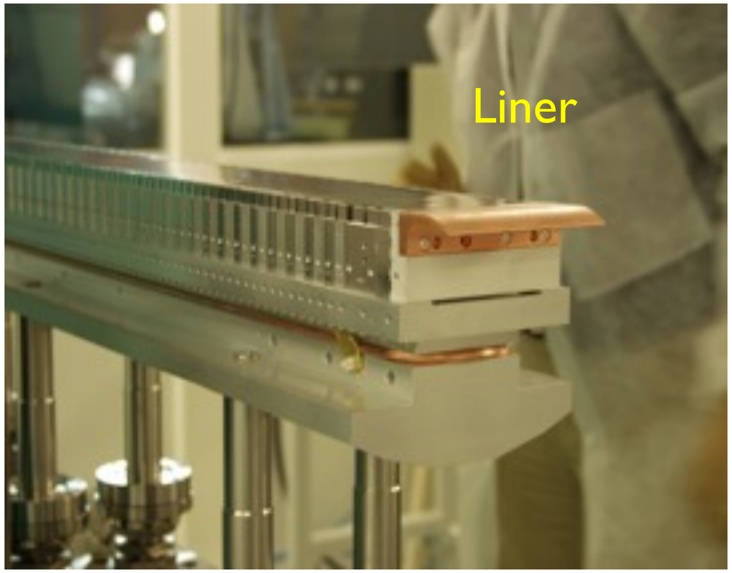

I- In vacuum undulators and wigglers

Impedance issues : Liner

Some observations of liner degradation

ALS

A. Madur et al., PAC 2009; 333

0.7mm off axis, 0.4 mm excitation

Section	SDC					SDM				
Position	T		L		Pt	T		L		Pt
Type	RS	CS	RS	CS		RS	CS	RS	CS	
4 /4	1.2	9.8	3	13.1	**27.1**	2.4	9.8	3.4	13.1	**28.7**
3 /4	1.2	13.2	3	17.5	**34.8**	2.4	13.2	3.4	17.5	**36.5**
hybrid	1.2	13.3	3	18	**35.5**	2.4	13.3	3.4	18	**37.1**
8 b 120	0.3	2.6	0.7	21.4	**25**	0.6	2.6	0.8	21.4	**25.4**
8 b 80	0.2	2.3	0.5	9.5	**12.5**	0.4	2.3	0.5	9.5	**12.7**
1 bunch	0.05	2.57	0.1	4.7	**7.4**	0.09	2.57	0.14	4.7	**7.5**

Section	SDL9					SDL13				
Position	T		L		Pt	T		L		Pt
Type	RS	CS	RS	CS		RS	CS	RS	CS	
4/4	6.4	9.8	3.4	13.1	**32.7**	17.6	9.8	1	13.1	**41.5**
3 /4	6.4	13.2	3.4	17.7	**40.5**	17.6	13.2	1	17.5	**49.3**
hybrid	6.4	13.3	3.4	18	**41.1**	17.6	13.3	1	18	**49.9**
8 b 120	1.5	2.6	0.8	21.4	**26.3**	4.2	2.6	0.24	21.4	**28.5**
8 b 80	1	2.3	0.5	9.5	**13.3**	2.8	2.3	0.16	9.5	**14.8**
1 bunch	0.26	2.57	0.14	4.7	**7.7**	0.7	2.57	0.04	4.7	**8**

SOLEIL : burned thermocouple (U20 n°4), beam heating (U20 n°5)

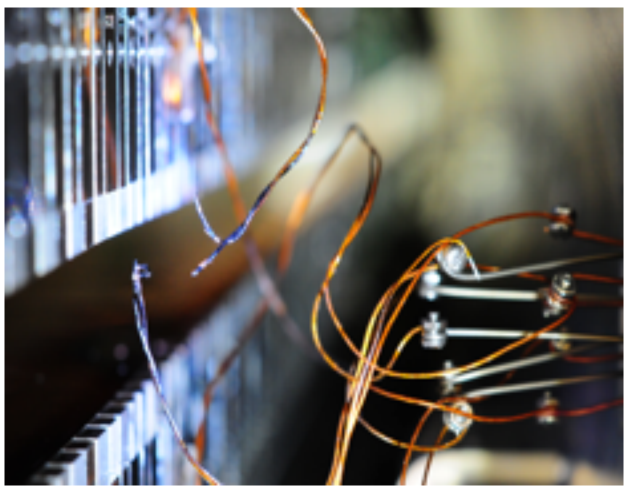

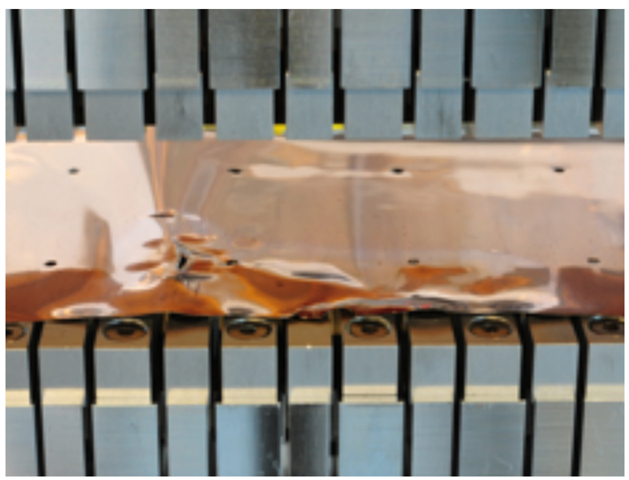

Solution : liner tensor

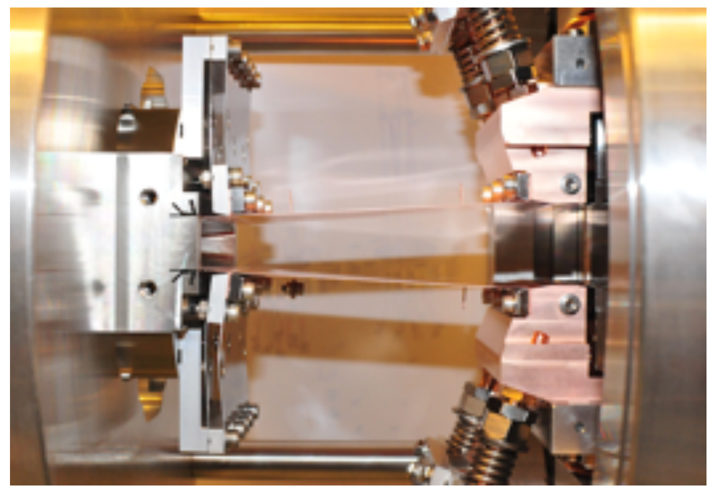

I- In vacuum undulators and wigglers

Magnetic measurements

- without in situ magnetic measurements

• Use of a conventional bench based on the displacement of the magnetic sensor (Hall probe, flopping coil) by an actuation stage of high precision

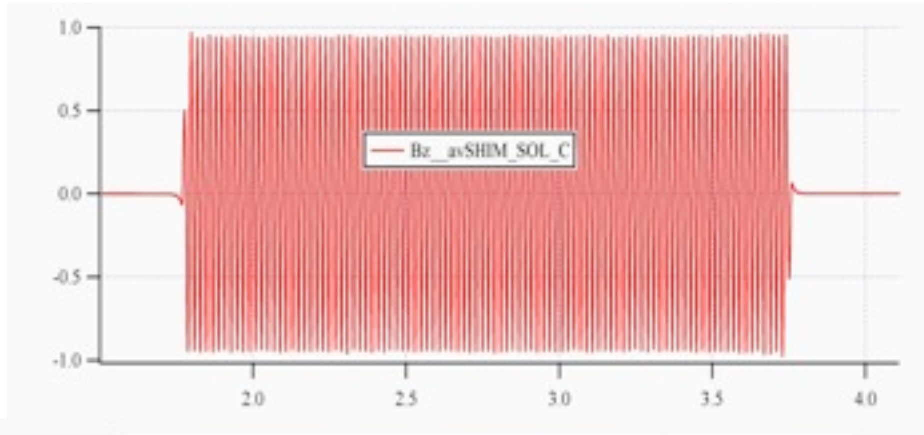

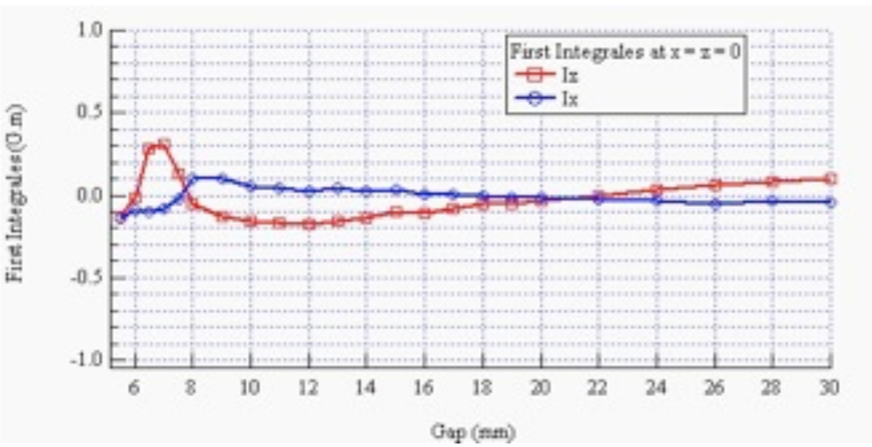

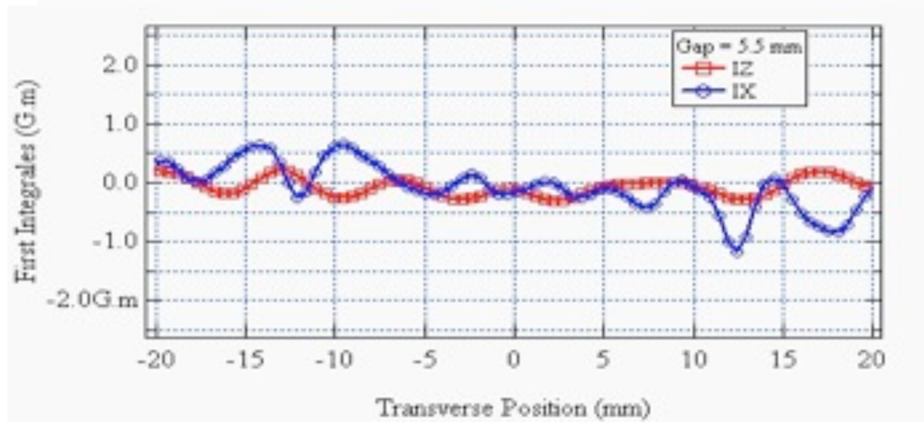

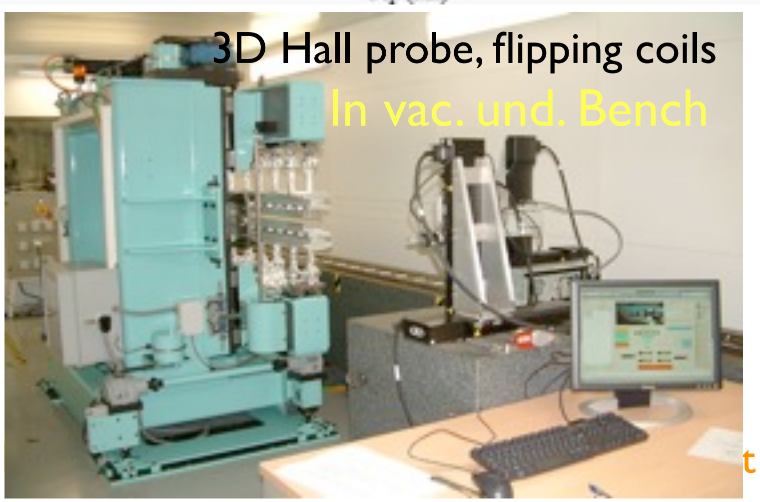

I- In vacuum undulators and wigglers

Magnetic measurements

- without in situ magnetic measurements, for no lateral access

• Use of the pulsed wire technique

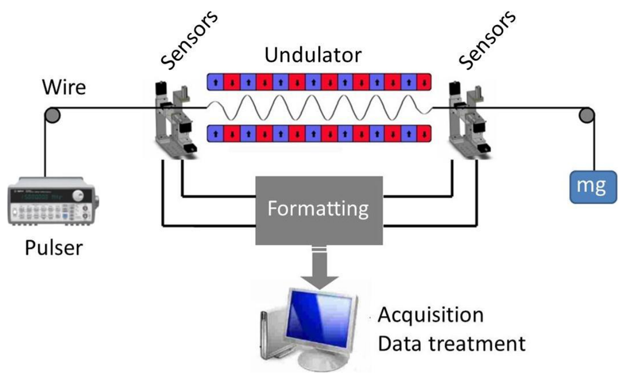

R.W.Warren, "Limitations on the use of the pulsed-wire field measuring technique", Nucl. Instr. and Meth. A272 (1988) 257

Swiss Light Source : 1 T, 19 mm period, Signal/Noise = 26.02 dB

The Pulse wire magnetic measurement system, T. Schmidt, International Magnetic Measurements Workshop 16, 2009

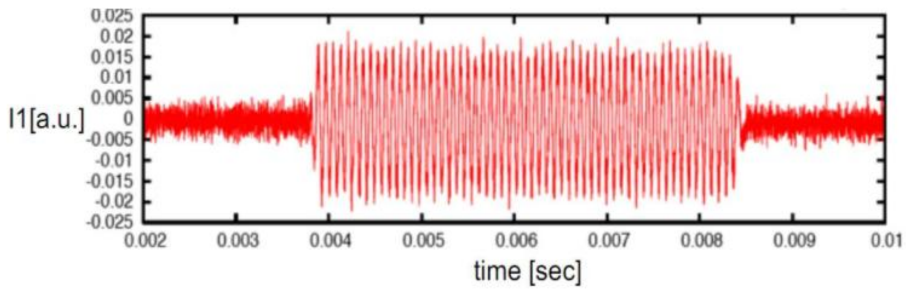

SOLEIL : 1 T, 18 mm period, 2 m long undulator

CuBe wire : 125 µm diameter, 10 N, sag : 65 µm
5 A 2 µs bipolar pulse generator developed in house
Photodiode for vibration detection

Pulse 4.5 A Δt=10 µs, Signal/Noise : 26.02 dB

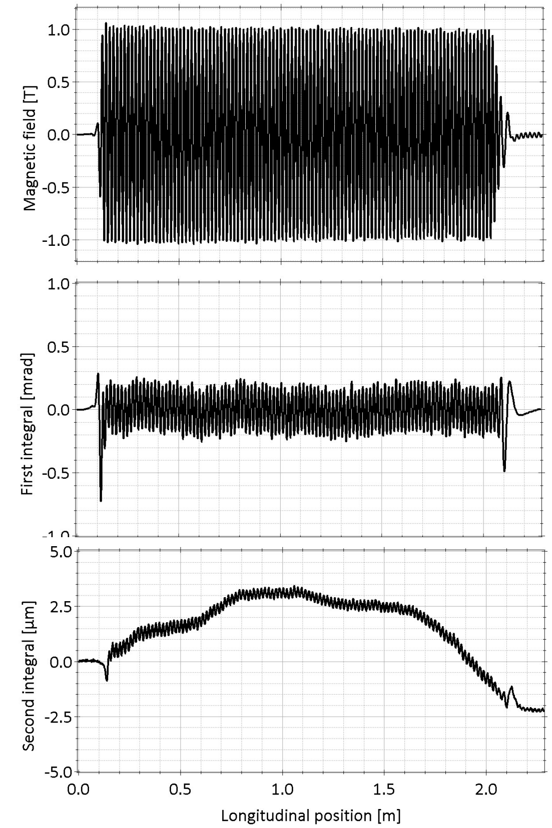

Measurements of SOLEIL Insertion Devices using Pulsed Wire Method , M.Valléau, C. Benabderrahmane, M.-E. Couprie, O. Marcouillé, F. Marteau, J.Vétéran , IPAC2011, San Sebastián, Spain, 3242-3244

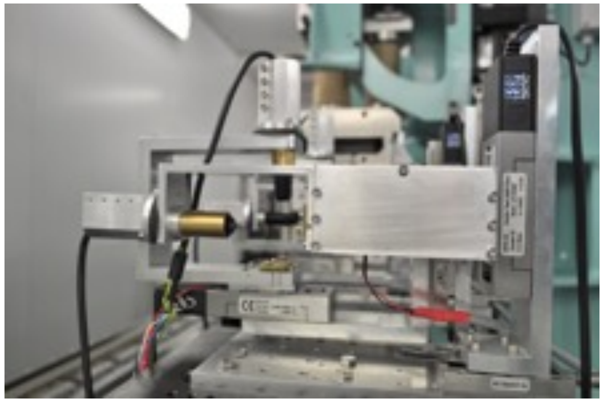

I- In vacuum undulators and wigglers

Magnetic measurements

- in situ magnetic measurements

ex : SAFALI (Self aligned field analyzer with laser instrumentation)

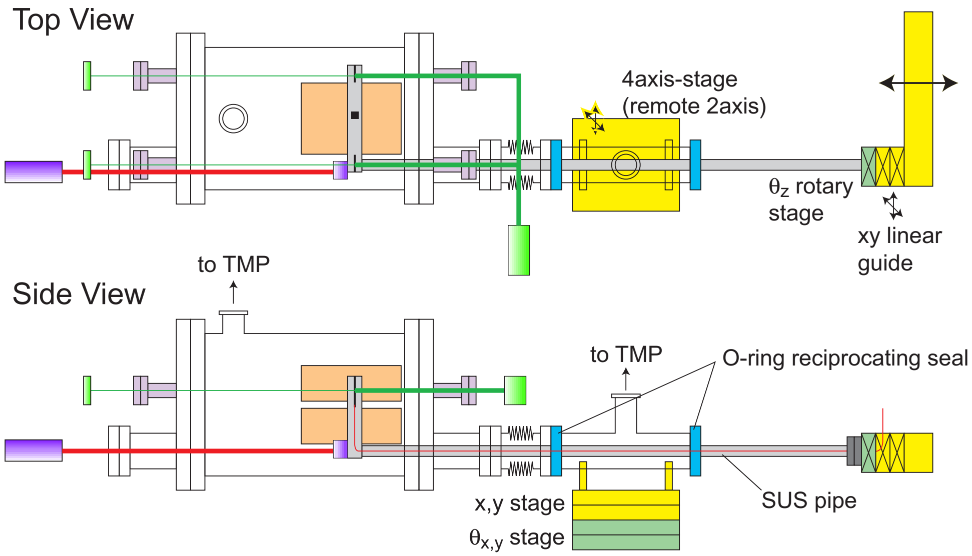

T. Tanaka et al, FEL 2007, Novosibirsk, 468;
T.Tanaka et al. FEL 2008, Gyeonju, 371;
T. Tanaka, et al., . Phys. Rev. Spec.Topics 12, 120702 (2009)

T. Tanabe, et al., . Design concept for a modular in vacuum probe mapper for use with CPMU convertible in vacuum undulators of varying magnetic length, PAC 2011, 2534

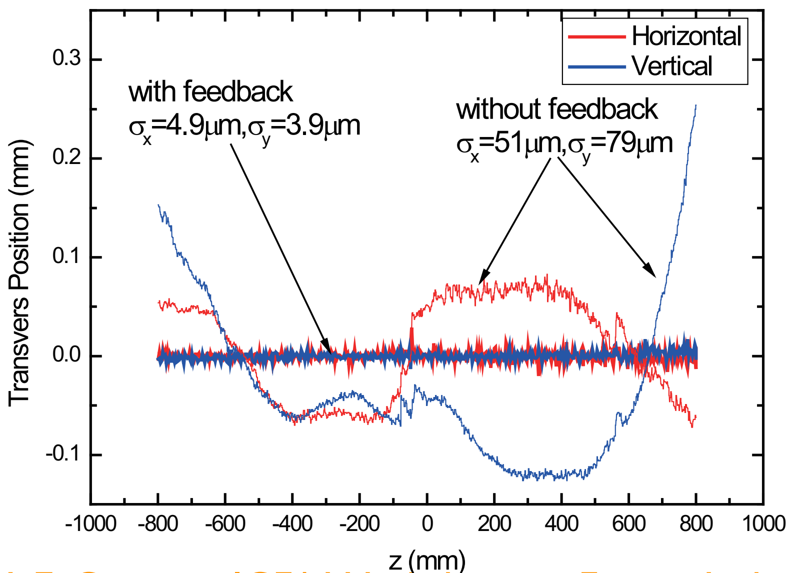

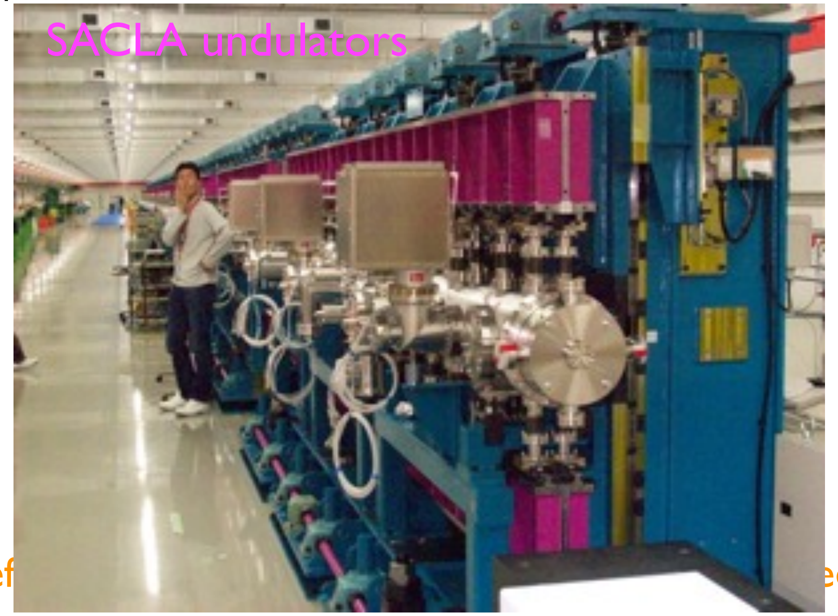

Magnetic corrections

Shimming

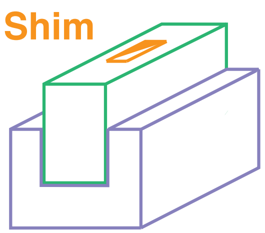

Change of the undulator inner gap

ex : 5.5 mm => 5.15 mm

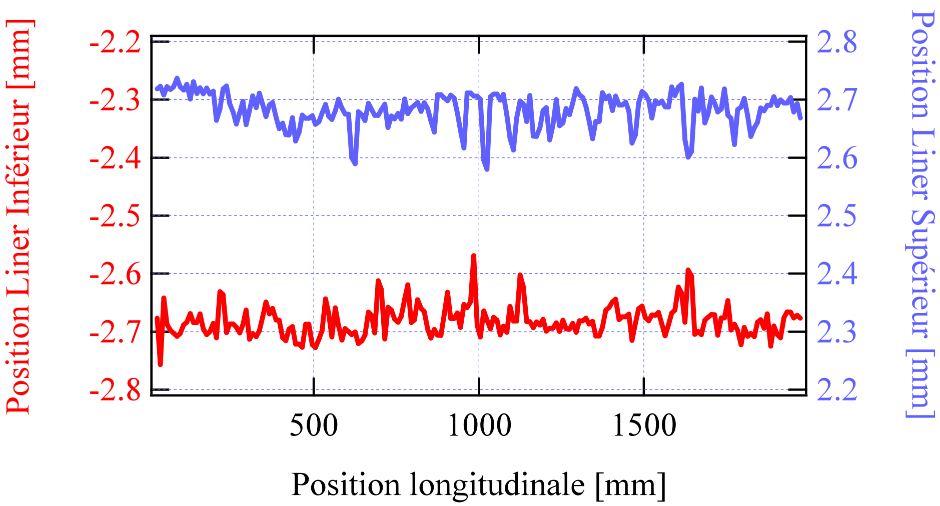

In Situ Sorting, Swapping

exchange (phase error), rotation (multiple components)

$$I_{1n} = \int_{z_n}^{z_{n+1}} B(z)\,\mathrm{d}z, \qquad z_n = -L/2 + n\lambda_u/2$$

$$ES_n = \sum_{m=1}^{n} i_m, \qquad i_n = \frac{|I_{1n}| - \langle I \rangle}{\langle I \rangle}$$

$$FS_n = \sum_{m=1}^{n} f_m \qquad f_n = I_{1n} - (-1)^n \langle I \rangle$$

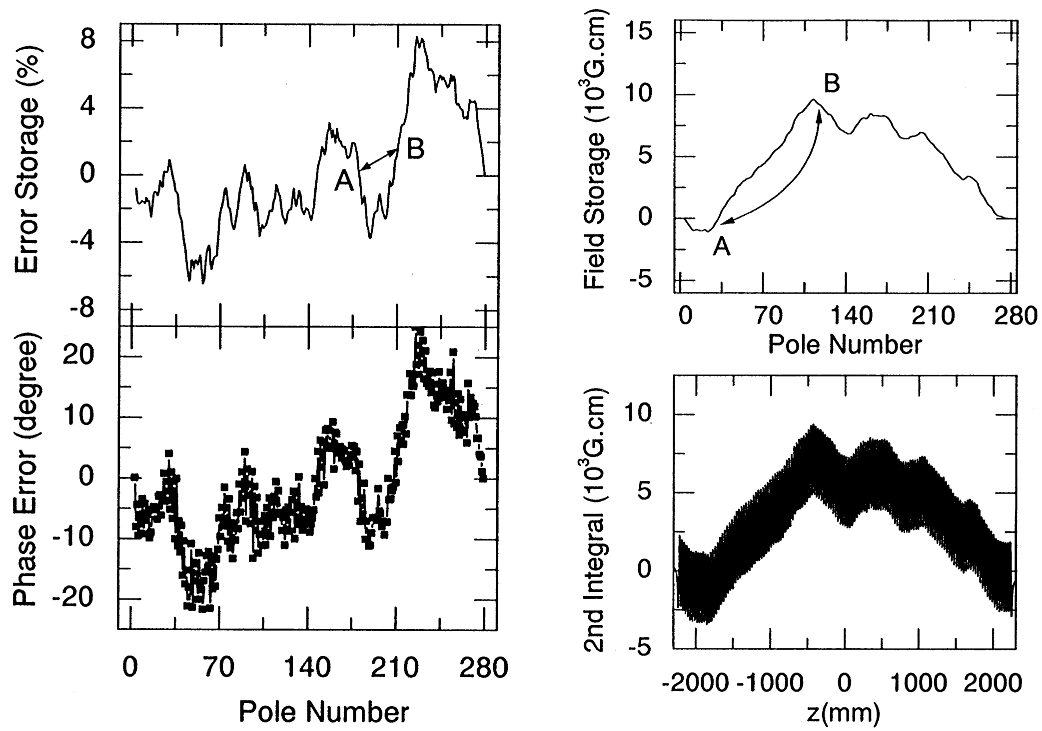

T. Tanaka et al, Undulator field correction by in situ sorting, NIMA 465 (2001) 600
ex : phase error 16° to 2.2°

Genetic algorithm based ID Builder

Evaluation:

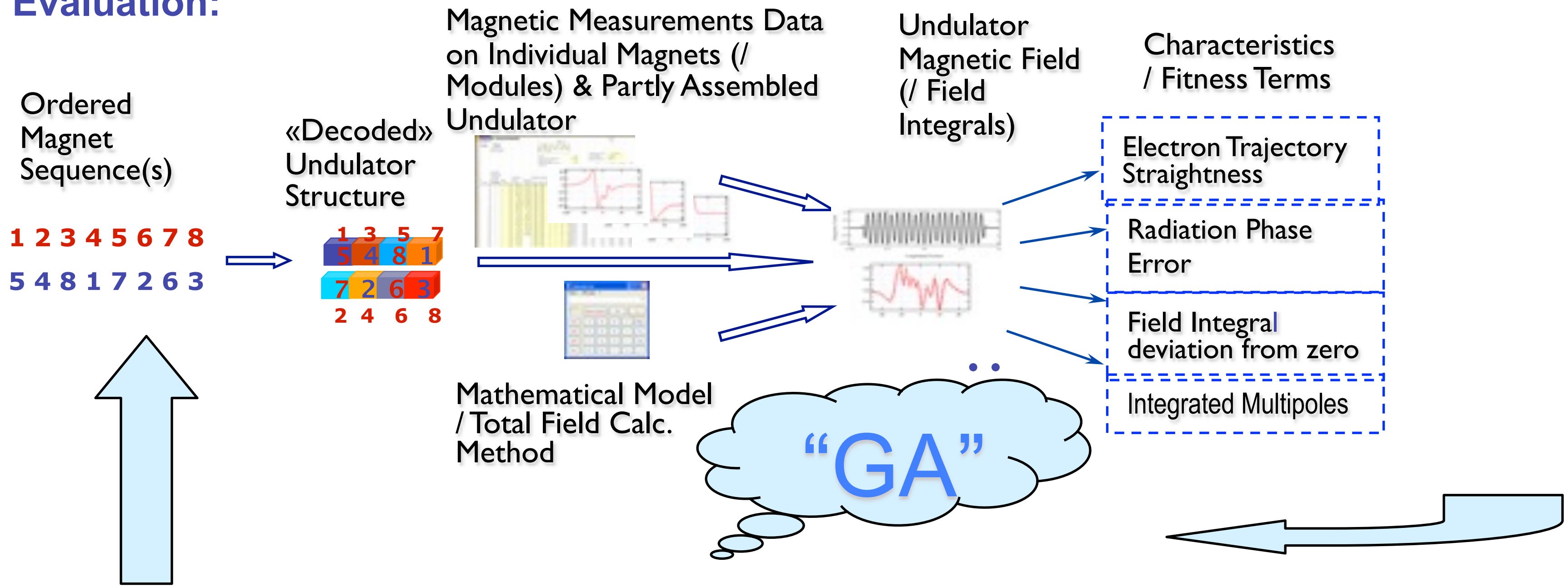

Variation Operators for Permutations:

Mutation : - e.g. swap items (magnets) at two randomly chosen positions - [5 4 8 1 7 2 6 3] ⟹

Crossover : - e.g. «order 1» - [1 2 3 4 5 6 7 8] [3 5 6 8 1 2 7 4] ⟹ [? ? ? 4 5 6 7 ?] ⟹

Advantages : object function, arbitrary search space, search from ap population, mutation and cross-over => global optimum, multi-modal/multi-objet

Efficient Computation of Coherent Synchrotron Radiation taking into account 6D Phase space distribution of emitting electrons, O. Chubar, M. E. Couprie, International Conference on Synchrotron Radiation Instrumentation Daegu (KO) 28 May-2 June 2006, AIP Conference Proceedings 2007, 879, 259-362

Towards short period high field in vacuum undulators

- Configuration : Pure Permanent magnet (magnet configuration) to Hybrid technology

K. Halbach, Jour. Physics, 44 (1983) 211

- Magnet and poles choices

SmCo magnets => NdFeB magnets
Vanadium Permendur poles =>Dysprosium poles

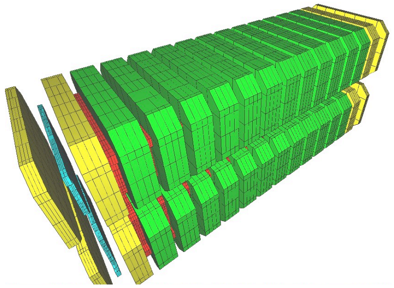

RADIA design

Proposed alternative to superconducting undulators : cryogenic undulators

- increase of remanent field and coercivity at low temperature
- operation at liquid nitrogen temperature => manageable heat budget
- easy operation on synchrotron light sources

T. Hara, T. Tanaka, H. Kitamura, T. Bizen, X. Maréchal, T. Seike, T. Kohda, Y. Matsuura, Phys. Rev. Spc.Topics 7, 050702 (2004)

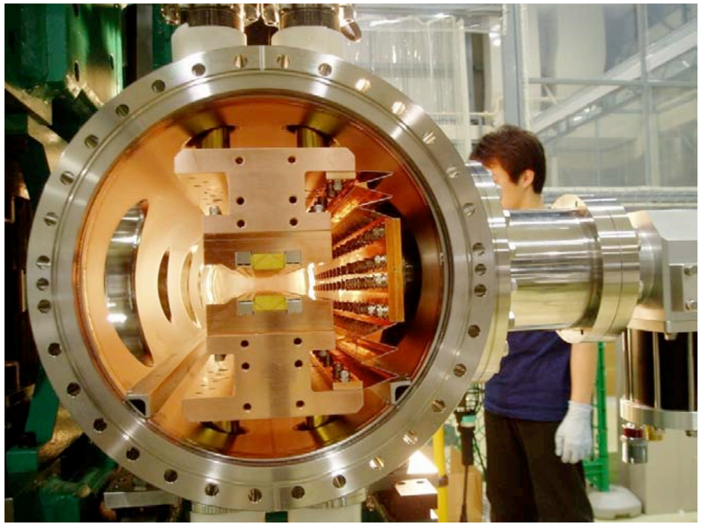

Cryogenic undulator with high Tc superconductors

T. Tanaka et al. PRSTAB 7, 090794 (2004)

Magnetic characterisation on sample magnets

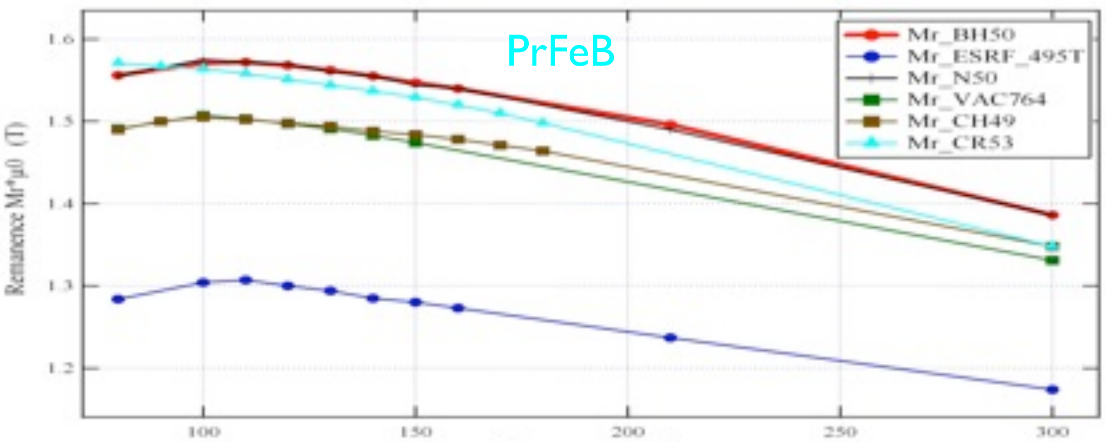

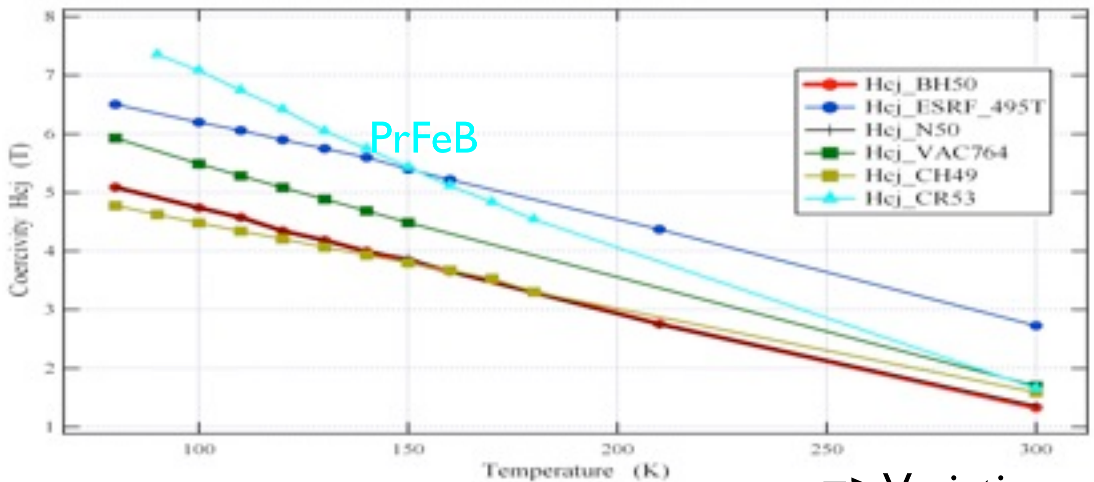

M. Sagawa et al. J. Magn. Magn. Mater. 70, 316 (1987)
T. Hara et al. APAC2004, Gyeongju, Korea, 216
C. Benabderrahmane et al, NIM A 669 (2012) 1-6
K. Uestuener et al., Sintered (Pt,Nd)FEB permanent magnets with $(BH)_{max}$ of 520 kJ/m^3 at 85 K for cryogenic applications, 20th Workshop on Rare Earth Permanent Magnets 2008, Crete

Spin Transition Reorientation
NdFeB strong Magneto-Crystalline Anisotropy (MCA) => orientation along [001]
Magneto-cristalline orientation given by the energy : $E(T) = K_1 \sin^2(\theta) + K_2 \sin^4(\theta)$, θ angle between the magnetisation and [001]
at room temperature : magnetisation // c
Fe MCA independant of T, Nd : K_1 // [001] dominant at room T and K_2//[110] at low T

=> Variation of the susceptibility vs T

Characteristics of different magnet samples at 20 °C: B_r remanence, H_{cj} coercivity. VAC stands for Vacuumschmeltze.

Characteristics Company	CR53 Hitach-Neomax	BH50	CH49	VAC764 VAC	495T Neorem	N50 Atlas-Yunshen
Type of magnet	$Pr_2Fe_{14}B$	$Nd_2Fe_{14}B$	$Nd_2Fe_{14}B$	$Nd_2Fe_{14}B$	$Nd_2Fe_{14}B$	$Nd_2Fe_{14}B$
Remanence B_r (T)	1.35	1.40	1.39	1.37	1.18	1.40
Coercivity H_{cj} (T)	1.65	1.39	1.63	1.63	2.81	1.38
Temp. Coef. ΔB_r (%/°C)	0.11	0.11	0.11	0.12	0.11	0.11
Temp. Coef. ΔH_{cj} (%/°C)	0.58	0.58	0.58	0.70	0.58	0.60
Dimensions (mm^3)	4 × 4 × 4	4 × 4 × 4	4 × 4 × 4	4 × 4 × 4	4 × 4 × 4	4 × 4 × 4

D. Givord et al. Solid State Comm. 51 (1984) 857
L. M. Garcia et al. Phys. Rev. Lett. 85 (2) 429

CPMU cooling strategy

Cryocoolers

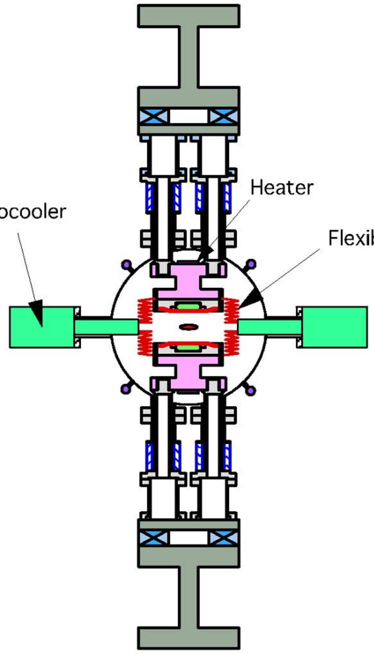

SPring-8
T. Hara et al. Phys. Rev. Spc. Topics 7, 050702 (2004)

Cryo Cooler: Power 2000 W (<300 W), Liquid LN2, Pump : 30 to 90 Hz (40 Hz), Flow : 1 to 30 l/mn (5 l/mn)

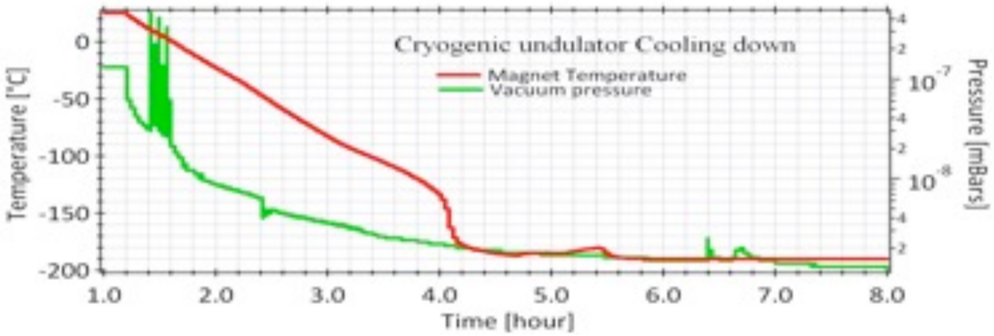

SOLEIL
C. Benabderrahmane et al 7, 050702 (2004)

Cooling to He temperature at BNL

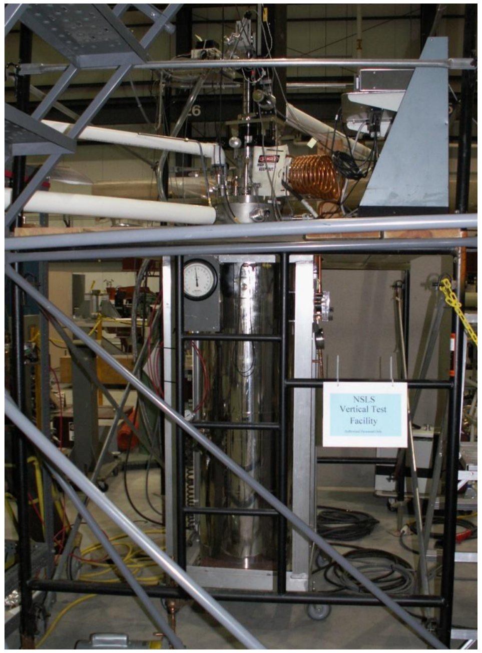

I- In vacuum undulators and wigglers

Mini Cryogenic undulators

at NSLS-II

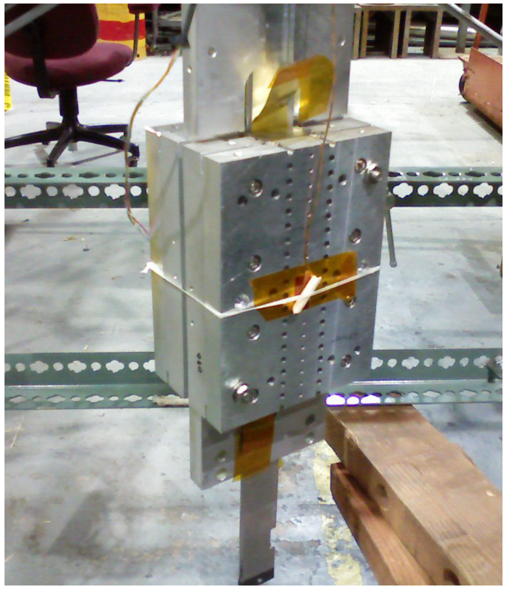

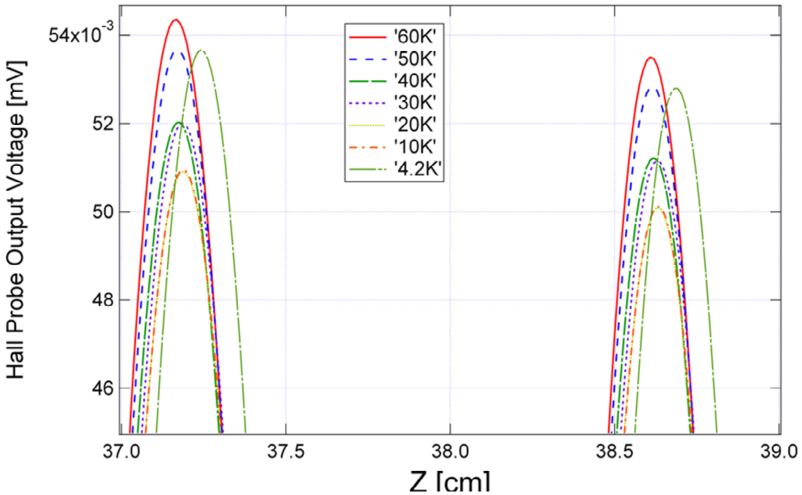

T.Tanabe, et. al., AIP Conference Proceedings, Vol. 1234, p.29 (2010). 4.85 mm gap

at SOLEIL

Validation of magnetic model at low temperature

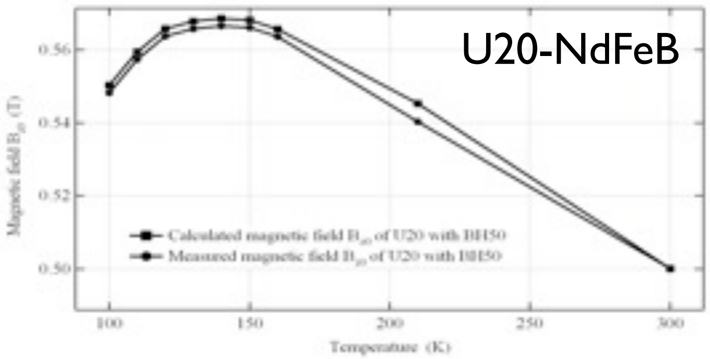

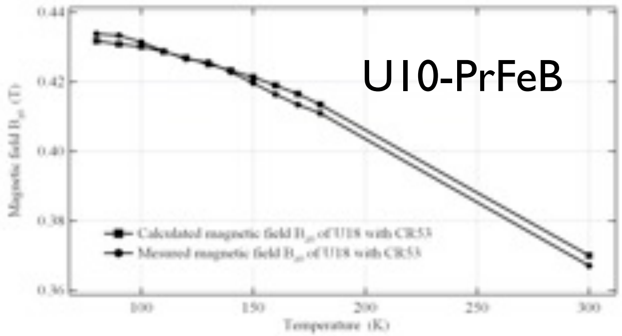

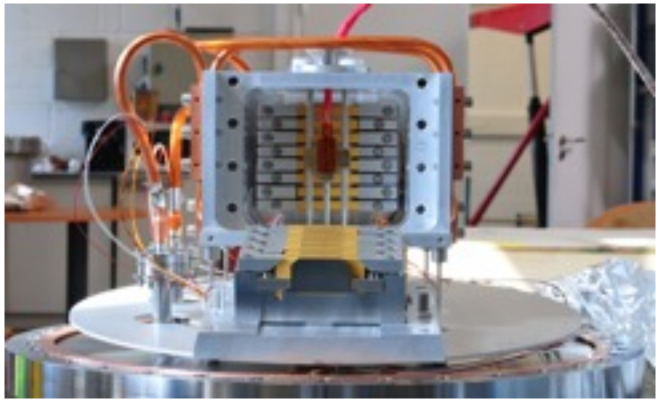

$Nd_2Fe_{14}B$ and $Pr_2Fe_{14}B$ magnets characterisation and modelling for cryogenic permanent magnet undulator applications, C. Benabderrahmane, P. Berteaud, M. Valléau, C. Kitegi, K. tavakoli, N. Béchu, A. Mary, J. M. Filhol, M. E. Couprie, Nucl. Instrum. Methods A 669 (2012) 1-6

at BESSY

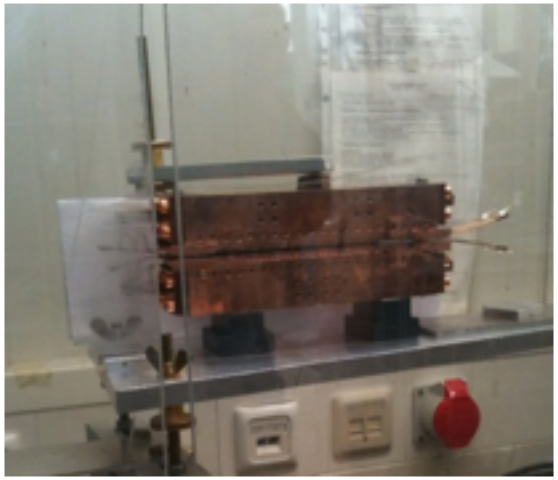

J. Bahrdt et al. IPAC10, 3111

fixed gap=2.5 mm

In vacuum low temperature measurements

ESRF

Stretched wire
Field integral measurement

Laser

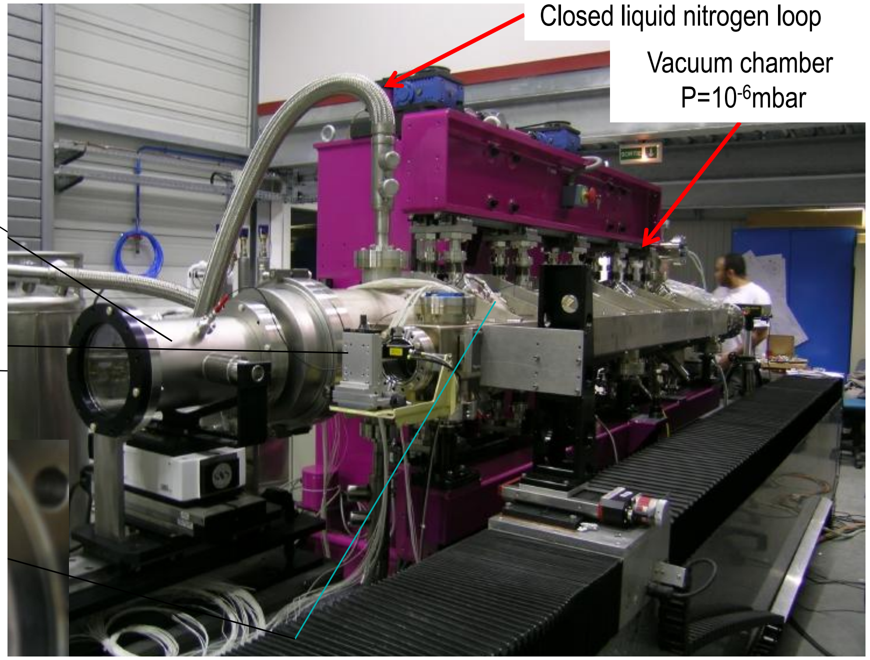

SOLEIL

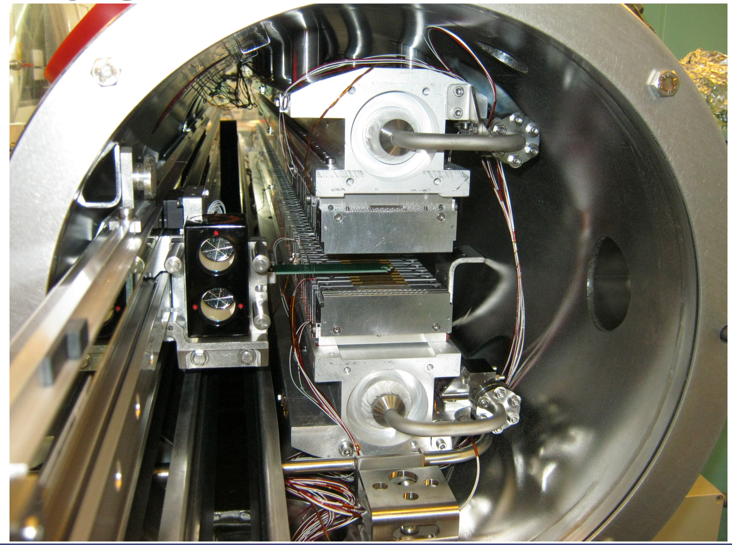

SPring-8

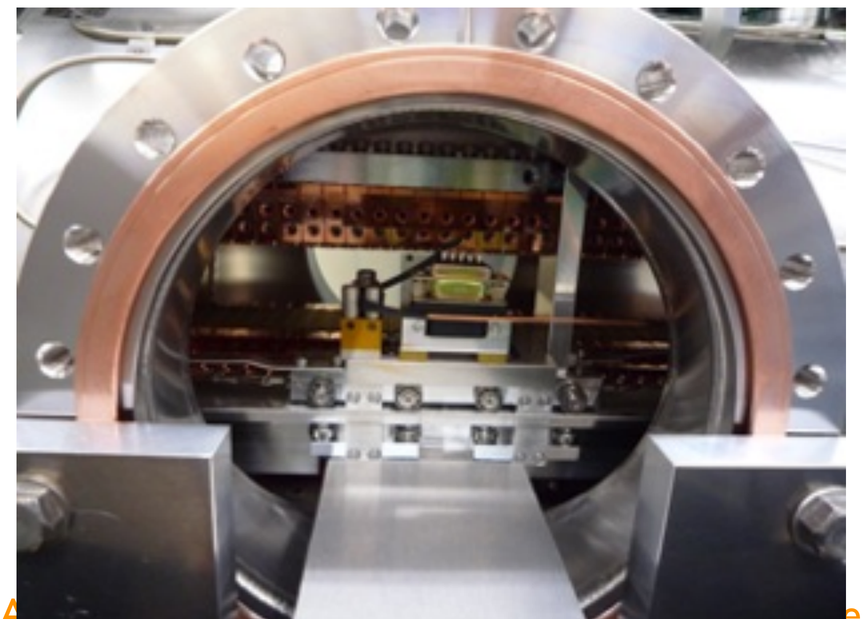

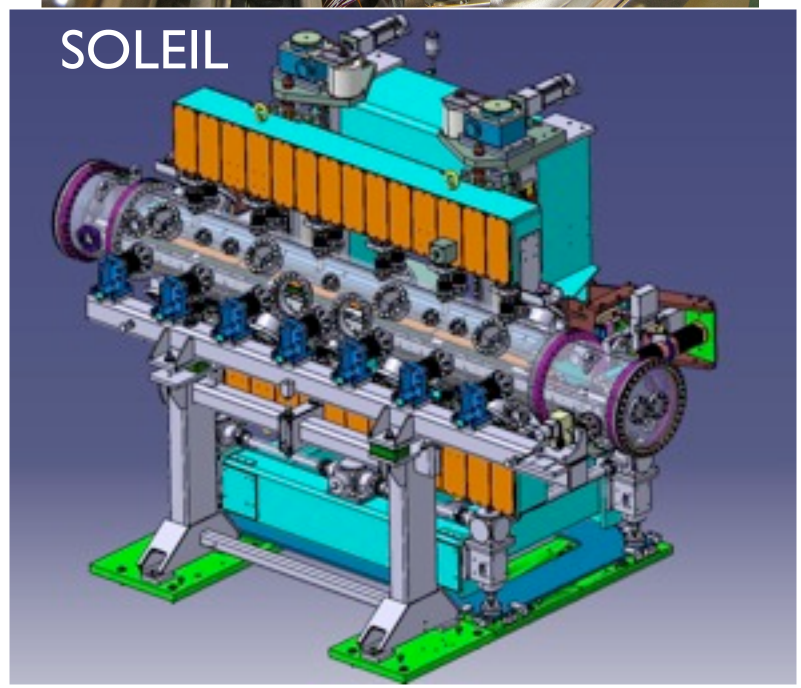

Mechanical changes at low temperature

- Gap opening due to thermal contraction of the supporting rods to be compensated
  Measurement :
  Capacitance type displacement monitors (Nantex Corp.) SPring-8
  Wire resistivity : ESRF, SOLEIL

- Period reduction due to girder contraction, ex at SOLEIL 9 mm over 2 m, i.E. 38 µm / period)

- Phase error correction via rod shimming

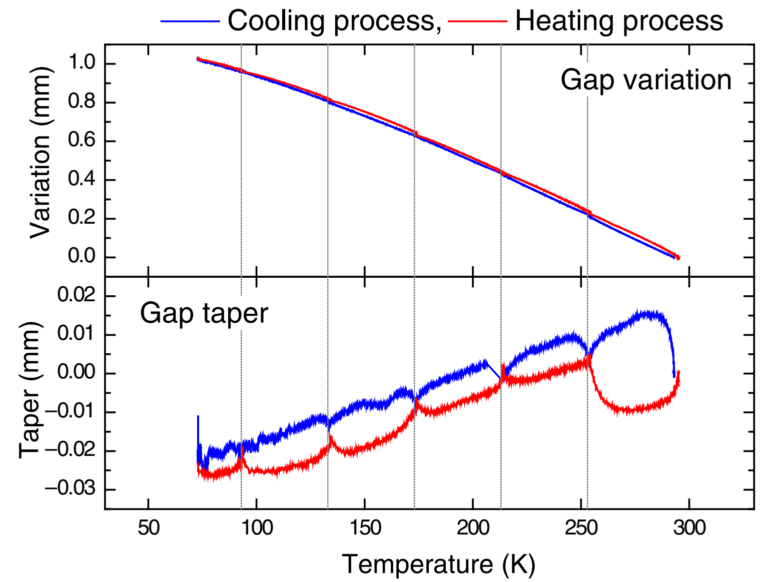

T. Tanaka et al., New Journal of Physics, Development of cryogenic permanent magnet undulaotrs operating around liquid nitrogen temperature, New Jour. Physics 6, 2011, 287

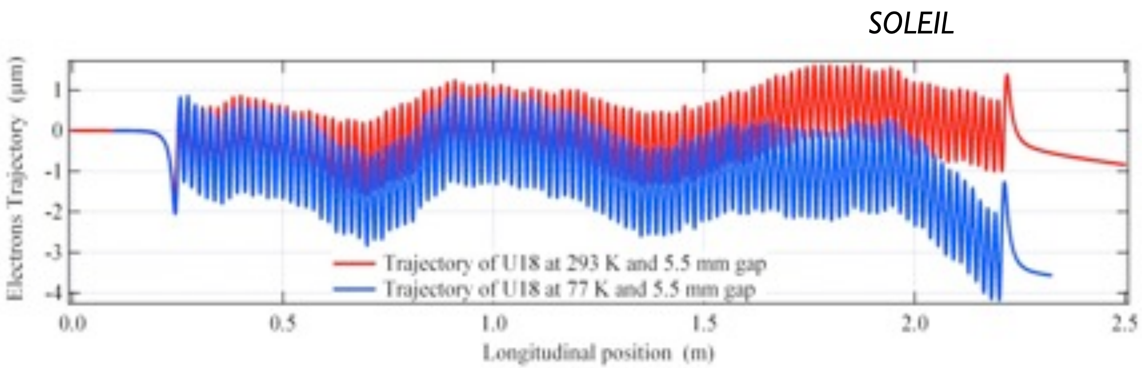

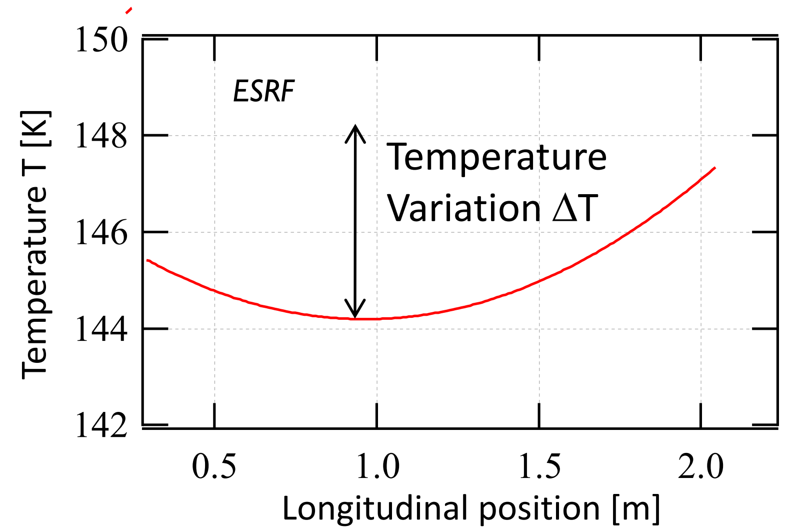

Cryogenic undulators on operation

ESRF

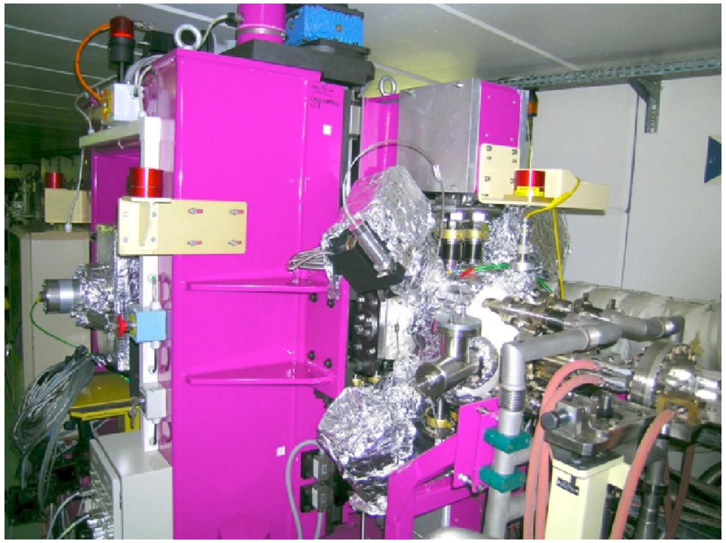

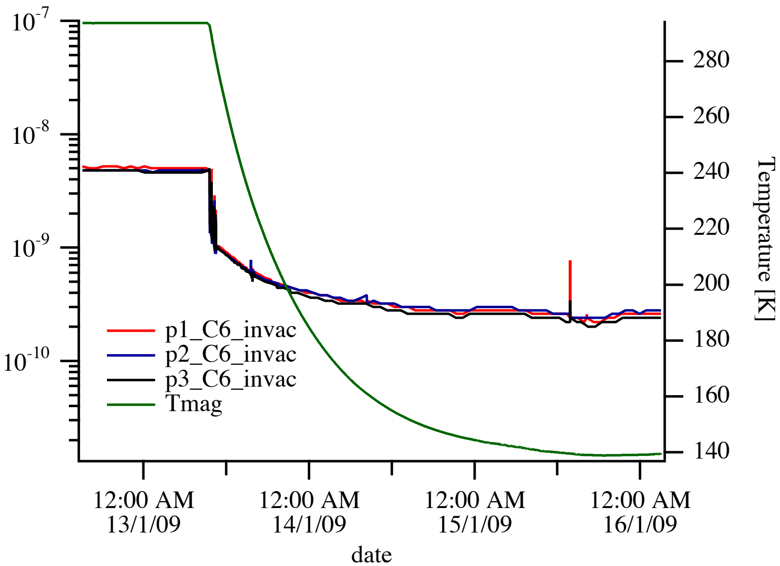

J. Chavanne et al., First operational experience with a cryogenic permanent magnet undualtor at the ESRF, PAC09, 2414

SLS

T. Tanaka et al., in situ magnetic correction for cryogenic undulators, IPAC 2010, 3147

Tanaka, et al., . Phys. Rev. Spec.Topics 12, 120702 (2009)

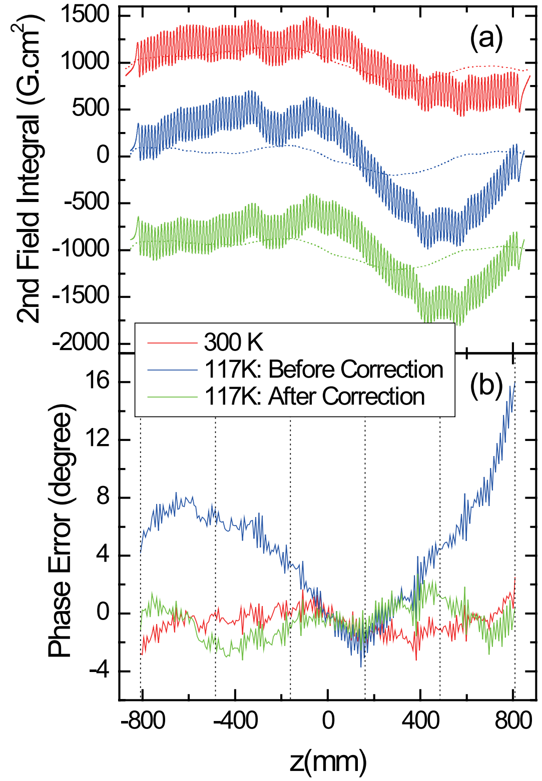

I- In vacuum undulators and wigglers

Cryogenic undulators on operation

SOLEIL Cryo U18 PrFeB

operation at 77 K, Non baked, B= 1.16 T @5.5 mm gap

C. Benabderrahmane et al. IPAC 2011

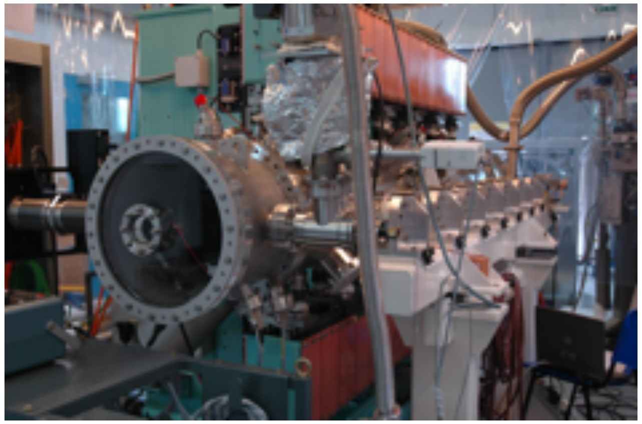

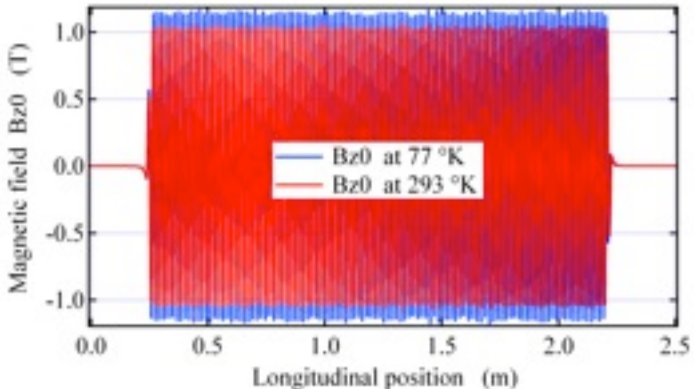

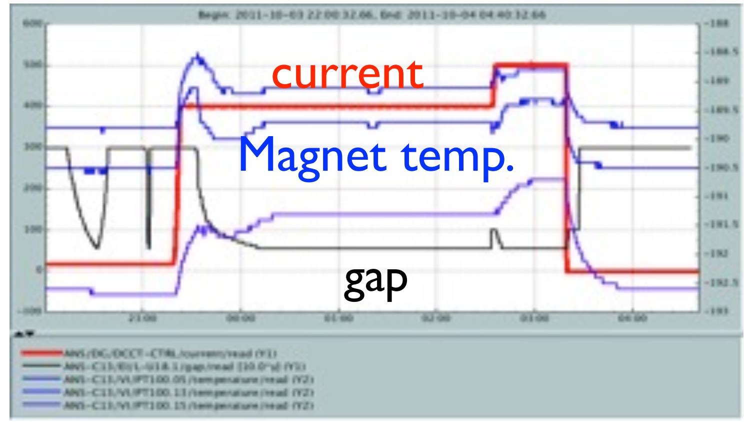

Thermal gradient on the magnetic system **< 1.2 K/m**

Total temperature variation due to electron beam (500 mA) and gap variation **< 2.5 K**

DIAMOND

NdFeB, operation at 157 K, Non baked, B= 1.04 T@ 4 mm gap

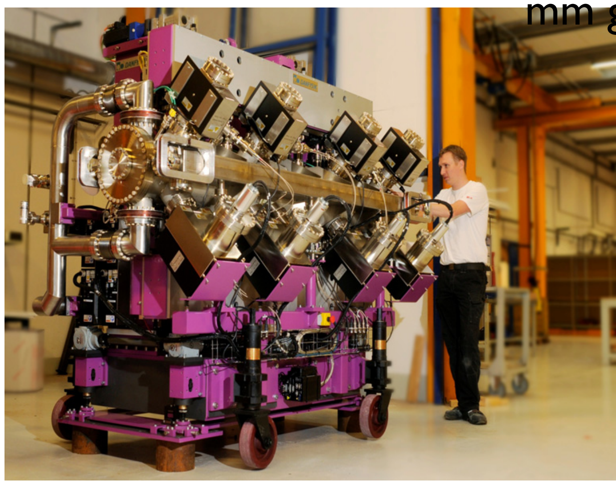

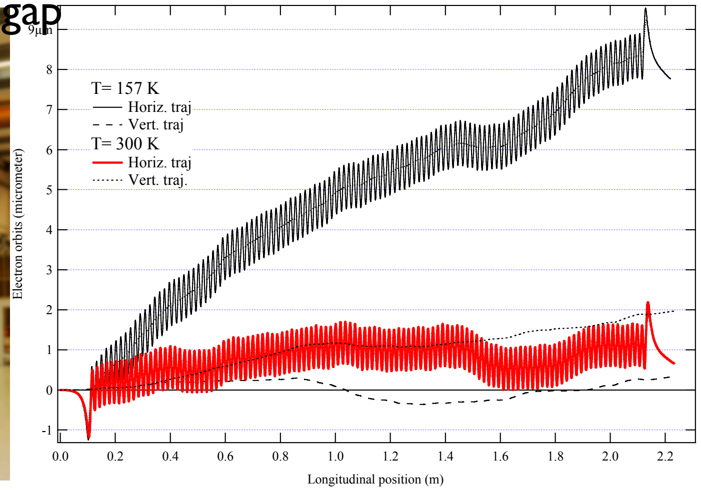

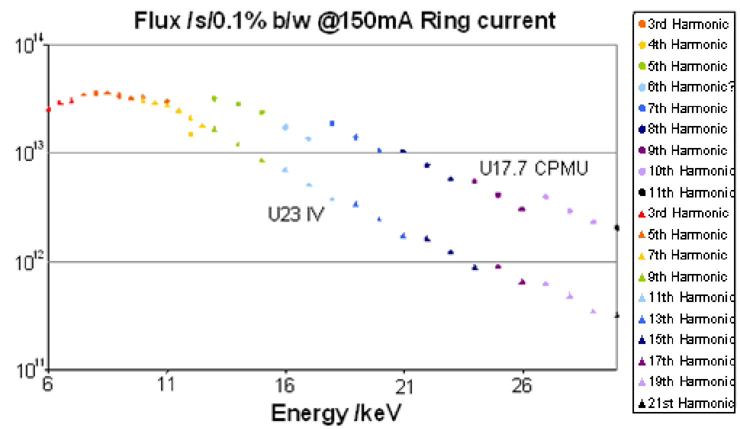

C.W. Ostenfeld et al., Cryoegnic in vacuum unduator at Danfysik, IPAC2010, 3093

J. Schouten et al, Electron beam heating and operation of the cryogenic undulator and superconducting wigglers at DIAMOND, IPAC 2011, 3323

I- In vacuum undulators and wigglers

Cryogenic undulators radiation

SOLEIL

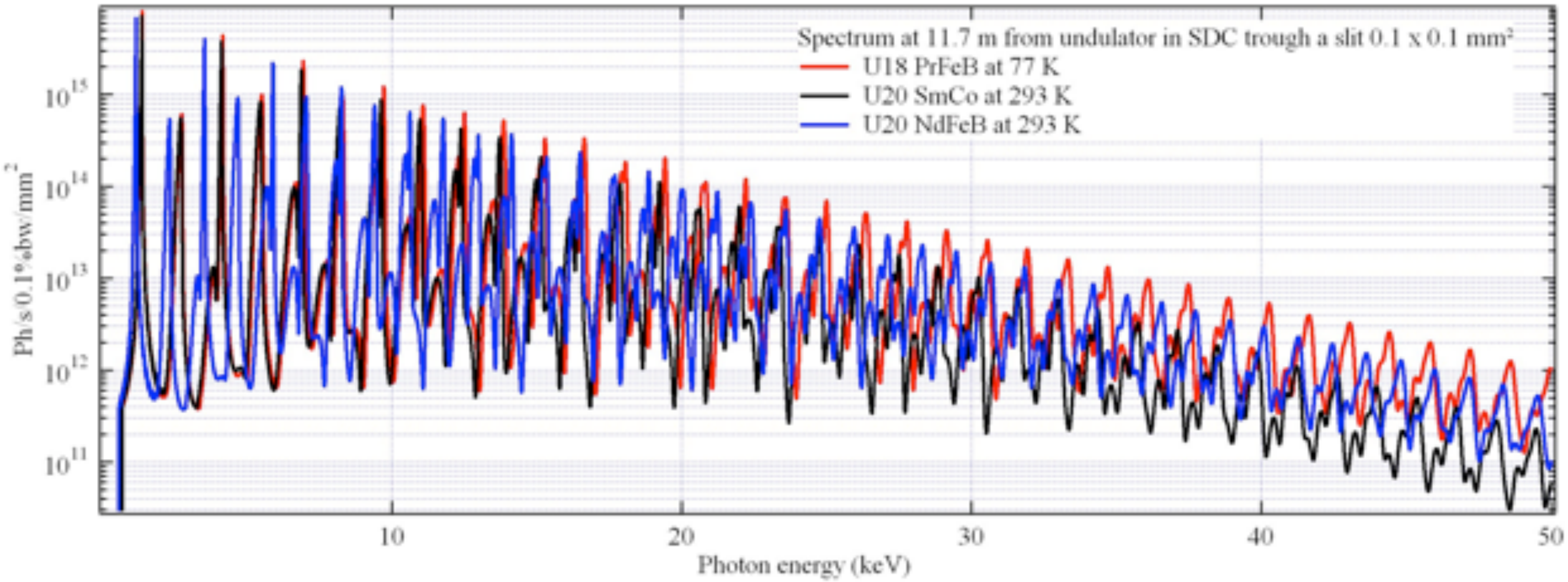

Test RP : 13 décembre 2011

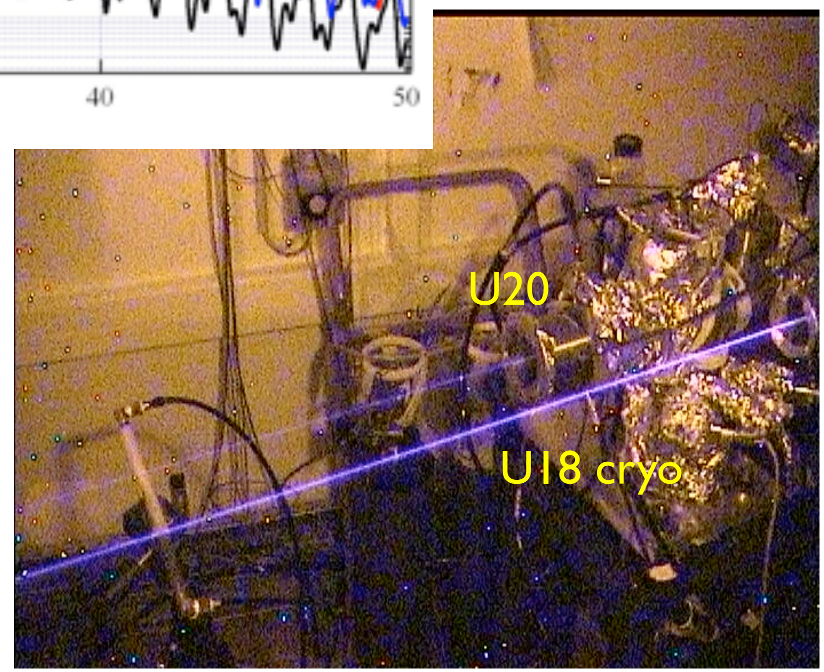

In vacuum wiggler

Choice of an in vacuum wiggler rather than a superconducting wiggler

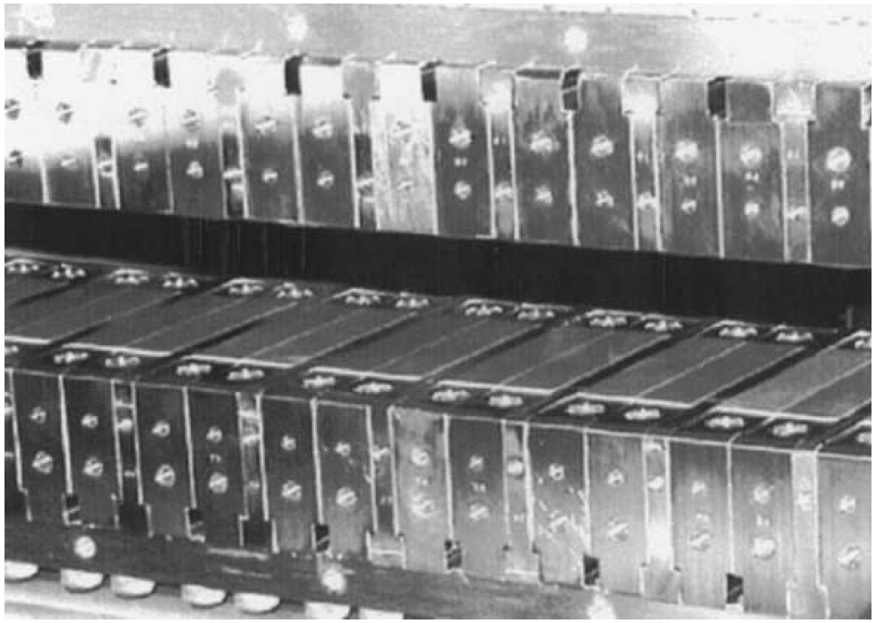

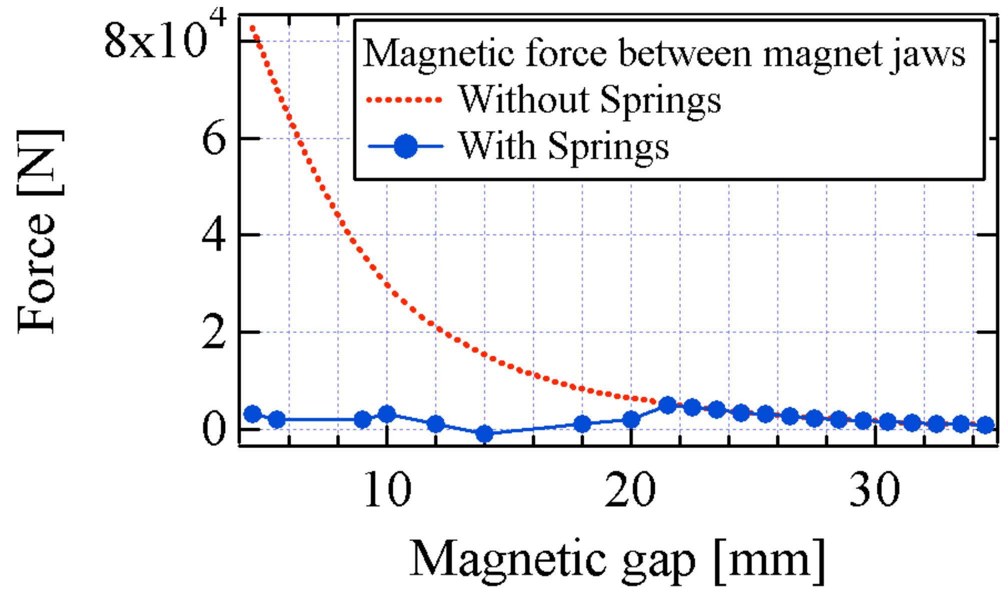

SPring-8 : 1.95T, gap=7 mm, 10x90 mm

X.M. Marechal et al, NIMA 4676-468 (2001) 138-140

SOLEIL : 2.1T, gap=5.5 mm, 10x150 mm

O. Marcouillé et al., SRI 09

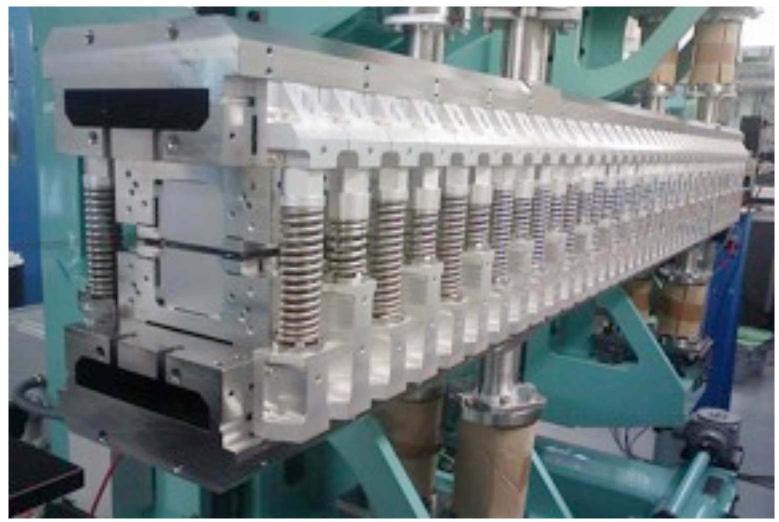

In vacuum wiggler

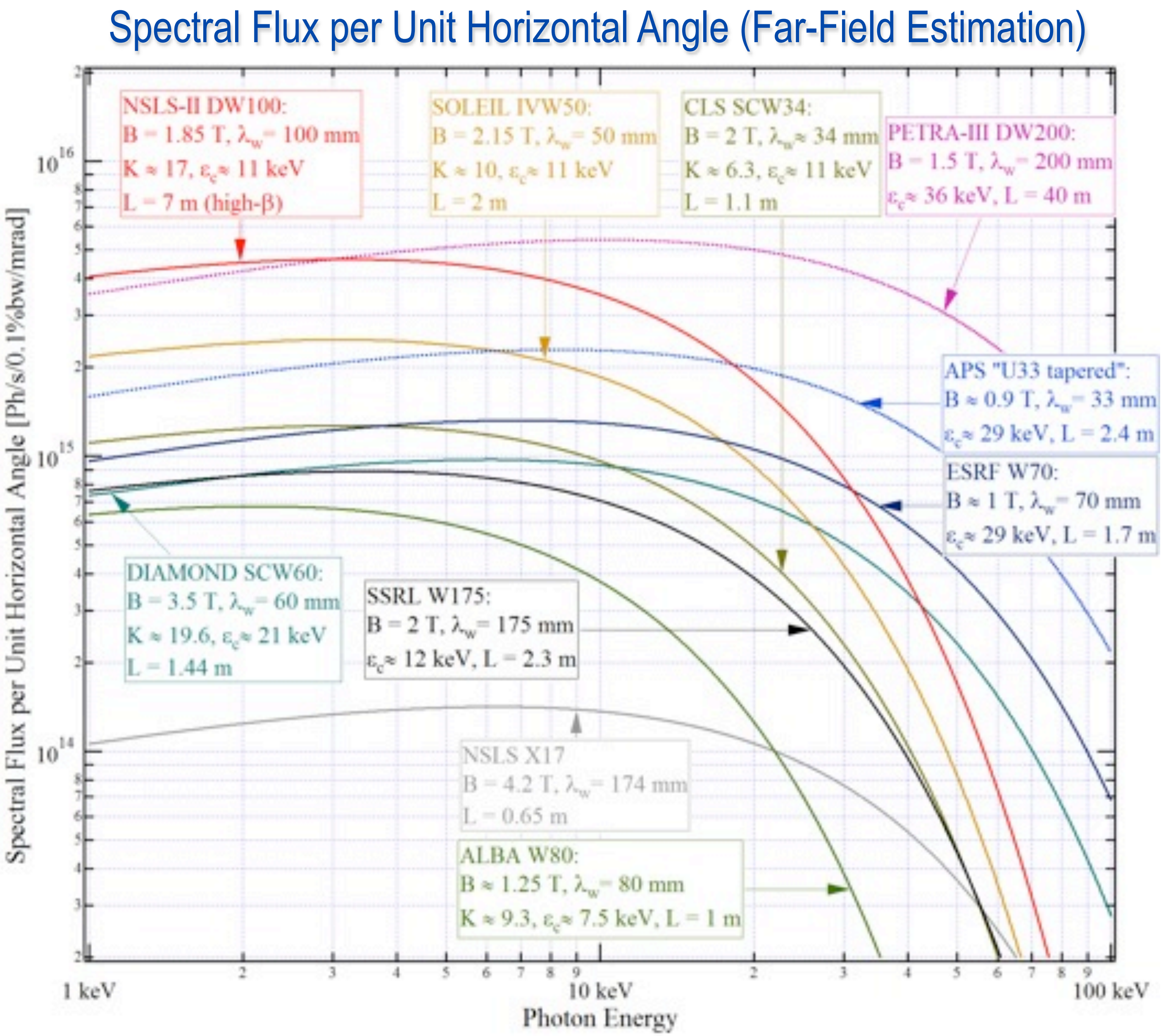

O. Chubar

2- EPU and fast polarisation switching

Electromagnetic undulators

Ex of the SOLEIL 10 m HU640

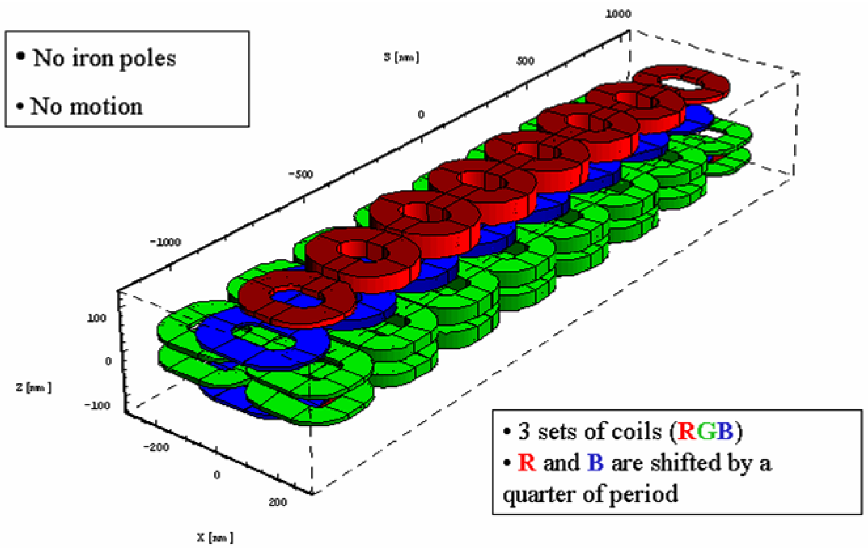

Radia code: http://www.esrf.fr

$$B_z(s)=B_B.\cos[2\pi s/\lambda_o]+B_R.\sin[2\pi s/\lambda_o]=B_{zo}.\cos[2\pi s/\lambda_o+f]$$

Fast switching : 1 Hz : 270 ms for switching -±600 A on PS1, 300 ms flat top for data acquisition
SOLEIL conception- Realisation Danfysik, Magnetic measurements SOLEIL

Design, Construction and Magnetic Measurements of the DESIRS Undulator at SOLEIL, O. Marcouillé et al., International Conference on Synchrotron Radiation Instrumentation Daegu (KO) 2006, AIP Conference Proceedings 2007, 879, 396-399

Electromagnetic undulators

Ex of the SOLEIL 526

Linear H,V, + Quasi periodic, Circular

Coll. BINP

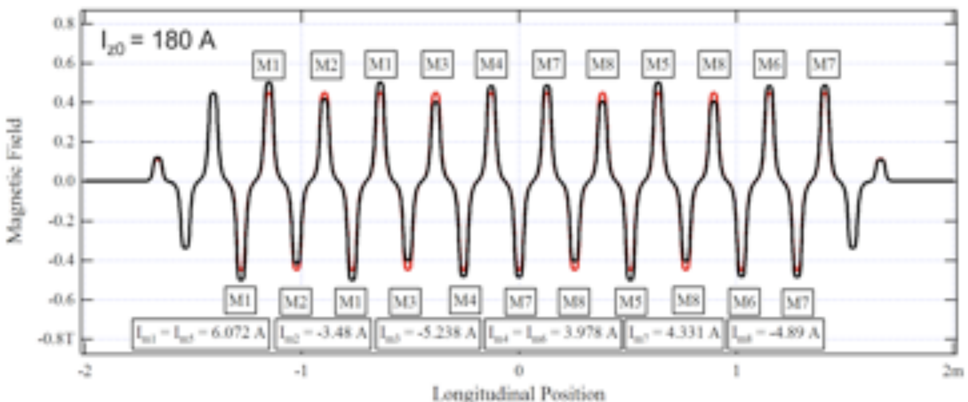

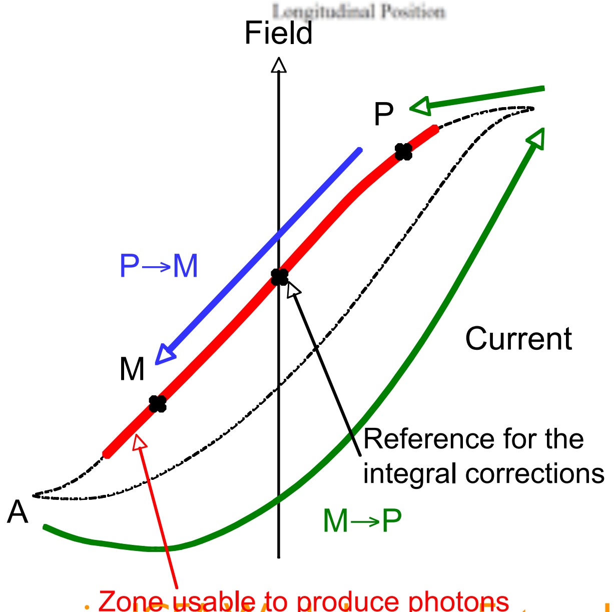

28 Bx dipoles (Asymmetric field)

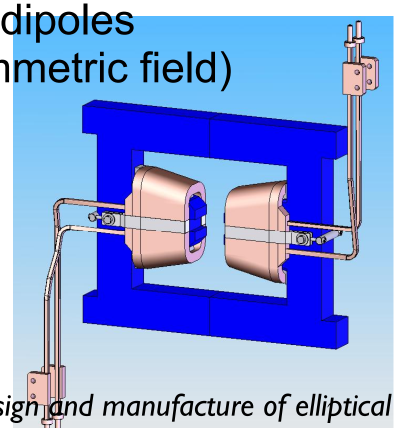

27 Bz dipoles (Symmetric field)

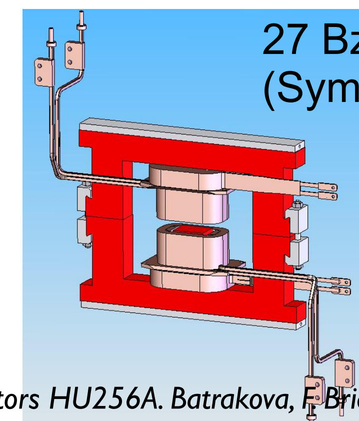

Magnetic design and manufacture of elliptical undulators HU256A. Batrakova, F. Briquez, O. Chubar, I. Churkin, M.-E. Couprie, A. Dael, I. Ilyin, Yu. Kolokolnikov, G. Roux, E. Rouvinski, E. Semenov, A. Steshova, M. Valleau, P. Vobly, Nuclear Instruments and Methods in Physics Research A 575 (2007) 29–32

Permanent magnets EPU: Crossed undulators

Onuki undulators

Modes	Bz [T]	Bx [T]
Linear H.	0,4	
Linear V.		0,4
Circular	0,28	

Undulator :

- Period : 30 mm
- Minimal gap : 15,5 mm

Magnets :

- NdFeB
- Size : 8 x 15,5 mm
- B_r : 1,26 T
- $\Theta_{mag} = 0\,°$
- $X_{dist} = 1$ mm

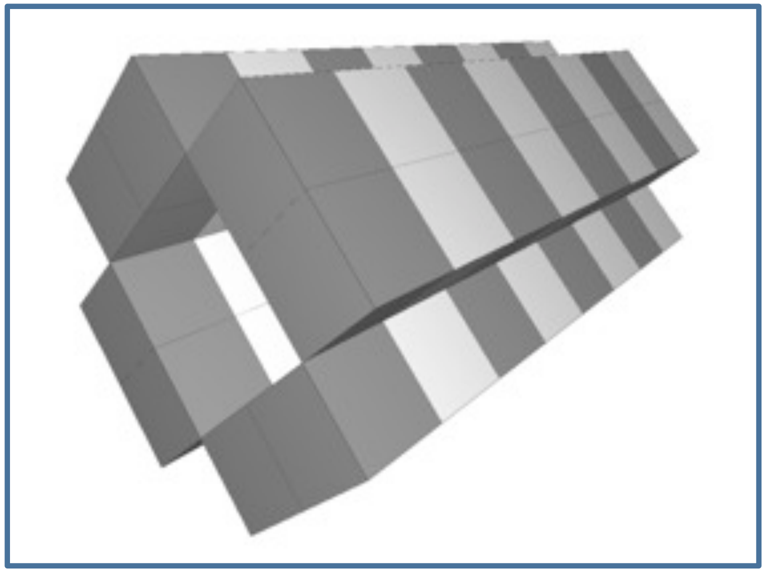

- Crossed and overlapped type polarizing undulator

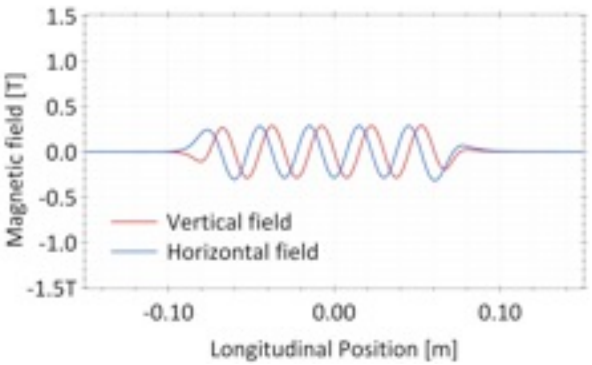

H. & V. field values in circular polarisation.

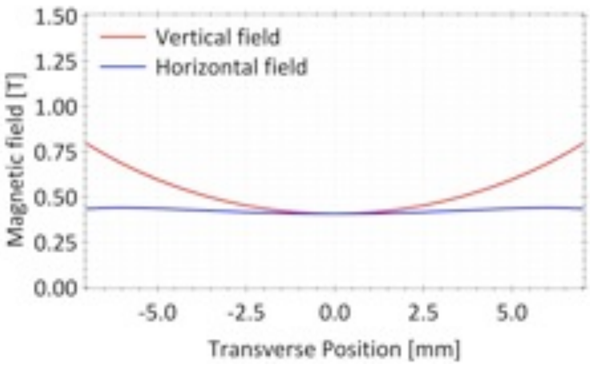

H. & V field roll-off at minimal gap

M. Moissev et al. Sov. Phys. J. 21, 332, 1978
K. J. Kim NIMA219, 426 (1986)

H. Onuki, Nucl. Instr. Meth., A246, 94, (1986)
H. Onuki et al, Appl. Phys. Lett., 52, 173, (1988)

3- EPU and fast polarisation switching

Permanent magnets EPU: HELIOS

Helios undulators

Modes	Bz [T]	Bx [T]
Linear H.	0,173	
Linear V.		0,125
Circular	0,1	0,1

Undulator :

- Period : 30 mm
- Minimal gap : 15,5 mm

Magnets :

- NdFeB
- Size : 30 x 30 mm
- B_r : 1,26 T
- $\Theta_{mag} = 0°$
- $X_{dist} = 1$ mm

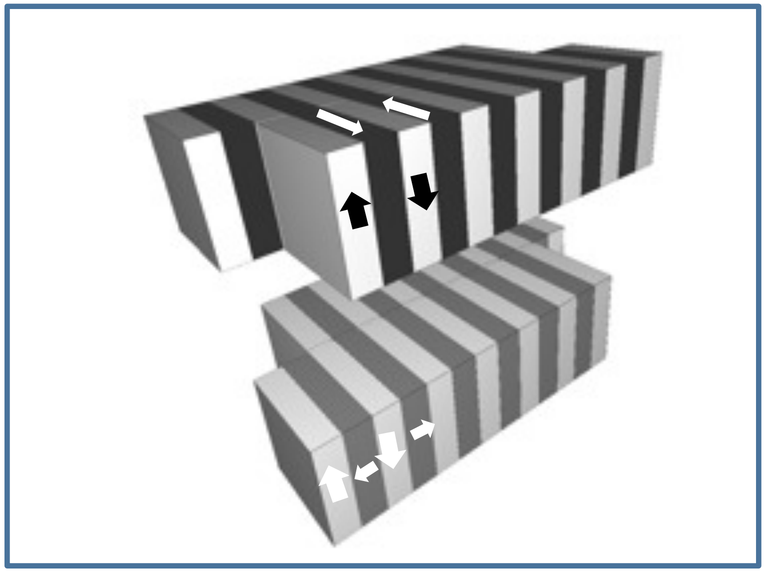

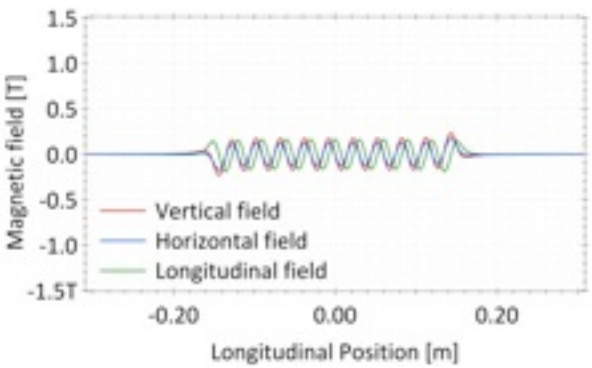

H. & V. field values versus gap at 0 mm shift.

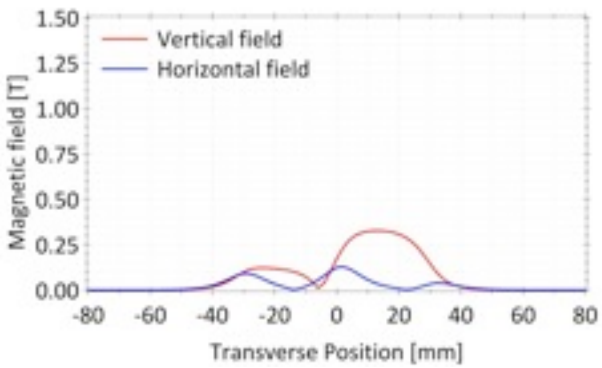

H. & V field roll-off at minimal gap,

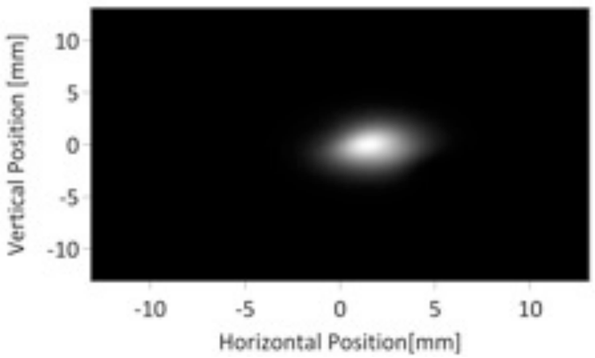

P. Elleaume, A flexible planar / helical undulator design for synchrotron radiation sources, Nucl. Instr. Meth., A291, 371 (1990)

P. Elleaume, J. Synch. Rad.,1, 19 (1994)

Permanent magnets EPU: Diviacco/Walker

Diviacco/Walker undulators

Modes	Bz [T]	Bx [T]
Linear H.	-	
Linear V.		-
Circular	0,13	

Undulator :

- Period : 30 mm
- Minimal gap : 15,5 mm

Magnets :

- NdFeB
- Size : 30 x 30 mm
- B_r : 1,26 T
- $\Theta_{mag} = 0$ °
- $X_{dist} = 1$ mm

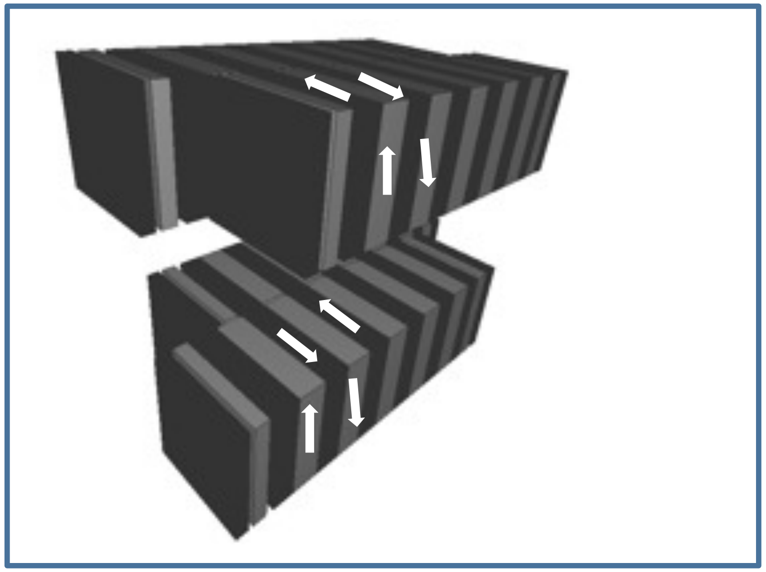

- No phase shift
- No longitudinal component

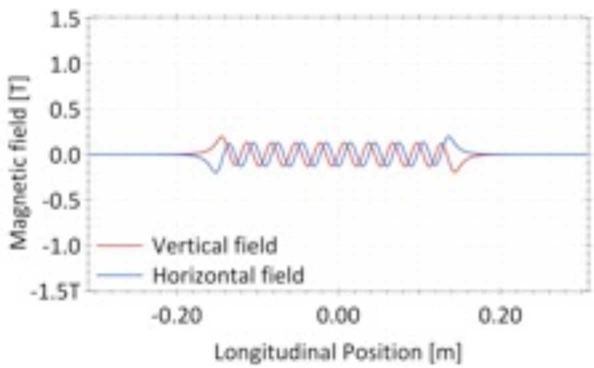

H. & V. fields at minimal gap

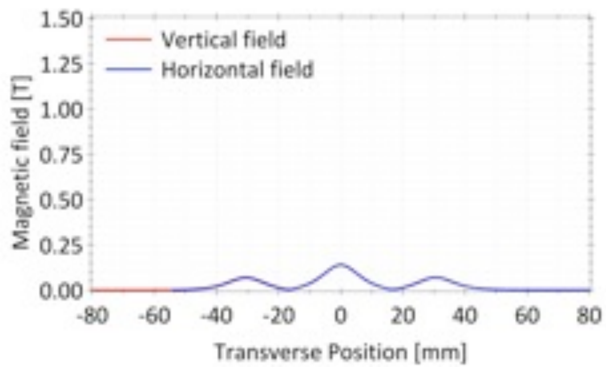

H. & V. fields roll-off at minimal gap

B. Diviacco and R. P. Walker, Nucl. Instrum. Meth., A292, 517 (1990)

Permanent magnets EPU : APPLE I

Apple I undulators

Modes	Bz [T]	Bx [T]
Linear H.	0,456	
Linear V.		0,21
Circular	0,135	0,135

Undulator :

- Period : 30 mm
- Minimal gap : 15,5 mm

Magnets :

- NdFeB
- Size : 30 x 30 mm
- B_r : 1,26 T
- Θ_{mag} = 45 °
- X_{dist} = 1 mm

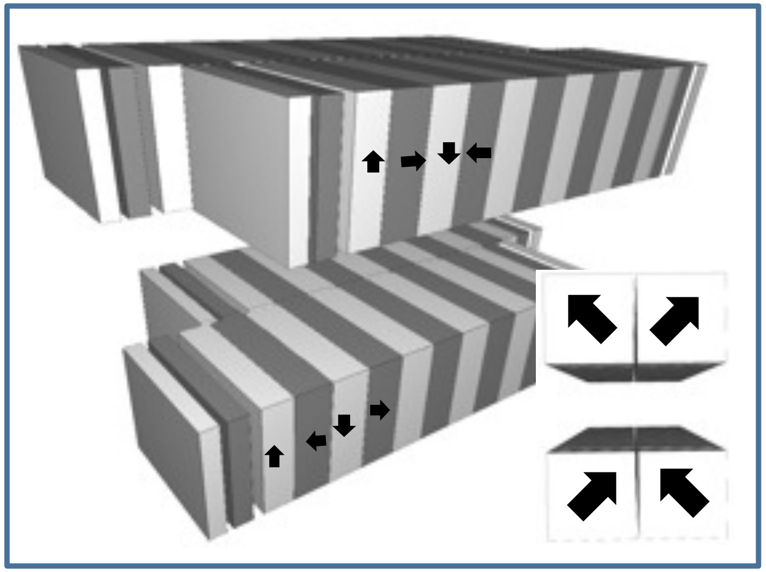

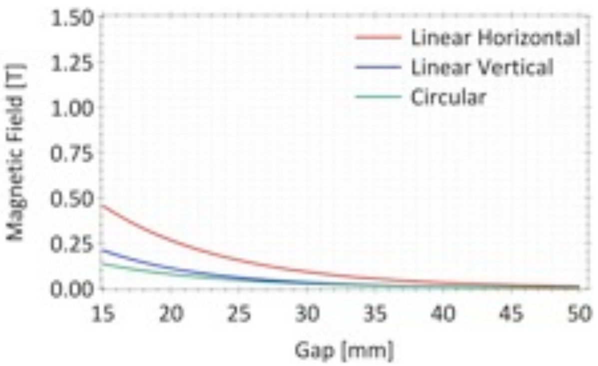

H. & V. field values versus gap at 0 mm shift.

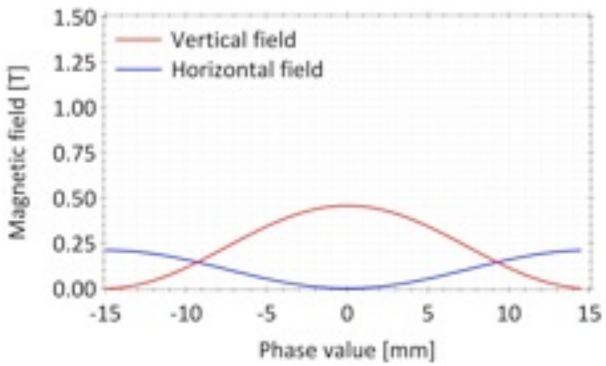

H. & V. field values versus shift at minimal gap

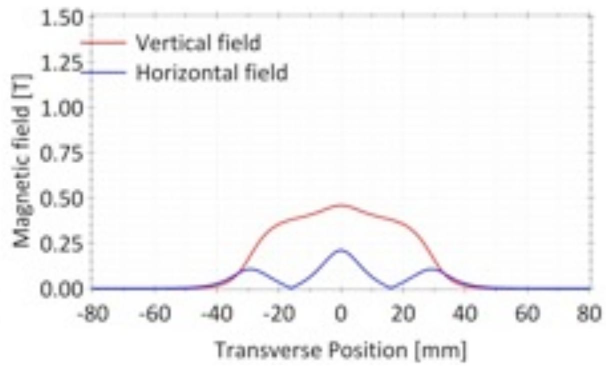

H. & V field roll-off at minimal gap,

S. Sasaki et al, A new undulator for generating variably polarized radiation, Jpn. J. Appl. Phys., 31, L194 (1992)
S. Sasaki et al, Nucl. Instr. Meth., A331, 763 (1993)
S. Sasaki et al, Nucl. Instr. Meth., A347,87 (1994)

3- EPU and fast polarisation switching

Permanent magnets EPU : APPLE II

Apple II undulators

Modes	Bz [T]	Bx [T]
Linear H.	0,421	
Linear V.		0,247
Circular	0,145	0,145

Undulator :

- Period : 30 mm
- Minimal gap : 15,5 mm

Magnets :

- NdFeB
- Size : 30 x 30 mm
- B_r : 1,26 T
- Θ_{mag} = 0 °
- X_{dist} = 1 mm

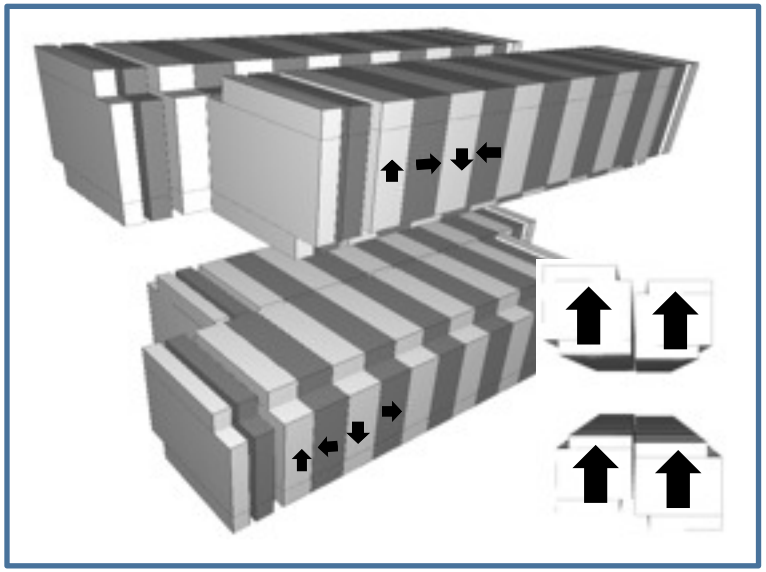

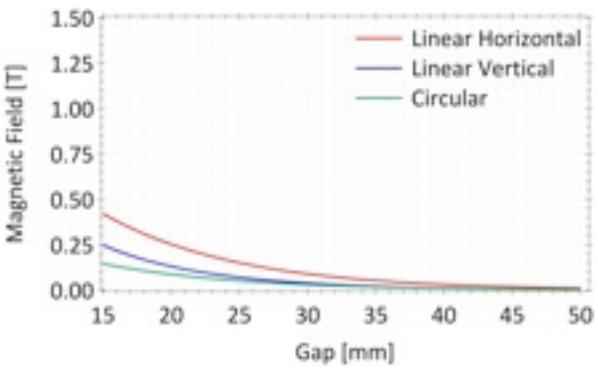

H. & V. field values versus gap at 0 mm shift.

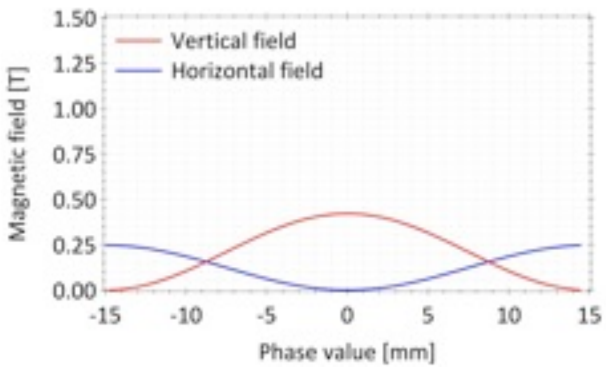

H. & V. field values versus shift at minimal gap

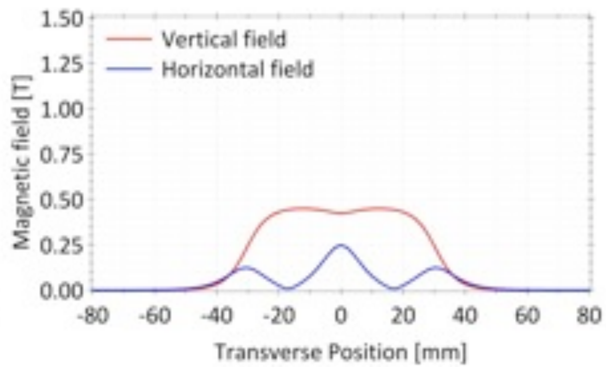

H. & V field roll-off at minimal gap,

R. Carr , Nucl. Instr. Meth., A306, 391 (1991)
R. Carr et al , Rev. Sci. Instrum., 63, 3564 (1992)
R. Carr, Proceedings of 1992 EPAC, p489 (1992)

Permanent magnets EPU : APPLE III

Apple III undulators

Modes	Bz [T]	Bx [T]
Linear H.	1,29	
Linear V.		0,83
Circular	0,52	0,52

Undulator :

- Period : 30 mm
- Minimal gap : 5,4 mm

Magnets :

- NdFeB
- Size : 40 x 40 mm
- B_r : 1,13 T & 1,19 T
- Θ_{mag} = 45 °
- X_{dist} = 1 mm

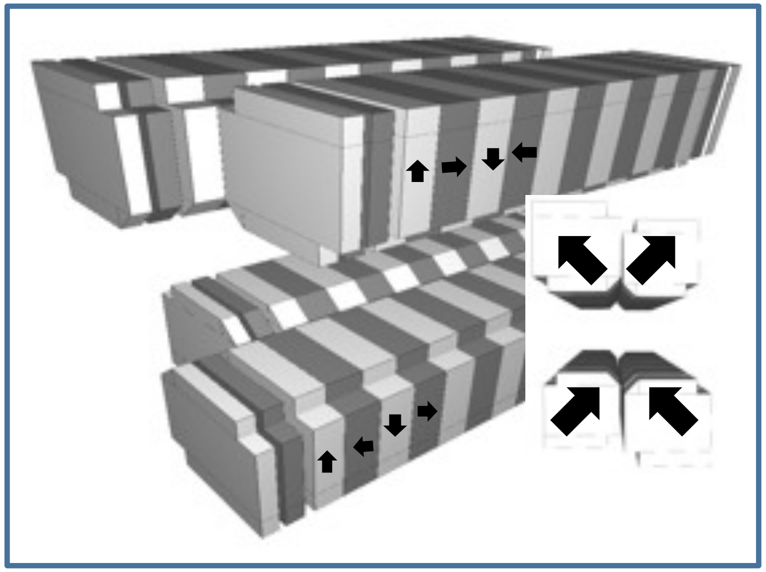

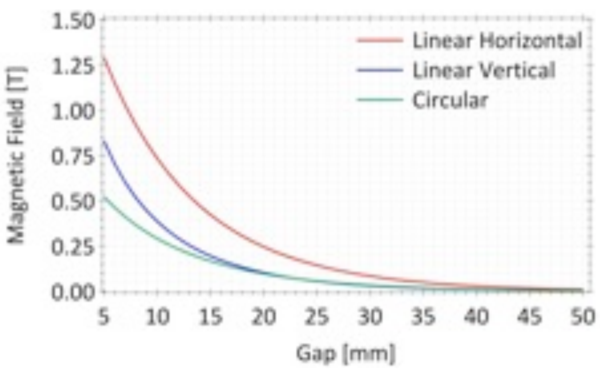

H. & V. field values versus gap at 0 mm shift.

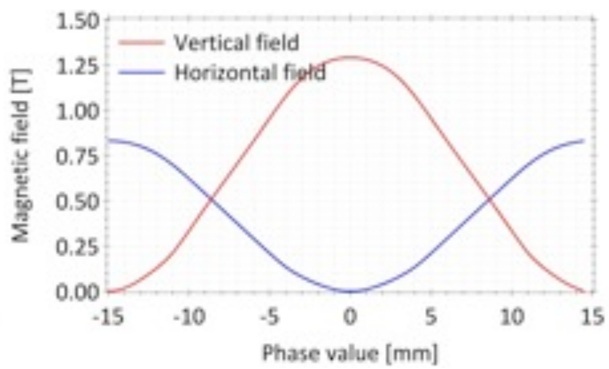

H. & V. field values versus shift at minimal gap

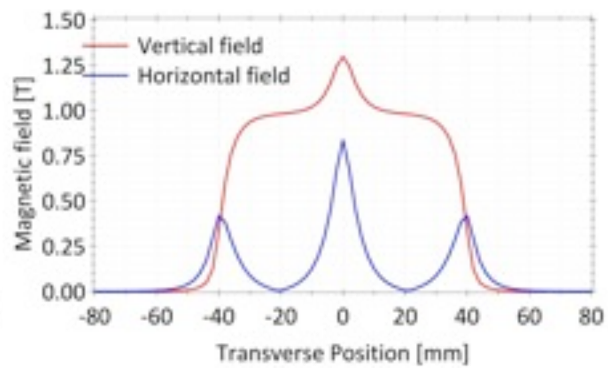

H. & V field roll-off at minimal gap,

[1] J. Bahrdt et al, Proceedings of the 2004 FEL Conference, Triestre, ITALY, p610 (2004)

Permanent magnets EPU : APPLE III

Apple III undulators
(SOLEIL model)

Modes	Bz [T]	Bx [T]
Linear H.	0,463	
Linear V.		0,23
Circular	0,16	

Undulator :

- Period : 30 mm
- Minimal gap : 15,5 mm

Magnets :

- NdFeB
- Size : 45 x 45 mm
- B_r : 1,26 T
- Θ_{mag} = 33 °
- X_{dist} = 1 mm

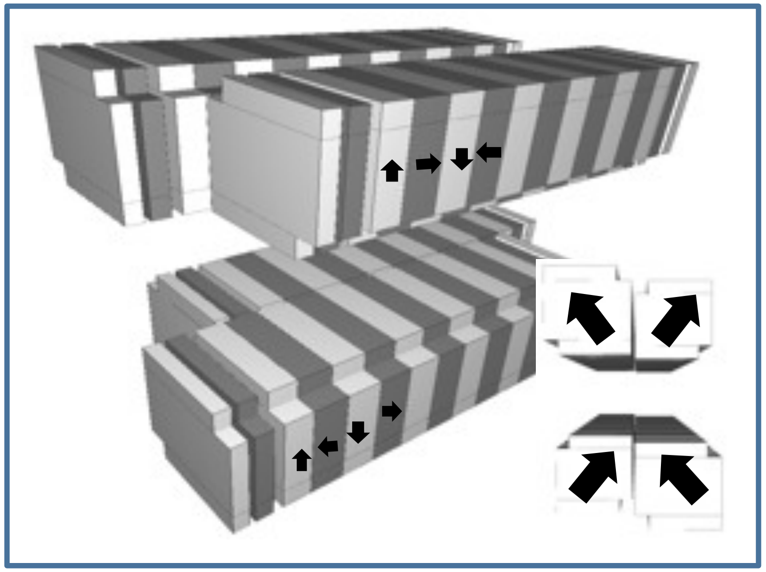

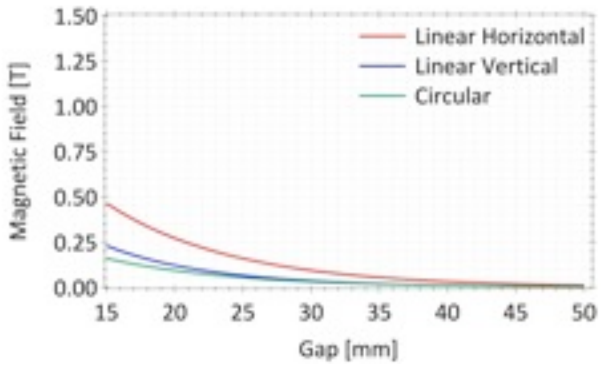

H. & V. field values versus gap at 0 mm shift.

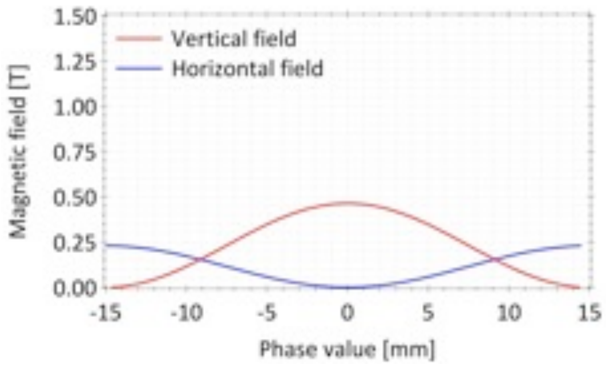

H. & V. field values versus shift at minimal gap

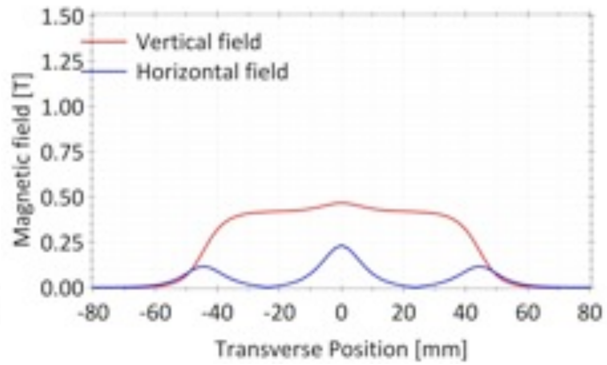

H. & V field roll-off at minimal gap,

J. Bahrdt et al, Proceedings of the 2004 FEL Conference, Triestre, ITALY, p610 (2004)

Permanent magnets EPU : DELTA

Delta undulators

Modes	Bz [T]	Bx [T]
Linear H.	1,04	
Linear V.		1,04
Circular	1,04	

Undulator :

- Period : 30 mm
- Minimal gap : 5 mm

Magnets :

- NdFeB
- Size : 25 x 9 x 9 mm
- B_r : 1,26 T
- $\Theta_{mag} = 0$ °
- $X_{dist} = 0,5$ mm

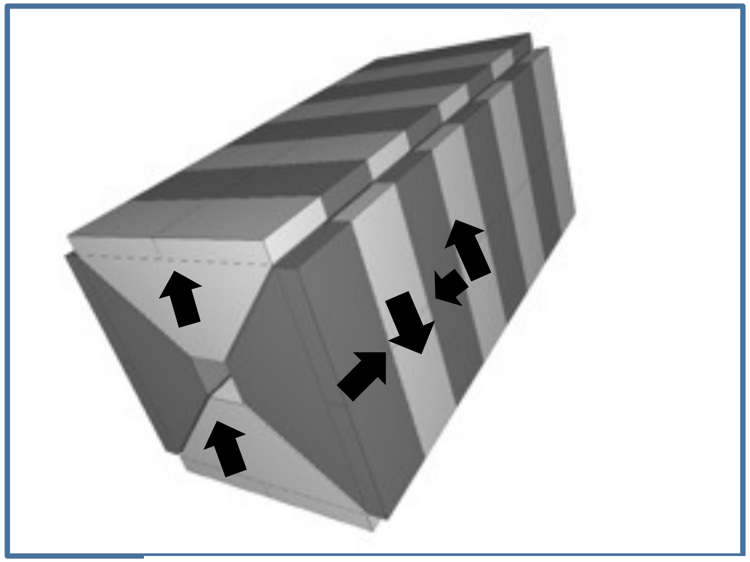

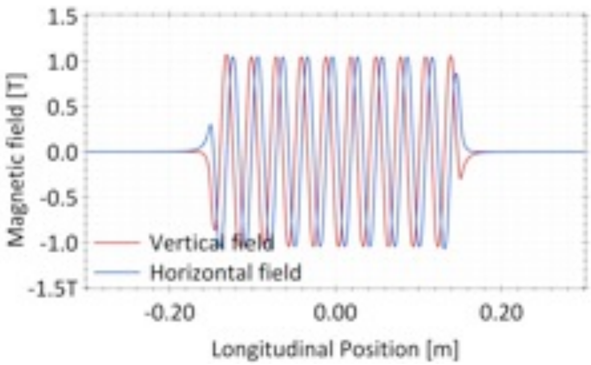

H. & V. fields at 0 mm shift.

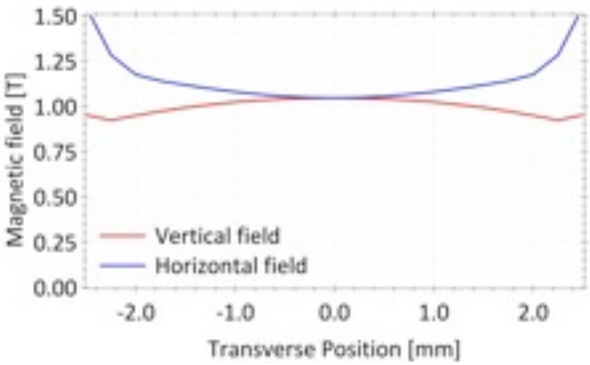

H. & V field roll-off at minimal gap,

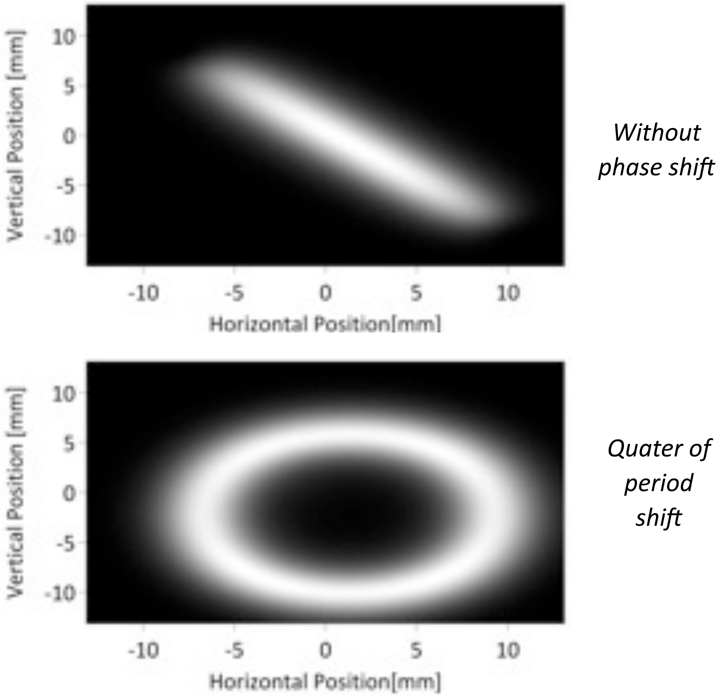

A. B. Temnykh, Phys. Res. Spec. Topics AB, 11,120702 (2008)

Permanent magnets EPU : DELTA

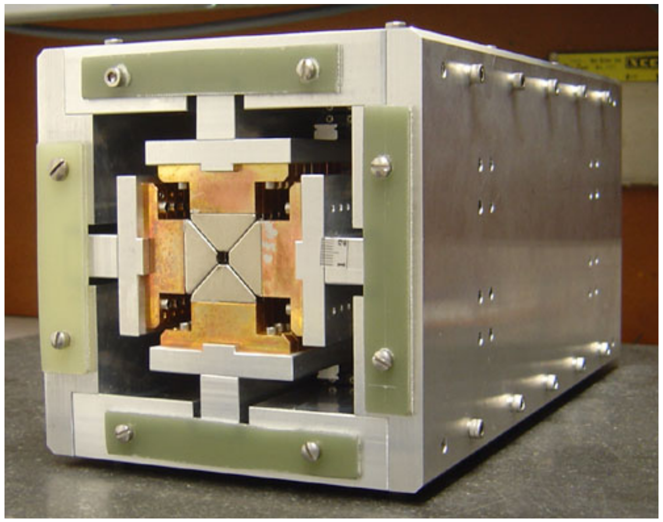

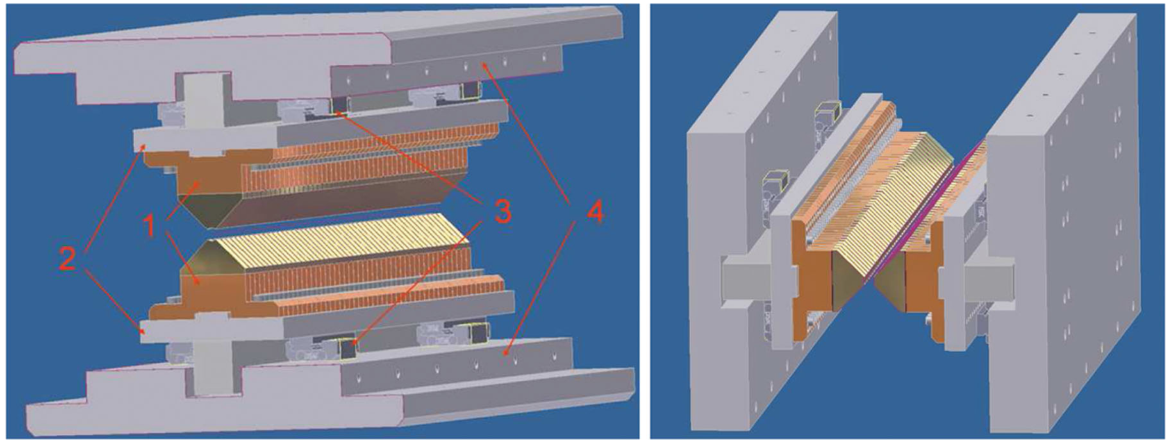

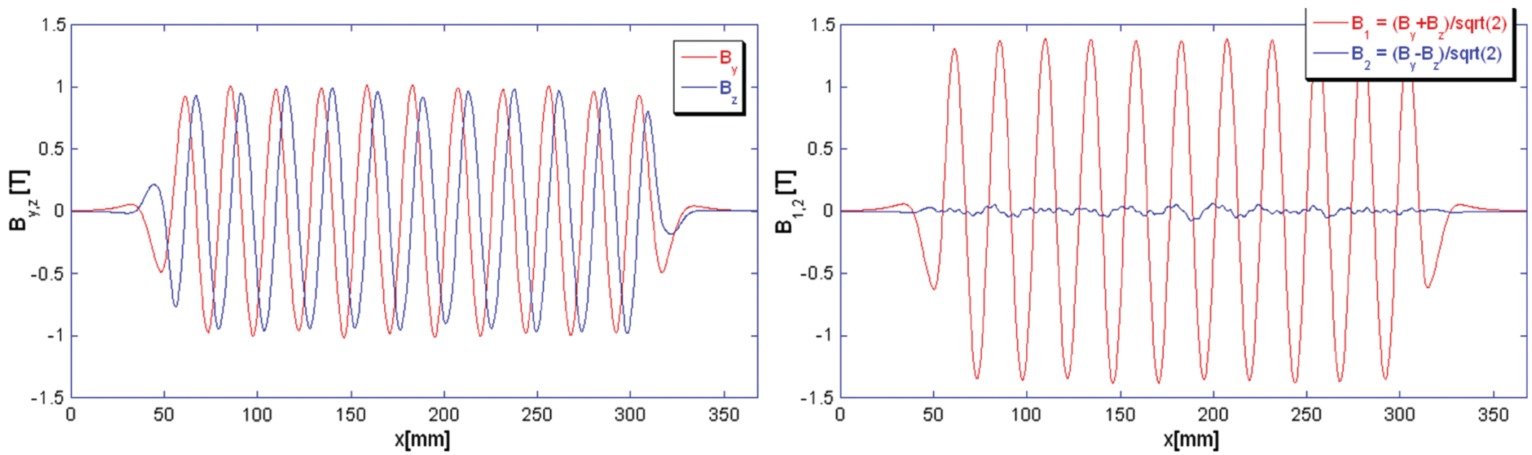

A. B. Temnykh, DELTA undulator for Cornell Energy Recovery Linac, Phys. Res. Spec. Topics AB, 11,120702 (2008)

Permanent magnets EPU: 6 arrays

Kitamura undulators

Modes	Bz [T]	Bx [T]
Linear H.	0,424	
Linear V.		0,06
Circular	-	

Undulator :

- Period : 30 & 60 mm
- Minimal gap : 15,5 mm

Magnets :

- NdFeB
- Size : 30 x 30 mm
  - 10 x 50 mm
- B_r : 1,26 T
- Θ_{mag} = 0 °
- X_{dist} = 1 mm

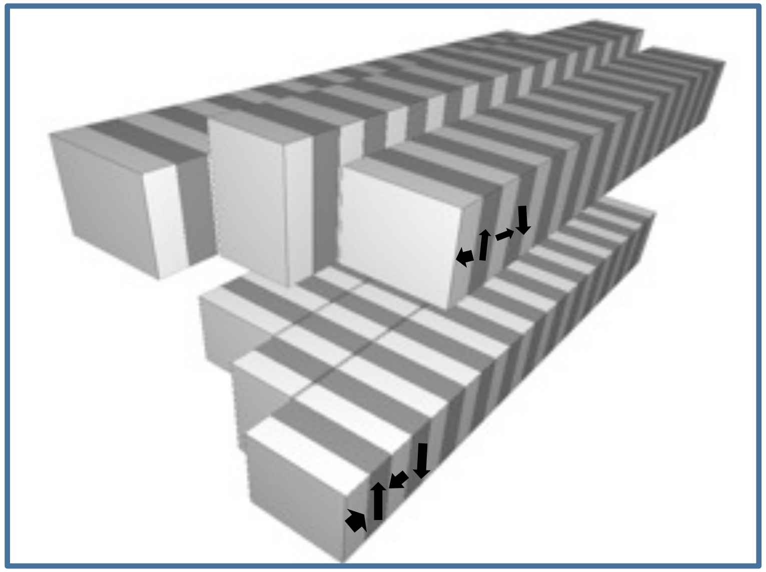

- Degree of circular polar. maintained while changing the photon energy

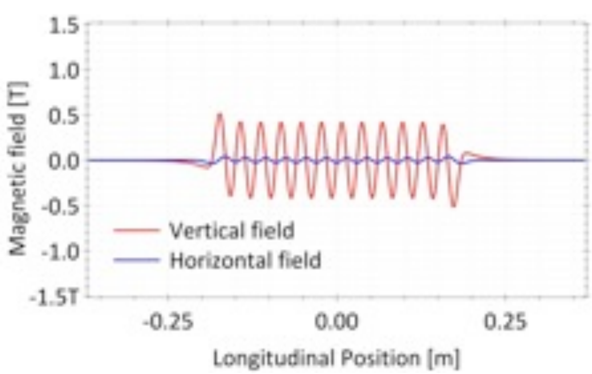

H. & V. field at minimal gap

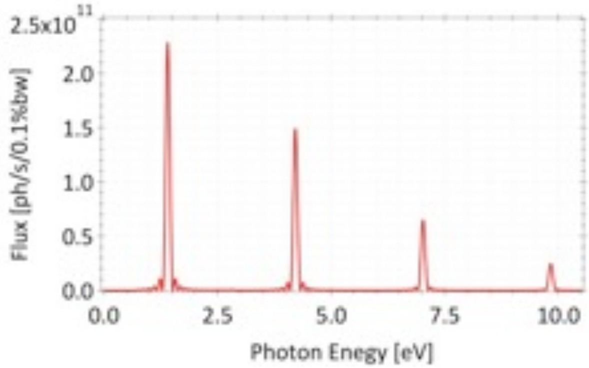

Flux density for a 400mA, 275 GeV beam without emittance an energy spread

H. Kitamura et al, J. Electron Spectr. Relate Phenom., 80 ,437, (1996)
A. Hiraya et al, J. Synchr. Rad., 5, 445, (1998)

3- EPU and fast polarisation switching

Permanent magnets EPU

Polarisation modes	LH	LV	C	Remarks
Apple I	0,45	0,21	0,135	
Apple II	0,42	0,24	0,14	
Apple III	0,46	0,23	0,16	
Delta (Apple IV?)	1,04	1,04	1,04	5mm round gap
Helios	0,173	0,125	0,1	
Diviacco-Walker	-	-	0,13	Circular only
Kitamura	0,424	0,06	-	Low field strength in circular
Onuki	0,4	0,4	0,28	

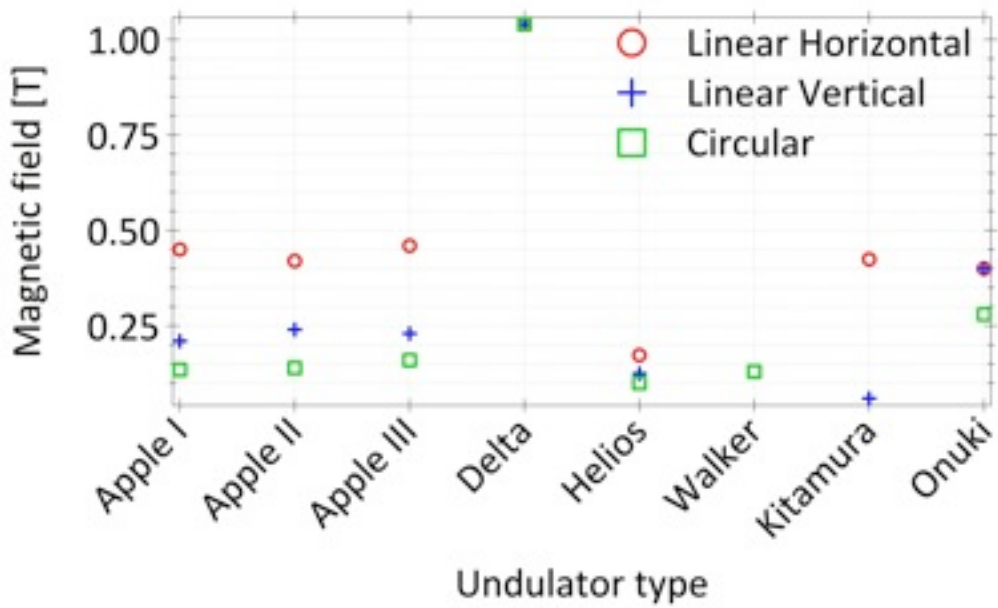

M. E. Couprie, ICFA Workshop on Future Light Source, Thomas Jefferson Nat. Acc. Facility. March. 5-9, 2012, Invited

Quasi periodic PM EPU: QP APPLE II

Apple II undulators

Modes	Bz [T]	Bx [T]
Linear H.	0,421	
Linear V.		0,247
Circular	0,145	

Undulator :
- Period : 30 mm
- Minimal gap : 15,5 mm

Magnets :
- NdFeB
- Size : 30 x 30 mm
- B_r : 1,26 T
- Θ_{mag} = 0 °
- X_{dist} = 1 mm

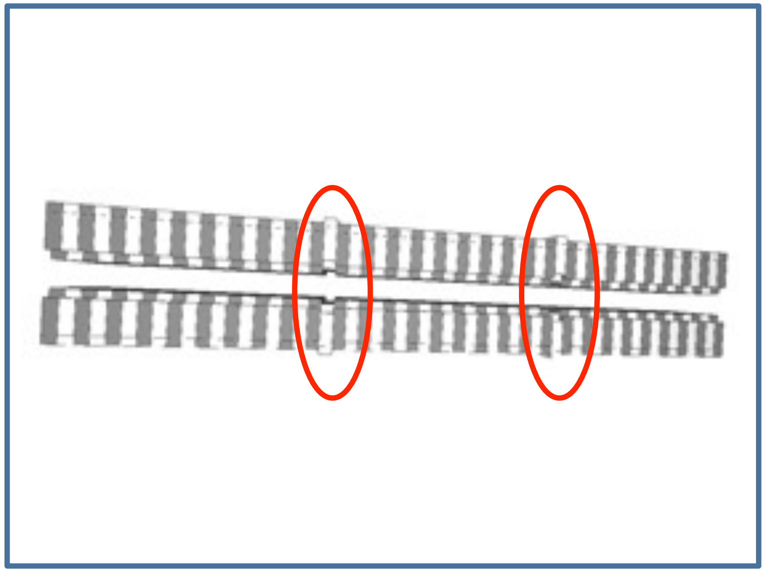

- Magnets creating aperiodicity are moved vertically

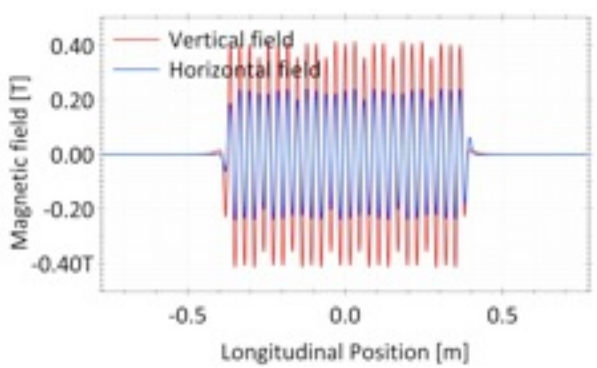

H. & V. field values in linear Horizontal (red line) and linear vertical (blue one)

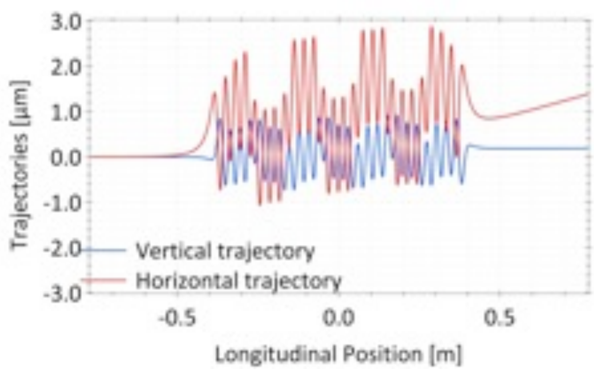

H. & V. trajectories in linear Horizontal (red line) and linear vertical (blue one)

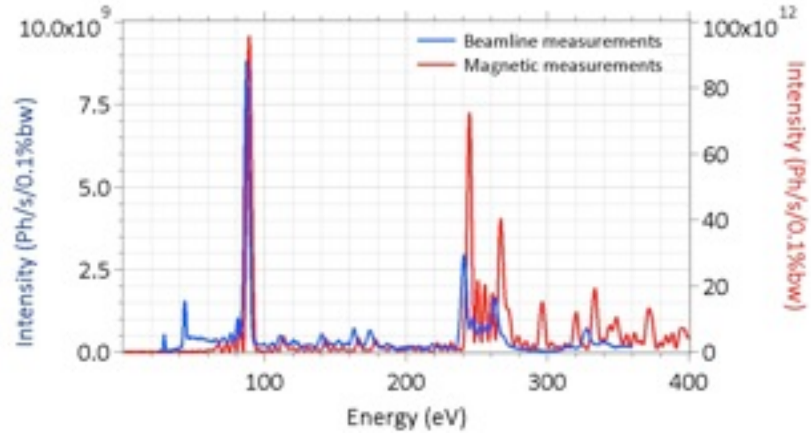

J. Chavanne et al, Proceedings of the European Particle Accelerator Conference, Sweden (1998)
B. Diviacco et al, Proceedings of the European Particle Accelerator Conference, Sweden (1998)

Quasi periodic PM EPU: Figure 8

T. Tanaka, H. Kitamura, Nuclear Instruments And Methods, A364, 368 (1995)

Figure8 undulators

Modes	Bz [T]	Bx [T]
Linear H.	0,42	
Linear V.		0,22
Circular		

Undulator :

- Period : 30 mm
- Minimal gap : 15,5 mm

Magnets :

- NdFeB
- Size : 30 x 30 mm
- B_r : 1,26 T
- Θ_{mag} = 0 °
- X_{dist} = 1 mm

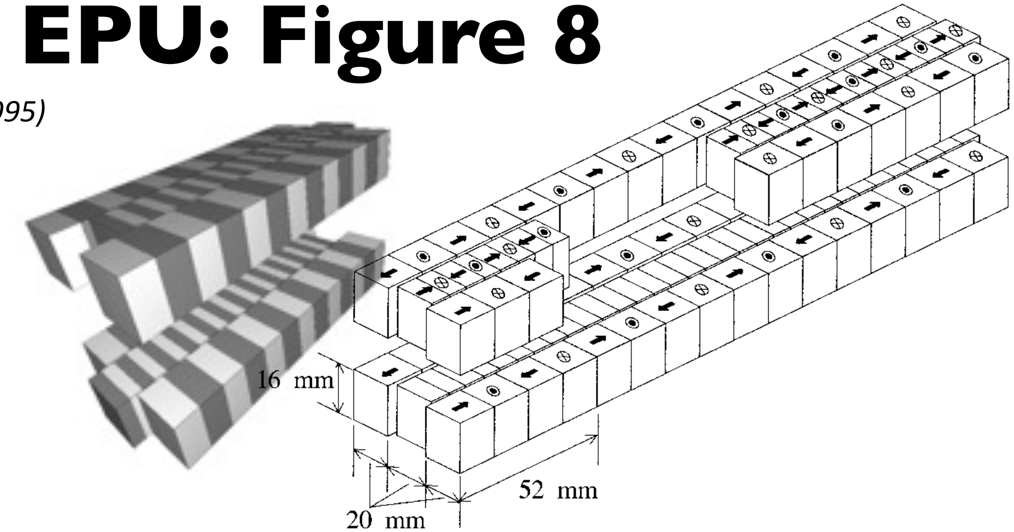

- odd (LH), integer (LH), and half integer harmonics (LV)

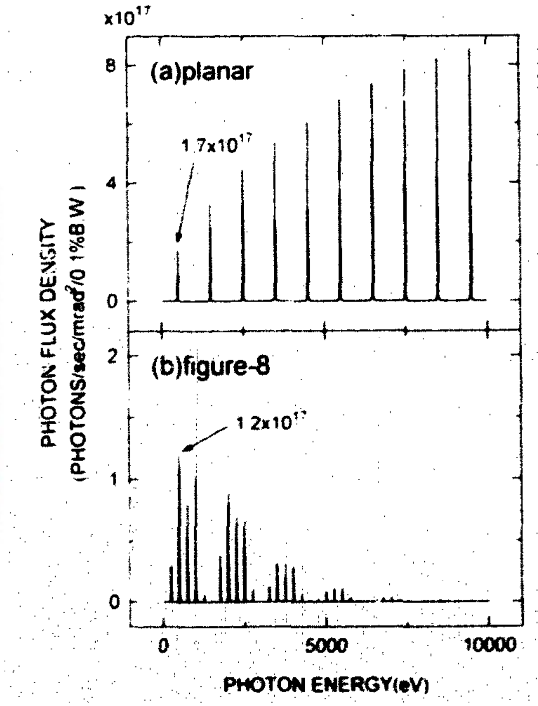

- Low on-axis power density in linear mode
- Combination of different period length

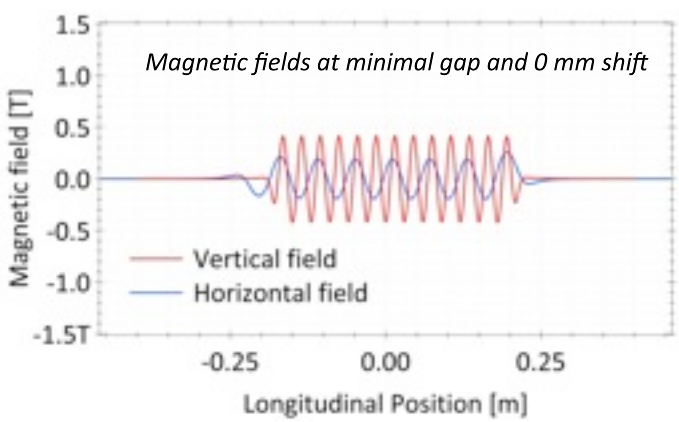

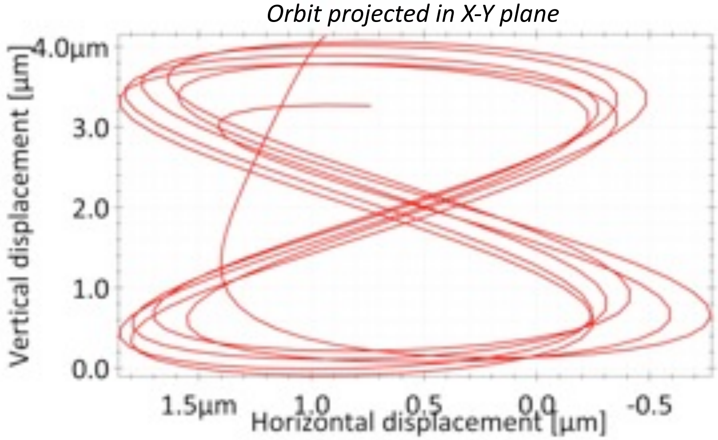

In vac helical

T. Tanaka, H. Kitamura, J. Synchrotron Radiation (1998), 5, 412-413
T. Hara et al. Nucl. Instrum. Methods A 467-468 (2001) 165-168

Permanent magnets EPU carriages

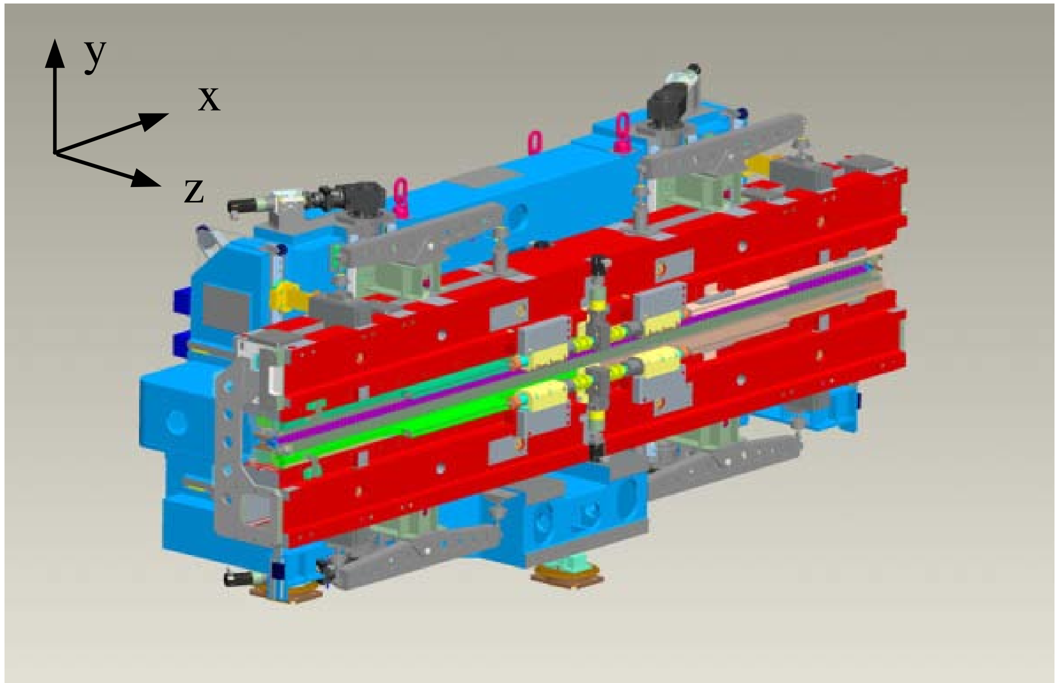

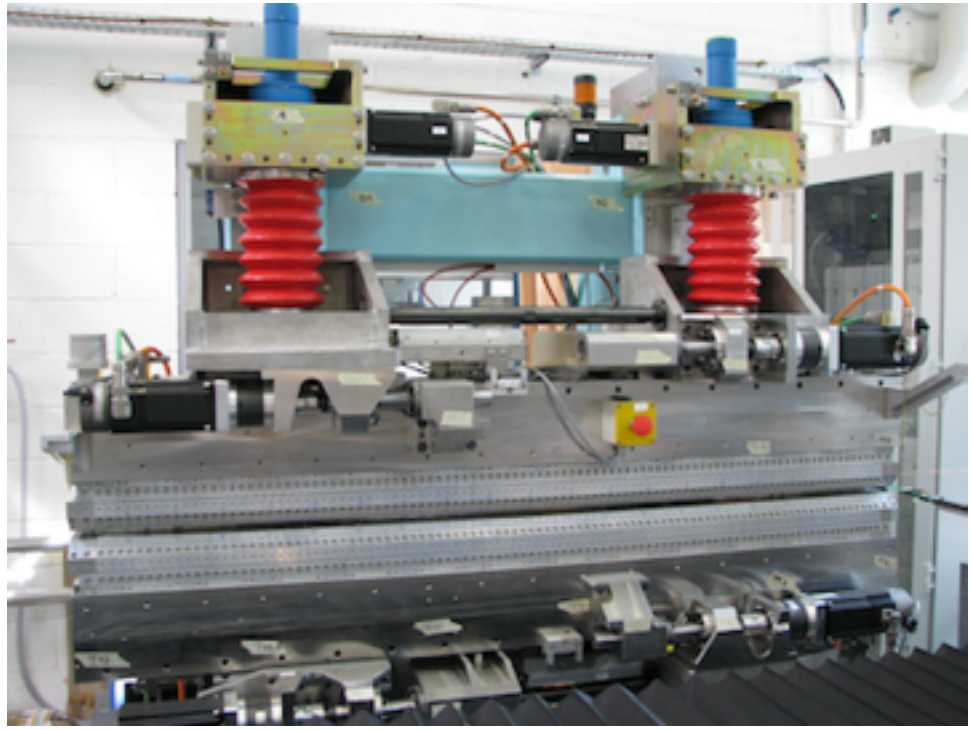

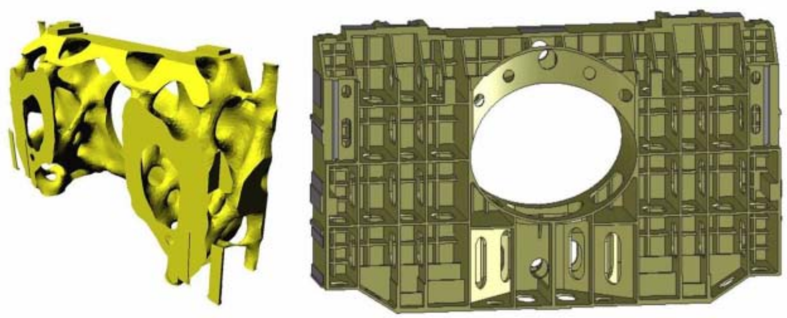

HU64 at SOLEIL : 4 arrays and gap movement

phase and gap variation
aperiodicity
taper
correction coils

J. Bahrdt et al., "APPLE Undulator for PETRA III", Proc. EPAC08, 2219 (2008)

In vacuum Fig8 type helical undulator

T. Tanaka, H. Kitamura, J. Synchrotron Radiation (1998), 5, 412-413
T. Hara et al. Nucl. Instrum. Methods A 467-468 (2001) 165-168

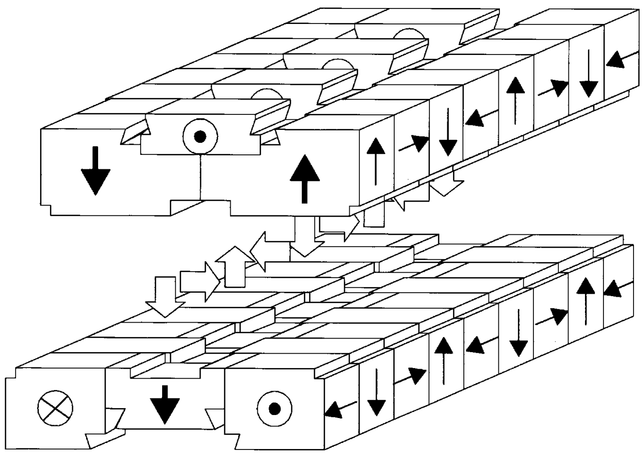

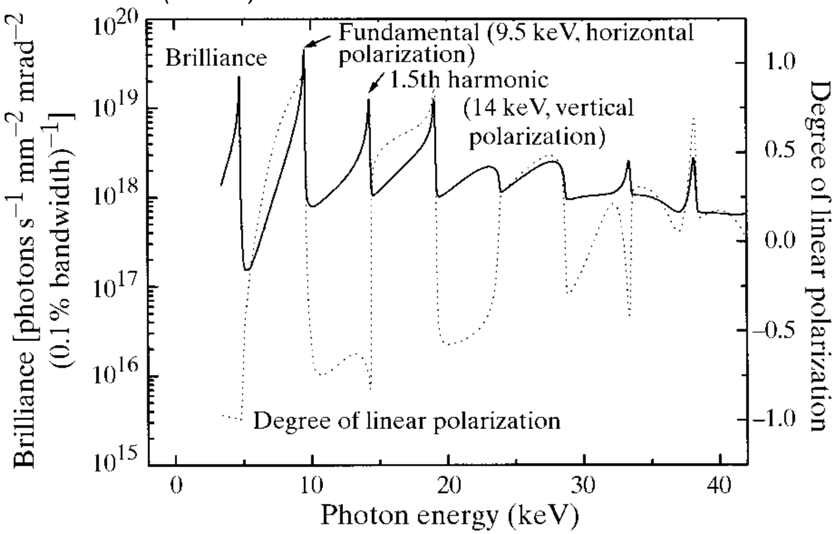

Central arrays : vertical field
side arrays : horizontal field

Gap : 11.6 mm (min . 8 mm)
Period : 26 mm
Length : 4.5 m
Bz=0.728 T @ 8 mm
Bx= 0.31 T @ 8 mm
22k W

TiN coating on the magnets
Cu Ni foil, baking 145 °C
no phasing mechanics

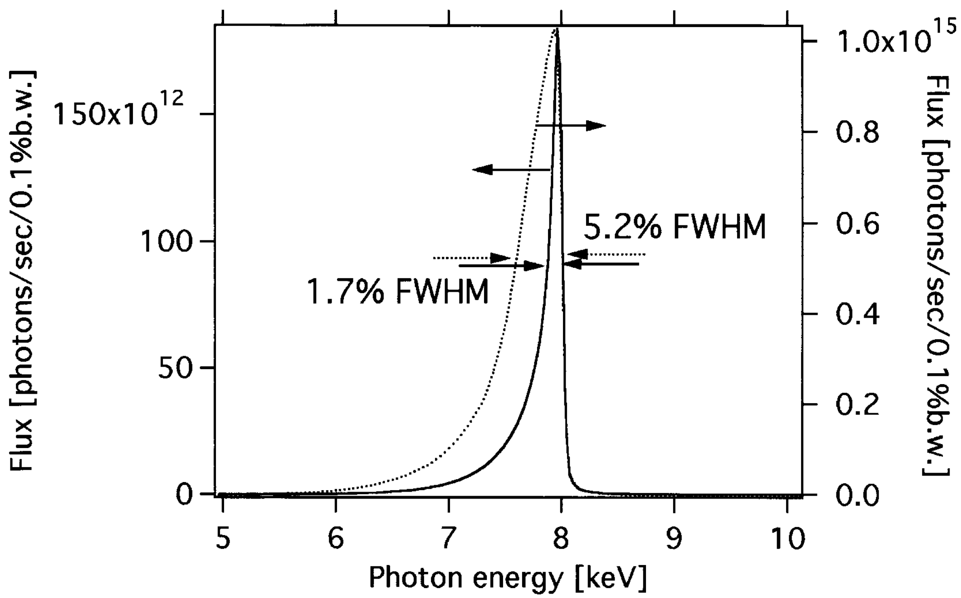

ElectroMagnetic Permanent magnet Helical Undulator

Vertical field : coil and laminated yoke, horizontal field : array of permanent magnets

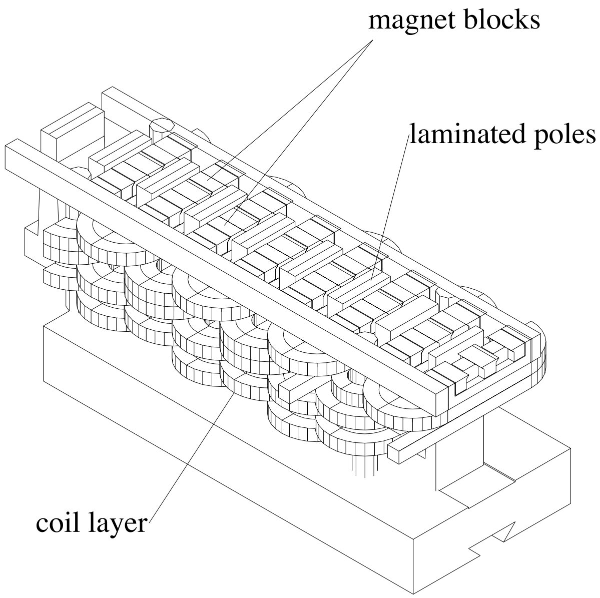

ESRF

19 x 80 mm, B=0.2T

flippling the current in the coil in 20 ms, ploarisaiton switching in 1 Hz

SmCo magnets

DSP card for real time synchronisation (eddy currents)

current flipping in 20 ms, gap 16 mm

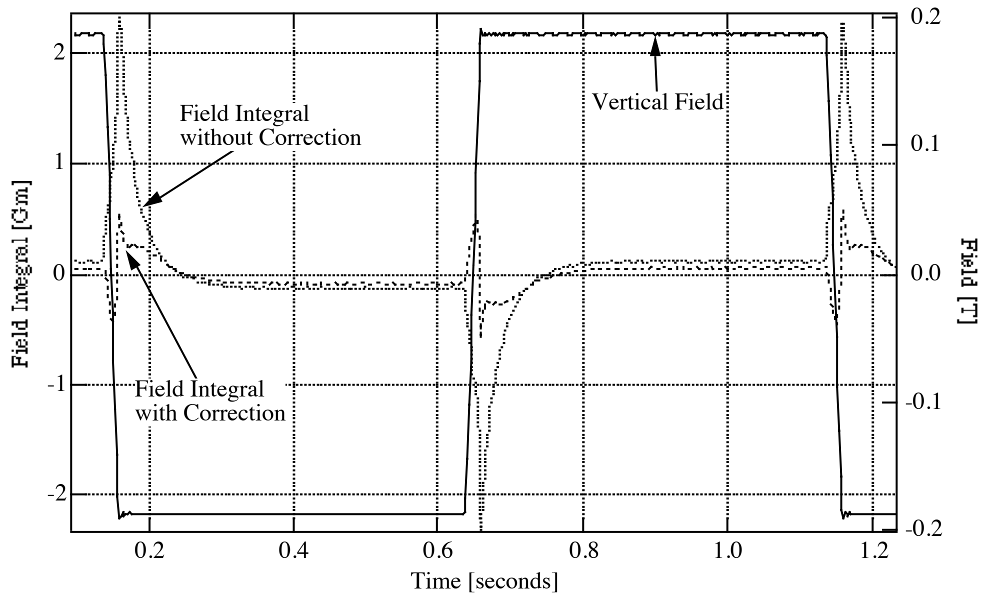

J. Chavanne, P. Elleaume, P. VanVaerenbergh, "A novel fast switching linear/helical undulator", Proceedings of EPAC 98, p. 317 (1998).

3- EPU and fast polarisation switching

EMPHU @ SOLEIL

Jefferson Lab
28 x 80 mm, B=0.134T

G. Biallas et al. an 8 cm period electromagnetic wiggler magnet with coils made from sheet copper“, Proceedings of PAC 2005, Knoxville, 4093 ; FEL04, 554-557

SOLEIL
26 x 64 mm, B=0.24T
flippling the current in 100 ms
NdFeB magnets
Coils: 25 layers of copper sheets stacked together 516 with current and 9 with cooling)
SPI controller for real time synchronisation (eddy currents)

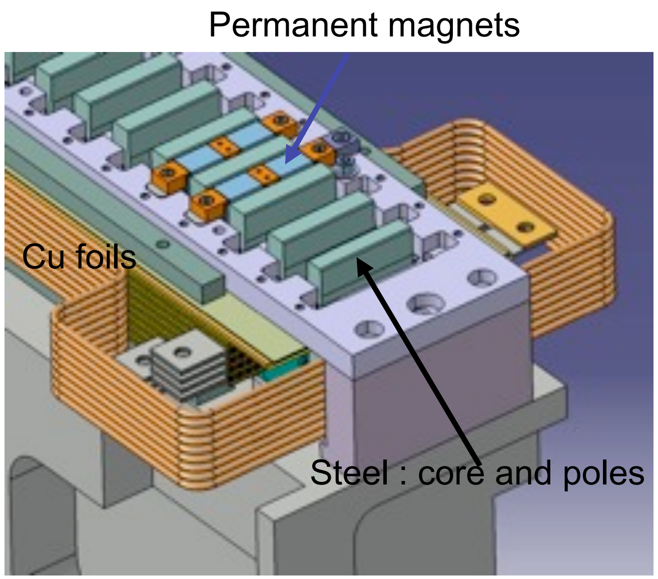

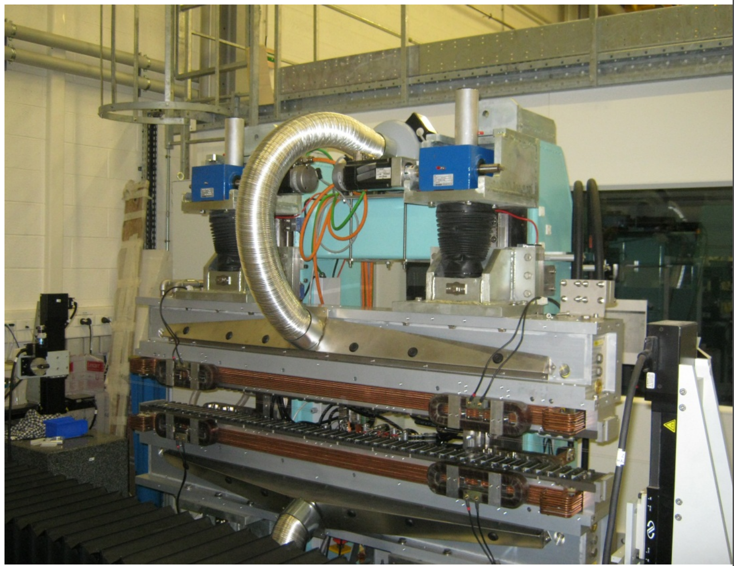

F. Marteau et al., Description of a EMPHU for fast polarisation switching , Proceedings MT, Marseille, Sept. 2011

3- Effect of the ID on the light source operation

Multipolar terms

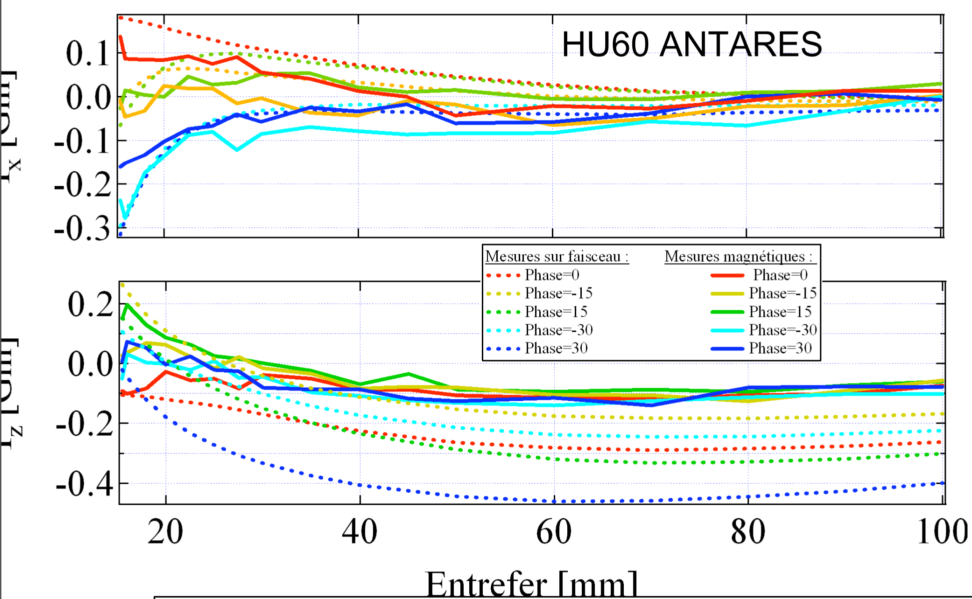

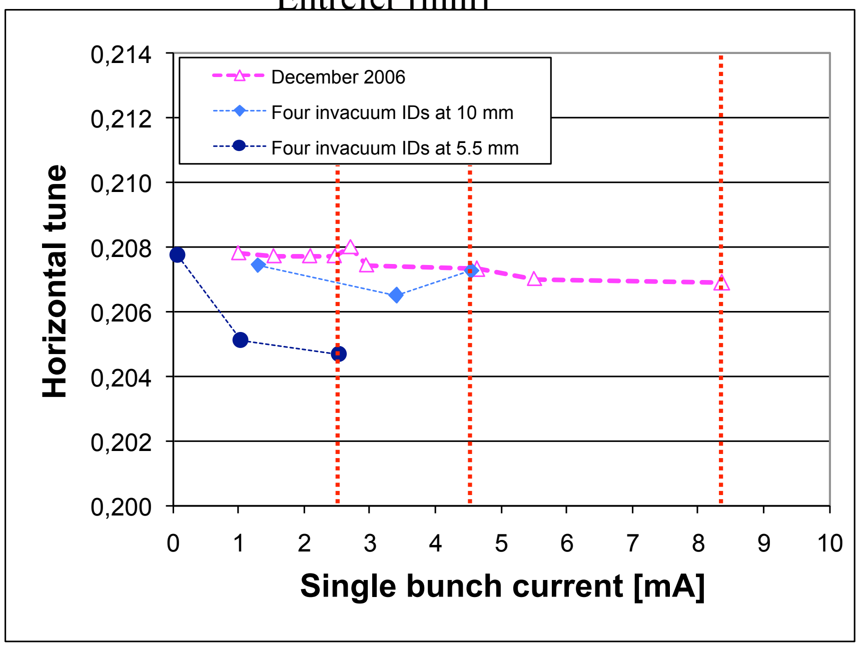

Dipolar terms: field integral

Comparison magnetic measurement/ electron beam

=> FFWD tables

+ Fast/slow orbit feedback to keep to source position and divergence in 10% of the electron beam size

Dynamic field integral compensation

J. Safranek et al, Phys. Rev. Special Topics (2002), Vol. 5, 010701, pp. 1-7

O. Marcoullé et al, IPAC 2011, 3236

Quadrupolar terms:

normal quadrupoles => tune shift => feedback on the tunes, or FFWD tables

Skew quadrupoles => coupling

Compensation : current sheet for APPLE-II devices

J. Bahrdt, et. al., "Active shimming of the dynamic multipoles of the BESSY UE112 Apple Undulator", Proceedings of EPAC'08, p. 2222 (2008).

Sextupolar terms=> chromaticity

General approach

Magnetic field maps (RADIA; measurements) introduced on TRACY electron beam simulation (on and off momentum) for injection efficiency and lifetime study

Modelisation with field maps

Simulation of the effect of the HU36 undulator located in a short straight section (betax=17.8 m)

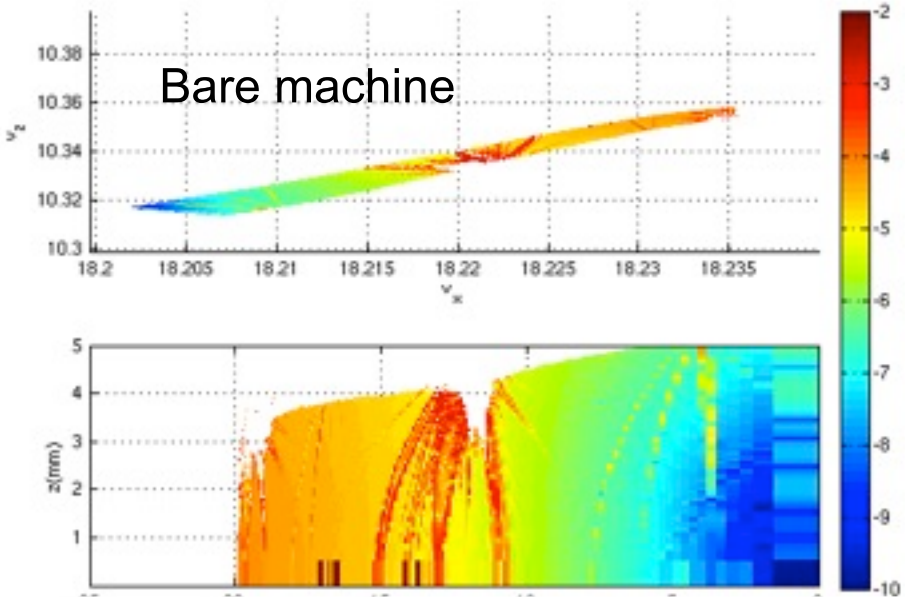

On-momentum dynamic aperture

11.5 mm minimum gap
Phase = 0

Injection rate :
bare machine, 88% => 80%
RP configuration 52% => 55%

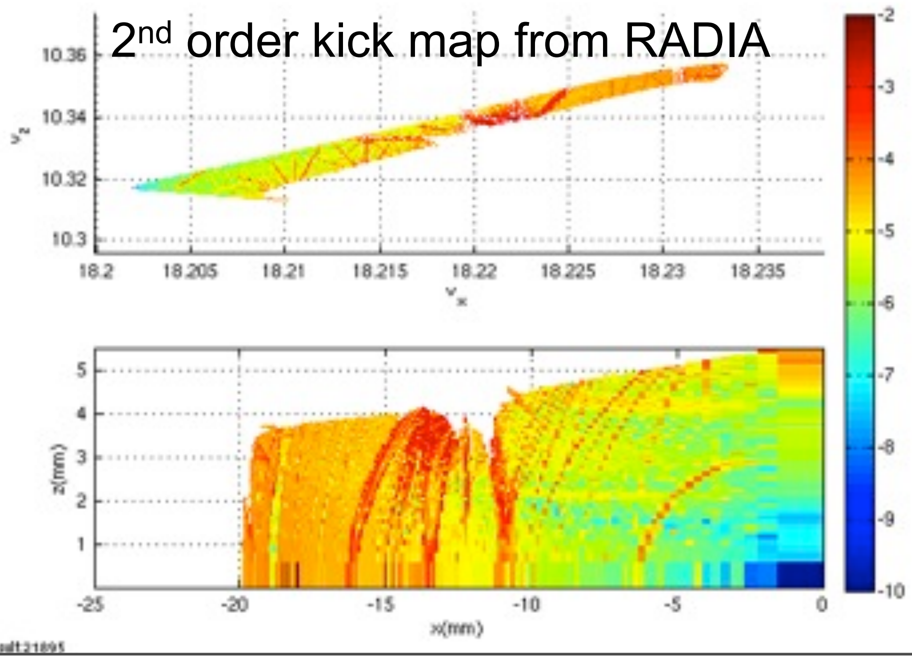

2nd order kick map from RADIA
+ magnetic measurement map

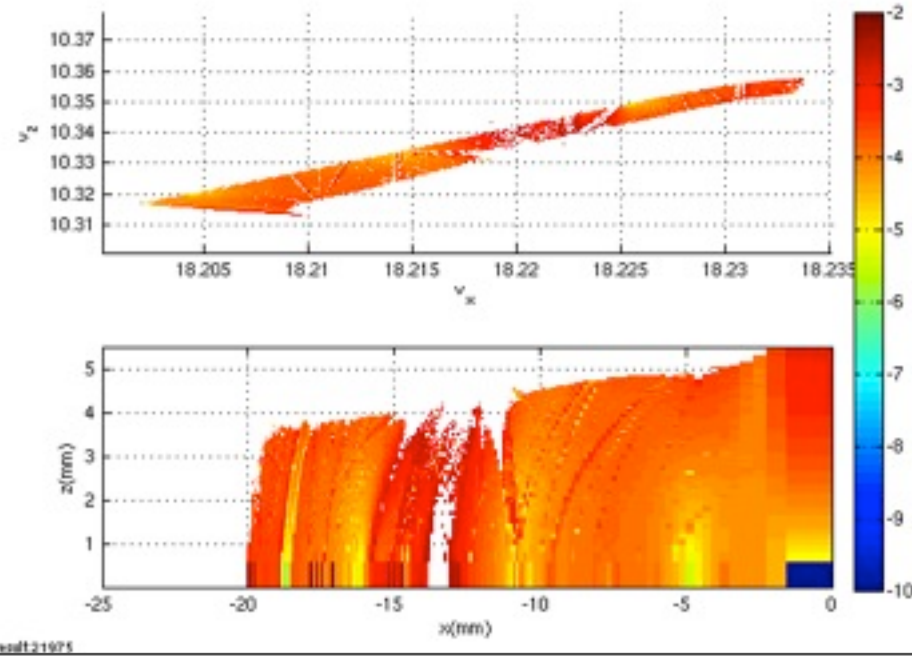

ur… , Invited

3- Effect of the ID on the light source operation

Modelisation with field maps

Simulation of the effect of the HU36 undulator located in a short straight section

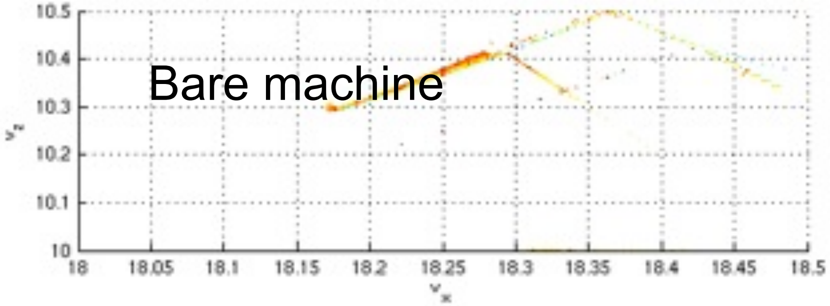

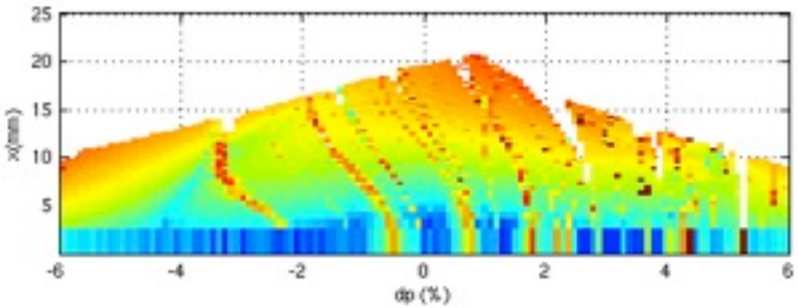

Off-momentum horizontal aperture

11.5 mm minimum gap
Phase = 0

Measured lifetime :
bare machine, 19.4 h@400 mA => 14.3 h
RP configuration 7.8 h => 6.6 h

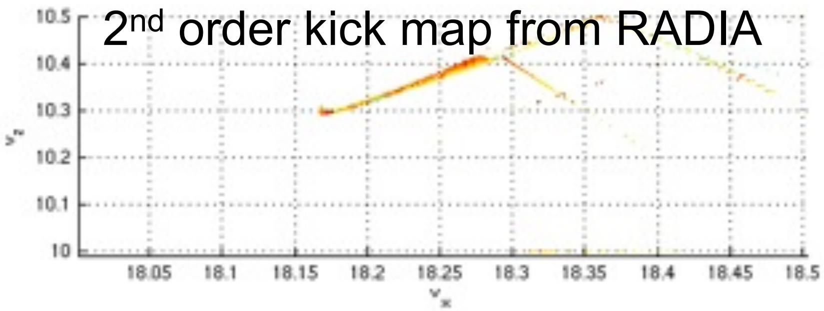

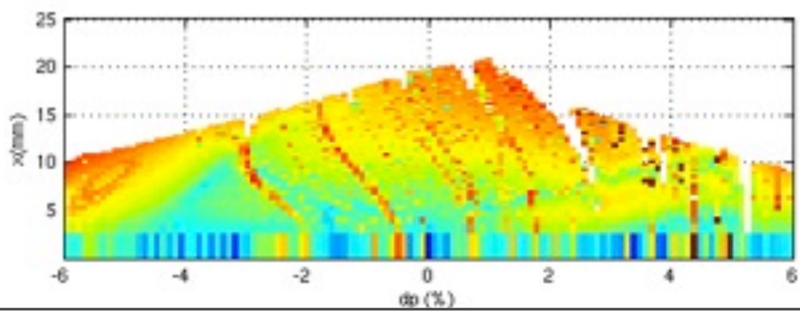

2nd order kick map from RADIA
+ magnetic measurement map

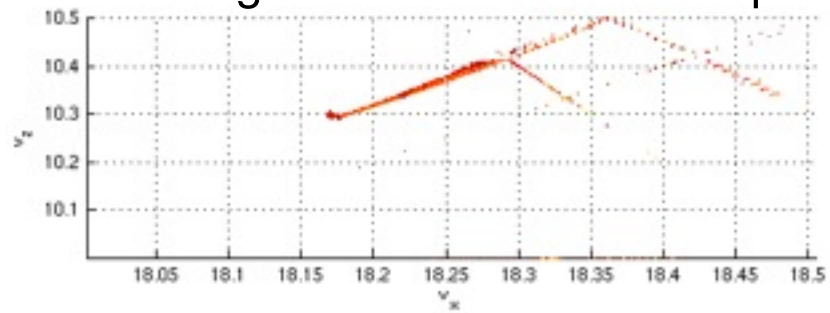

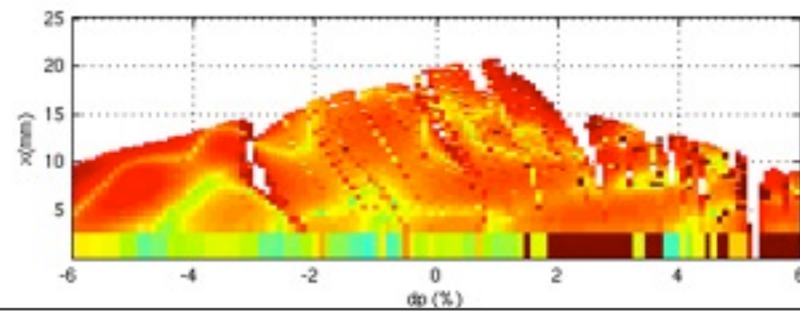

Desired ID effects: damping wiggler

More damping with additional synchrotron radiation through installation of strong wiggler magnets placed in a dispersion free location (for the equilibrium orbit to be independant of the particle energy) => emittance reduction

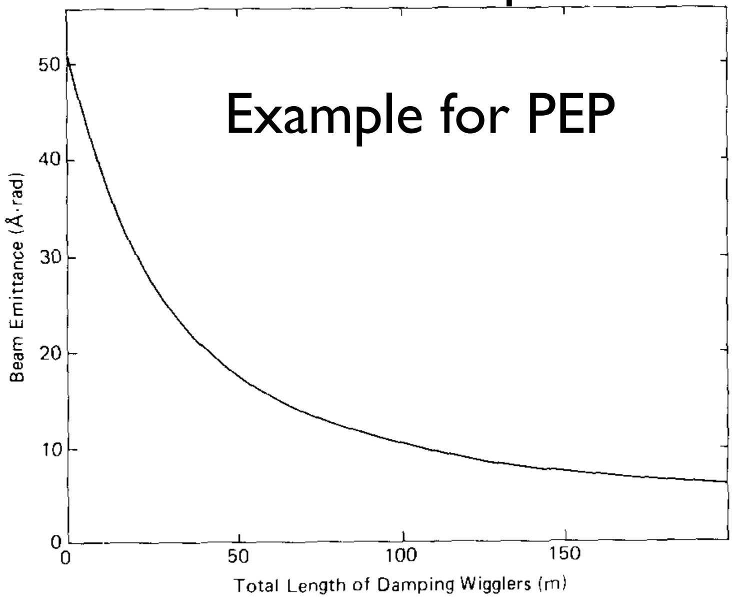

PETRAIII:Horizontal emittance : 1 nm.rad, Vertical emittance : 0.01 nmrad

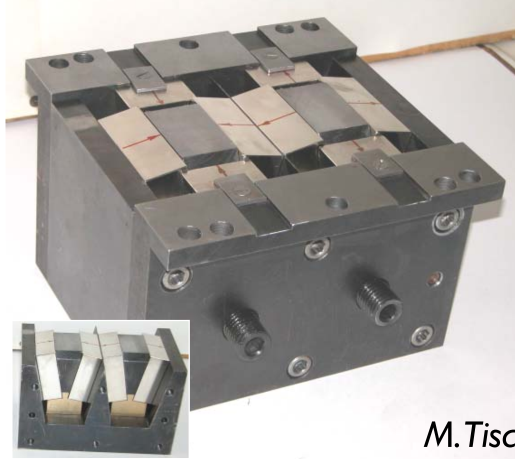

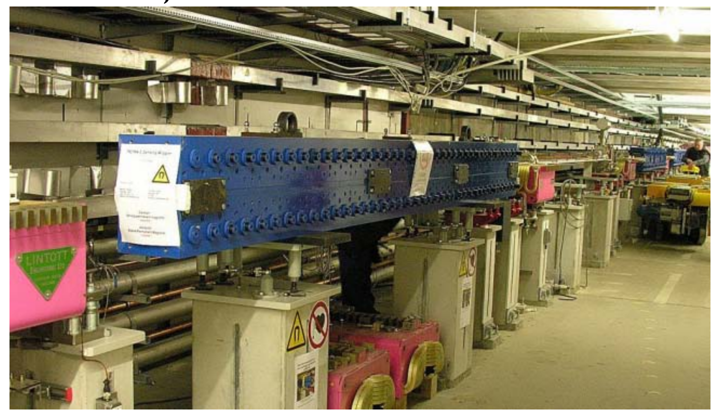

M.Tischer et al. Damping wigglers for the PETRA III light source, PAC 2005, Knoxville, 2446; EPAC08, 2317

H.Wiedemann, An ultra-low emittance mode for PEP using damping wigglers, Nucl. Instr. Meth. A266 (1988) 24-31.
T. Raubenheimer et al. SLAC PUB 4808, 1988

NSLSII (3 GeV):
Horizontal emittance : 0.55 nm.rad
Vertical emittance : 0.008 nmrad
2x3.4 mperiod 9 cm, gap 12.5 mm, K=15.2

MAX-IV (3 GeV):
Horizontal emittance : 0.24 nm.rad

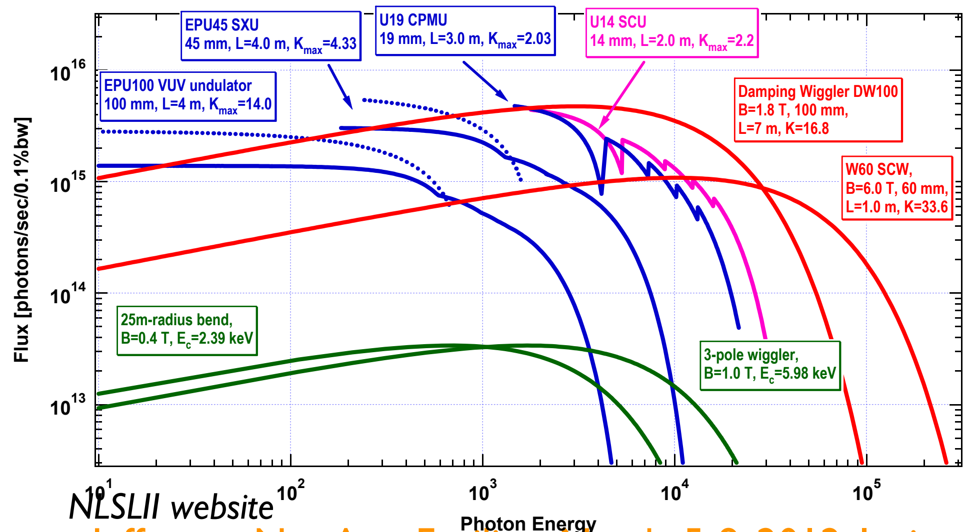

NLSLII website

Desired ID effects: Robinson wiggler

$$\varepsilon_x = \frac{C_q \gamma^2 \langle H \rangle_{dipole}}{J_x \rho_x}$$

D: partition number due to radiation damping

Generally, D ~ 0 and J_x ~ 1

Robinson theorem : $J_x + J_z + J_s = 4$

D=-1 => $\varepsilon_x/2$ and energy spread $x\sqrt{2}$

$B^*dB/dx \neq 0$ and $\eta_x \neq 0$

Short straight section : η_x **= 0.28 m**

Application to SOLEIL

horizontal emittance : 3.7 nmrad⇒1.85 nmrad

D=-1 =>

Type	B(T)	g (mm)	dB/dx (T/
out of vacuum	1.4	11	140
In vacuum	1.0	5.5	182

- Js=1 damping in longitudinal plane
- high gradients?
- field homogeneity (injection, lifetime)
- radiation properties

Desired ID effects: Robinson wiggler

$$\varepsilon_x = \frac{C_q \gamma^2 \langle H \rangle_{dipole}}{J_x \rho_x}$$

D: partition number due to radiation damping $J_x = 1 - D$

Generally, D ~ 0 and J_x ~ 1

Robinson theorem : $J_x + J_z + J_s = 4$

$$\varepsilon_x = \varepsilon_{x,0} \frac{1}{1-D} \qquad \left(\frac{\sigma_E}{E_0}\right)^2 = \frac{2}{2+D}\left(\frac{\sigma_{E,0}}{E_0}\right)^2$$

D=-1 => $\varepsilon_x/2$ and energy spread x$\sqrt{2}$

B*dB/dx ≠0 and η_x≠0

Short straight section : η_x **= 0.28 m**

Application to SOLEIL

horizontal emittance : 3.7 nmrad⇒1.85 nmrad

D=-1 =>

Type	B(T)	g (mm)	dB/dx (T/
out of vacuum	1.4	11	140
In vacuum	1.0	5.5	182

- Js=1 damping in longitudinal plane
- high gradients?
- field homogeneity (injection, lifetime)
- radiation properties

Desired ID effects: Robinson wiggler

$$\varepsilon_x = \frac{C_q \gamma^2 \langle H \rangle_{dipole}}{J_x \rho_x}$$

D: partition number due to radiation damping $J_x = 1 - D$

Generally, D ~ 0 and J_x ~ 1

Robinson theorem : $J_x + J_z + J_s = 4$

$$\varepsilon_x = \varepsilon_{x,0} \frac{1}{1-D} \qquad \left(\frac{\sigma_E}{E_0}\right)^2 = \frac{2}{2+D}\left(\frac{\sigma_{E,0}}{E_0}\right)^2$$

D=-1 => $\varepsilon_x/2$ and energy spread x$\sqrt{2}$

$$D = \frac{\oint \frac{\eta_x}{\rho_x^3} ds + \frac{2}{B^2 \rho_x^2} \oint \eta_x B \frac{dB}{dx} ds}{\oint \frac{ds}{\rho_x^2}}$$

B*dB/dx ≠0 and η_x≠0

Short straight section : η_x **= 0.28 m**

Application to SOLEIL

horizontal emittance : 3.7 nmrad⇒1.85 nmrad

D=-1 =>

Type	B(T)	g (mm)	dB/dx (T/
out of vacuum	1.4	11	140
In vacuum	1.0	5.5	182

- Js=1 damping in longitudinal plane
- high gradients?
- field homogeneity (injection, lifetime)
- radiation properties

Desired ID effects: Robinson wiggler

$$\varepsilon_x = \frac{C_q \gamma^2 \langle H \rangle_{dipole}}{J_x \rho_x}$$

D: partition number due to radiation damping $J_x = 1 - D$

Generally, D ~ 0 and J_x ~ 1

Robinson theorem : $J_x + J_z + J_s = 4$

$$\varepsilon_x = \varepsilon_{x,0} \frac{1}{1-D} \qquad \left(\frac{\sigma_E}{E_0}\right)^2 = \frac{2}{2+D}\left(\frac{\sigma_{E,0}}{E_0}\right)^2$$

D=-1 => $\varepsilon_x/2$ and energy spread x$\sqrt{2}$

$$D = \frac{\oint \frac{\eta_x}{\rho_x^3} ds + \boxed{\frac{2}{B^2 \rho_x^2} \oint \eta_x B \frac{dB}{dx} ds}}{\oint \frac{ds}{\rho_x^2}}$$

B*dB/dx ≠0 and η_x≠0

Short straight section : η_x **= 0.28 m**

Application to SOLEIL

horizontal emittance : 3.7 nmrad⇒1.85 nmrad

D=-1 =>

Type	B(T)	g (mm)	dB/dx (T/
out of vacuum	1.4	11	140
In vacuum	1.0	5.5	182

- Js=1 damping in longitudinal plane
- high gradients?
- field homogeneity (injection, lifetime)
- radiation properties

Desired ID effects: Robinson wiggler

$$\varepsilon_x = \frac{C_q \gamma^2 \langle H \rangle_{dipole}}{J_x \rho_x}$$

D: partition number due to radiation damping $J_x = 1 - D$

Generally, D ~ 0 and J_x ~ 1

Robinson theorem : $J_x + J_z + J_s = 4$

$$\varepsilon_x = \varepsilon_{x,0} \frac{1}{1-D} \qquad \left(\frac{\sigma_E}{E_0}\right)^2 = \frac{2}{2+D}\left(\frac{\sigma_{E,0}}{E_0}\right)^2$$

D=-1 => $\varepsilon_x/2$ and energy spread x$\sqrt{2}$

$$D = \frac{\oint \frac{\eta_x}{\rho_x^3} ds + \boxed{\frac{2}{B^2 \rho_x^2} \oint \eta_x B \frac{dB}{dx} ds}}{\oint \frac{ds}{\rho_x^2}}$$

η_x= dispersion function

ρ_x = radius of curvature due to B

B*dB/dx ≠0 and η_x≠0

Short straight section : η_x **= 0.28 m**

Application to SOLEIL

horizontal emittance : 3.7 nmrad⇒1.85 nmrad

D=-1 =>

Type	B(T)	g (mm)	dB/dx (T/
out of vacuum	1.4	11	140
In vacuum	1.0	5.5	182

- Js=1 damping in longitudinal plane
- high gradients?
- field homogeneity (injection, lifetime)
- radiation properties

Desired ID effects: Robinson wiggler

$$\varepsilon_x = \frac{C_q \gamma^2 \langle H \rangle_{dipole}}{J_x \rho_x}$$

D: partition number due to radiation damping $J_x = 1 - D$

Generally, D ~ 0 and J_x ~ 1

Robinson theorem : $J_x + J_z + J_s = 4$

$$\varepsilon_x = \varepsilon_{x,0} \frac{1}{1-D} \qquad \left(\frac{\sigma_E}{E_0}\right)^2 = \frac{2}{2+D}\left(\frac{\sigma_{E,0}}{E_0}\right)^2$$

D=-1 => $\varepsilon_x/2$ and energy spread x$\sqrt{2}$

$$D = \frac{\oint \frac{\eta_x}{\rho_x^3} ds + \boxed{\frac{2}{B^2 \rho_x^2} \oint \eta_x B \frac{dB}{dx} ds}}{\oint \frac{ds}{\rho_x^2}}$$

η_x= dispersion function

ρ_x = radius of curvature due to B

B*dB/dx ≠0 and η_x≠0

Short straight section : η_x **= 0.28 m**

Application to SOLEIL

horizontal emittance : 3.7 nmrad⇒1.85 nmrad

D=-1 => $\boxed{\frac{\hat{B}_{w,z}^2}{2g} \approx 89\ \mathrm{T^2/m}}$

Type	B(T)	g (mm)	dB/dx (T/
out of vacuum	1.4	11	140
In vacuum	1.0	5.5	182

- Js=1 damping in longitudinal plane
- high gradients?
- field homogeneity (injection, lifetime)
- radiation properties

Desired ID effects: Robinson wiggler

Test in DCI

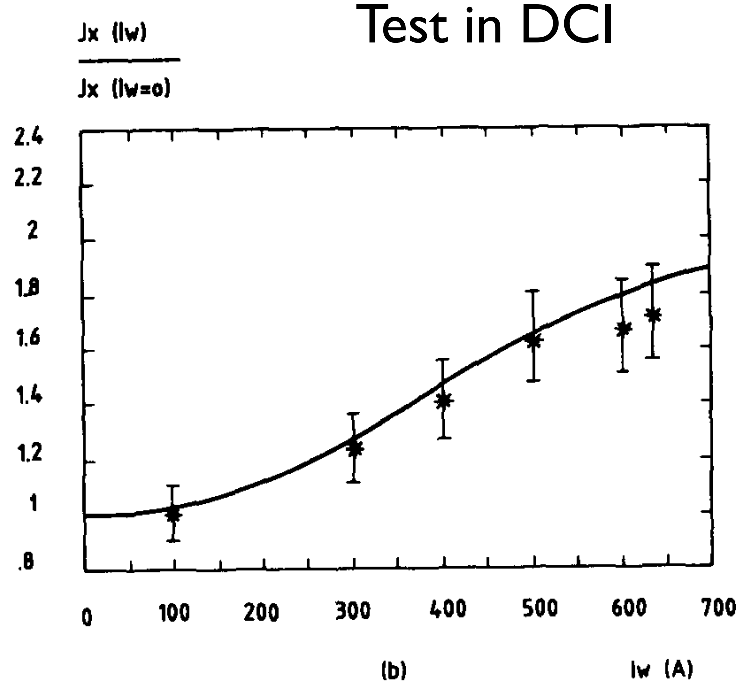

CERN PS (1983)

damping of horizontal betatron oscillations

J_x=3 et D = -2

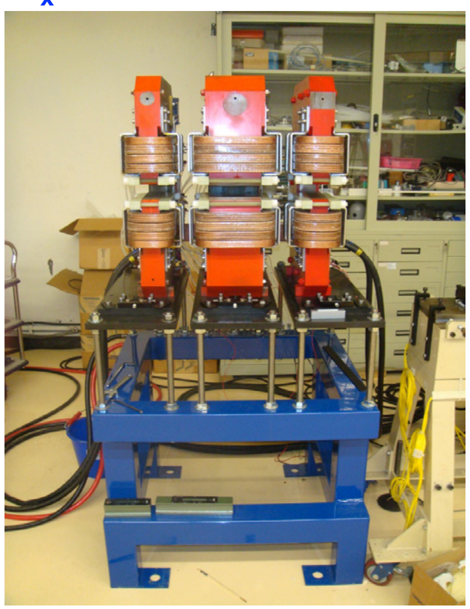

Y. Baconnier et al, Emittance control of the PSe± beamas using A Robinson wiggler, Nucl. Instr. Meth. A 234 (1985) 244-252 Nucl. Instr. Meth. A266 (1988) 24-31.

Lee SY Kolski J Review of Scientific Instruments 78, 075107 (2007)
Z.W Huang et al. IPAC 2010, 3186, PAC 2011, 1265

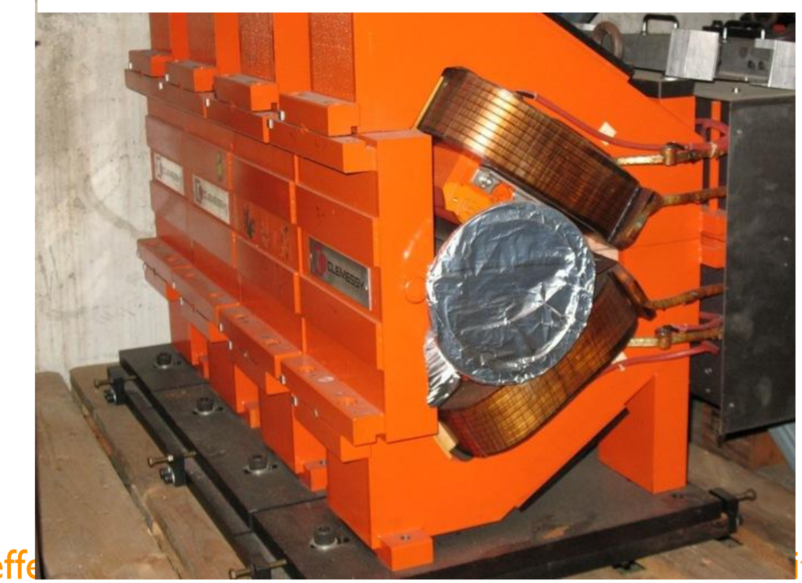

Desired ID effects: Robinson wiggler

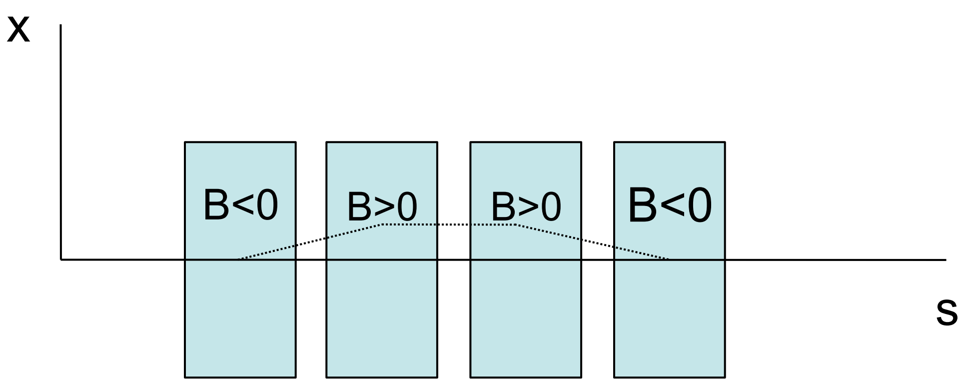

CERN PS (1983)

damping of horizontal betatron oscillations

J_x=3 et D = -2

Test in DCI

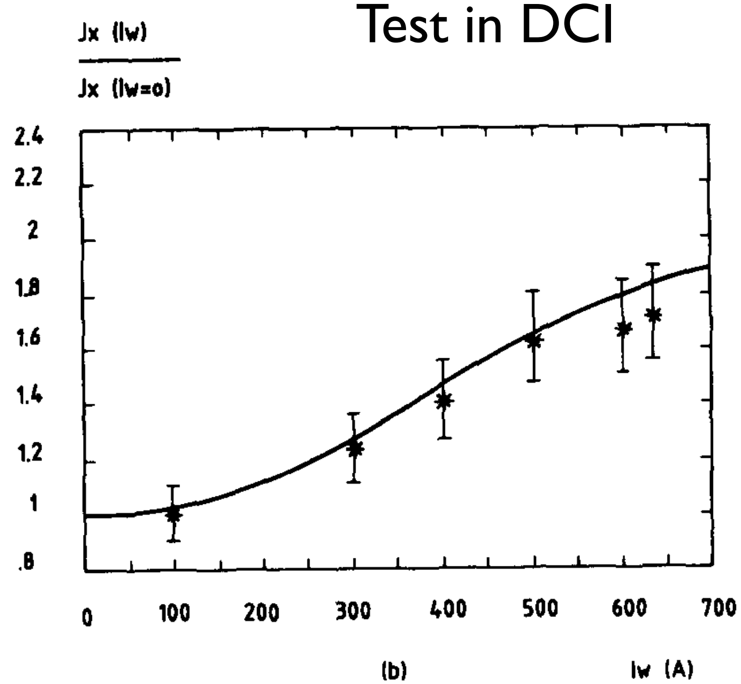

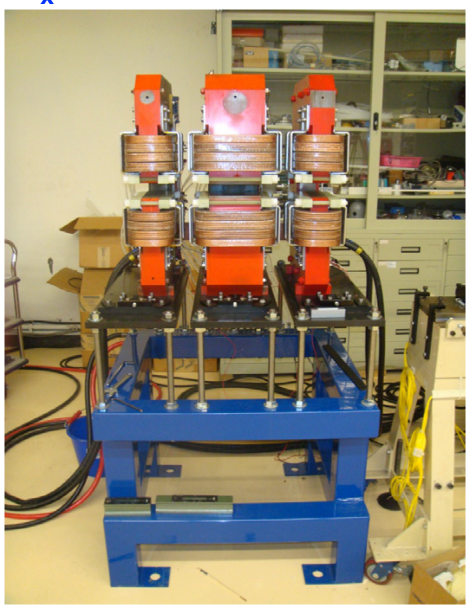

Y. Baconnier et al, Emittance control of the PSe± beamas using A Robinson wiggler, Nucl. Instr. Meth. A 234 (1985) 244-252 Nucl. Instr. Meth. A266 (1988) 24-31.

Lee SY Kolski J Review of Scientific Instruments 78, 075107 (2007)
Z.W Huang et al. IPAC 2010, 3186, PAC 2011, 1265

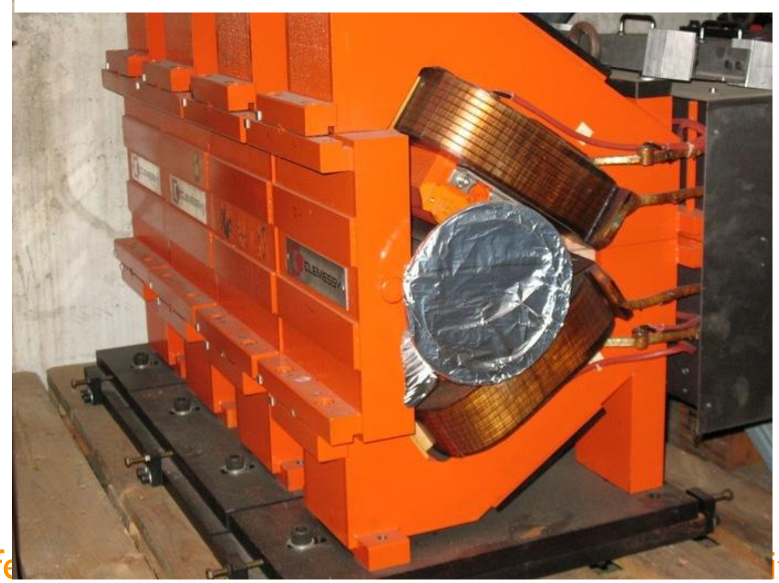

Conclusion

Interesting prospects with the advanced permanent magnet based insertion devices
New technological develpments towards short period high fields

Superconducting undulators and wiggler are also quickly developing :
Thermal budget (resistance wall and synchrotron radiation) =>with (larger gap) /without thermal shield
procedure of magnetic field correction

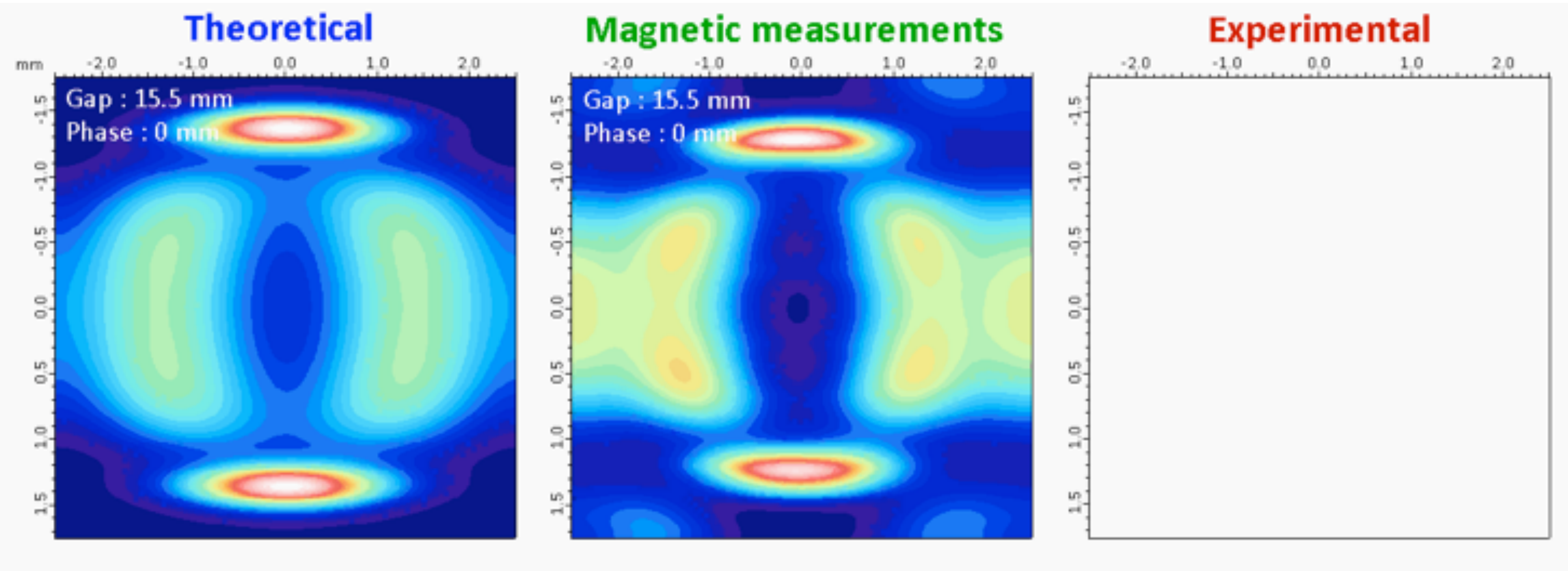

$$\phi(z) = \frac{2\pi}{\lambda}\left[\frac{z}{2\gamma^2} + \int_{-L/2}^{z} \frac{\beta_x^2(z') + \beta_y^2(z')}{2}\,\mathrm{d}z'\right]$$

In vac NSLS P. Stefan et al. J. Synchrotron Rad. (1998)

H. Hsieh et al. NIM A246, 1983, 79

Quasi periodic PM EPU: PERA undulators

PERA undulators

Modes	Bz [T]	Bx [T]
Linear H.	0,2	
Linear V.		0,26
Circular	-	

- No phase motion
- Linear polarization only
- Combination of different period length

Undulator :

- Period : 30 mm
- Minimal gap : 15,5 mm

Magnets :

- NdFeB
- Size : 30 x 30 mm
- B_r : 1,26 T
- $\Theta_{mag} = 0\ °$
- X_{dist} = 1 mm

S. Sasaki, B. Diaviacco and R. P. Walker, Synchrotrone Triestre Internal Report, ST/MTN-98/8
S. Sasaki, B. Diaviacco and R. P. Walker, Proceedings of EPAC 2008

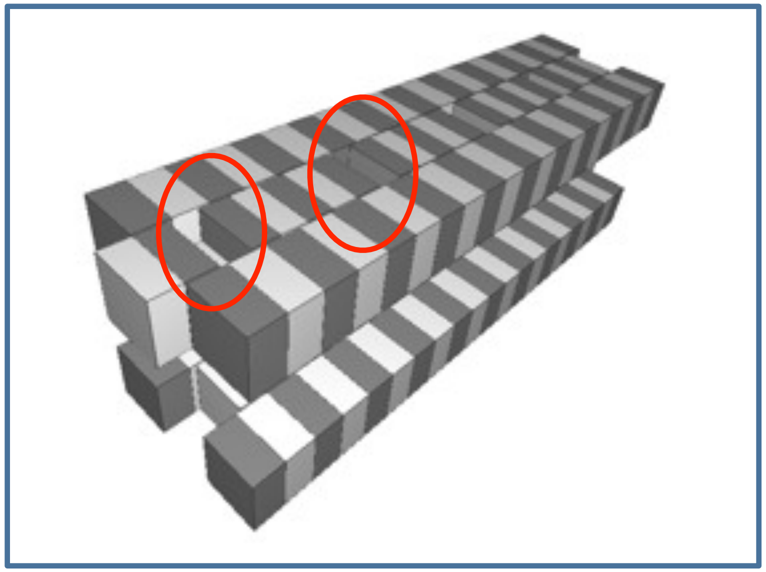

- Magnets creating aperiodicity have reduced height and opposite direction of magnetisation.

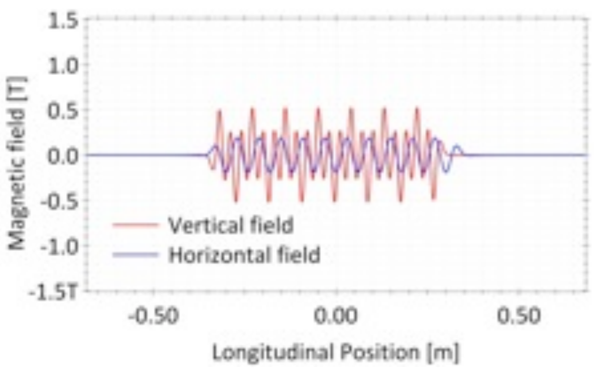

H. & V. field values in linear mode

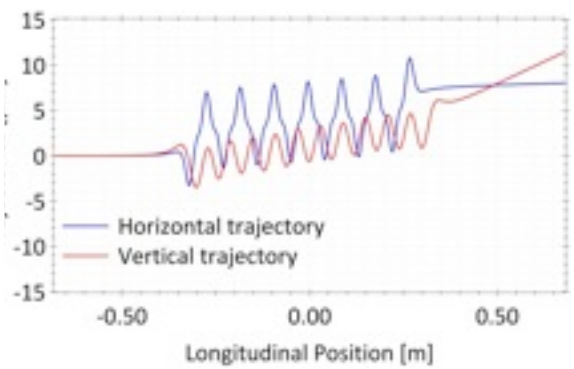

H. & V. trajectories in linear Horizontal (red line) and linear vertical (blue one)

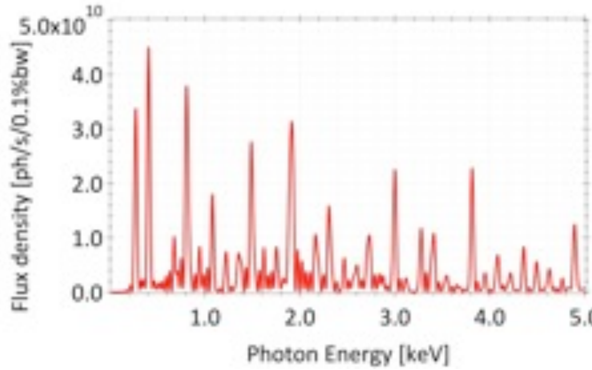

Spectrum calculated for 400 mA, 2,75 GeV and zero emittance and energy spread,

Quasi periodic PM EPU: APPLE VIII

Apple VIII undulators

Modes	Bz [T]	Bx [T]
Linear H.	0,42	
Linear V.		0,24
Circular	0,21	

Undulator :

- Period : 30 & 60 mm
- Minimal gap : 15,5 mm

Magnets :

- NdFeB
- Size : 30 x 30 mm
  - 50 x 50 mm
- B_r : 1,26 T
- Θ_{mag} = 0 °
- X_{dist} = 1 mm

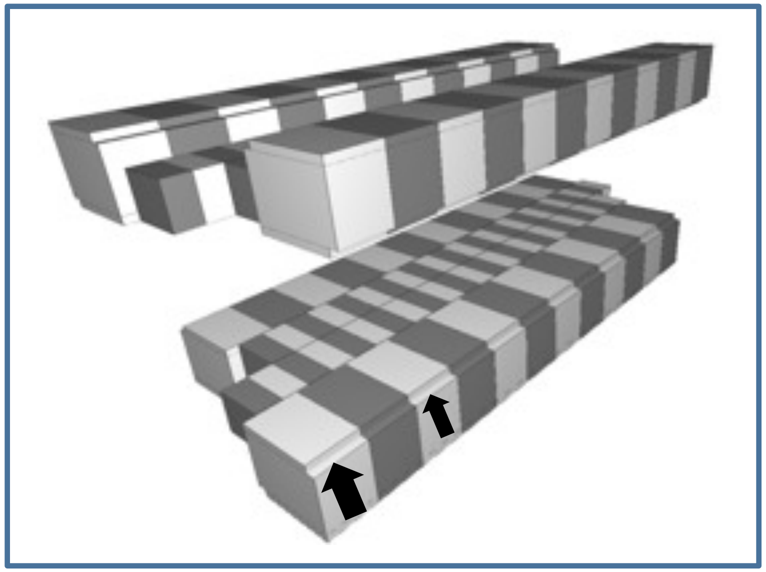

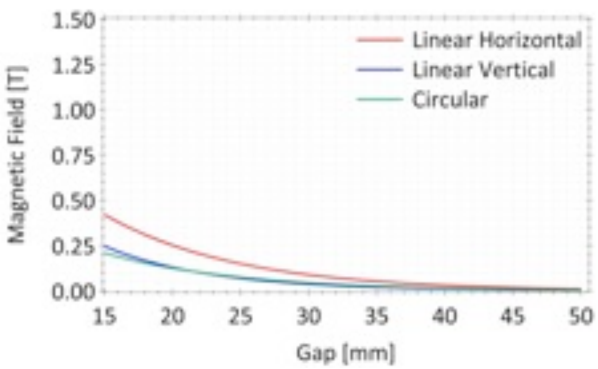

H. & V. field values versus gap at 0 mm shift.

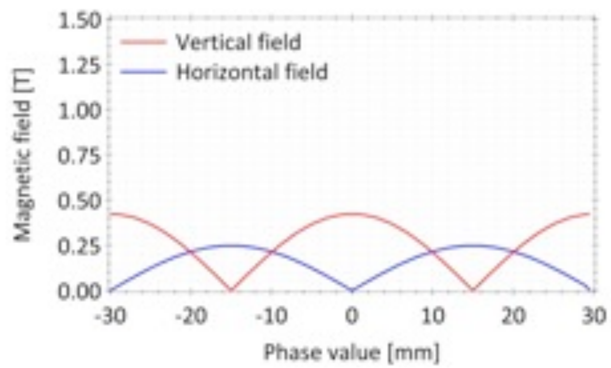

H. & V. field values versus shift at minimal gap

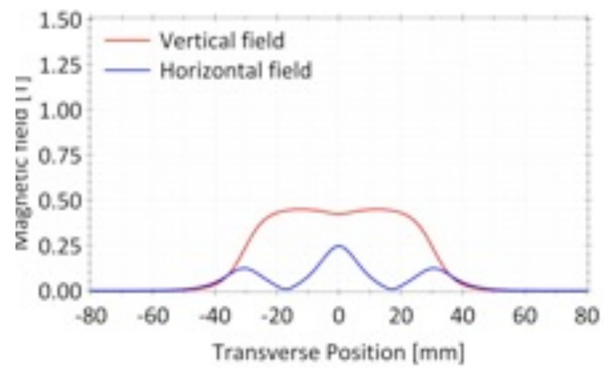

H. & V field roll-off at minimal gap,

S. Sasaki, B. Diviacco and R. P. Walker, Proceedings of European Particle Accelerator Conference, Sweden (1998)
S. Saski, Nuclear Instruments and Methods A347, 83 (1994)

3- EPU and fast polarisation switching

Quasi periodic PM EPU: APPLE VIII

Apple VIII undulators

- Complex structure
- Aperidodicity
- Low on-axis power density

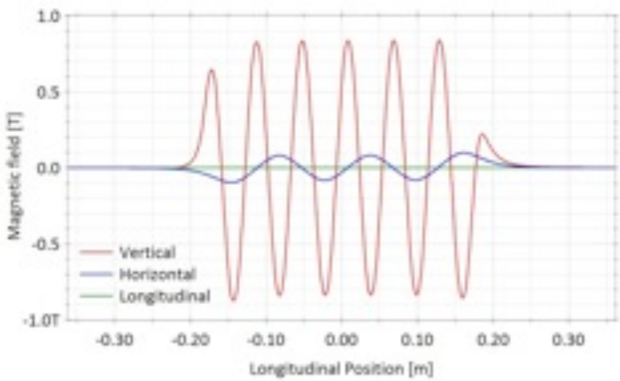

Fig. 1 : Magnetic fields at minimal gap and 0 mm shift

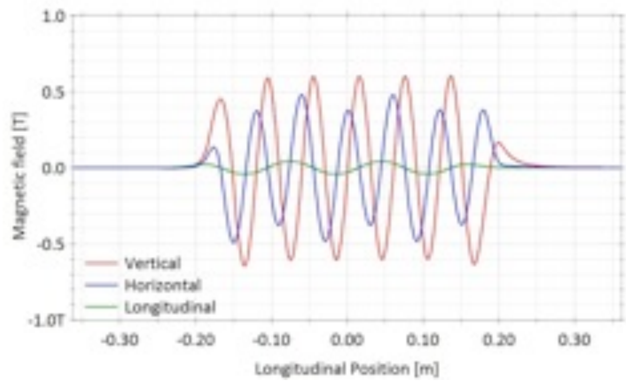

Fig. 1 : Magnetic fields at minimal gap and λ/4 mm shift

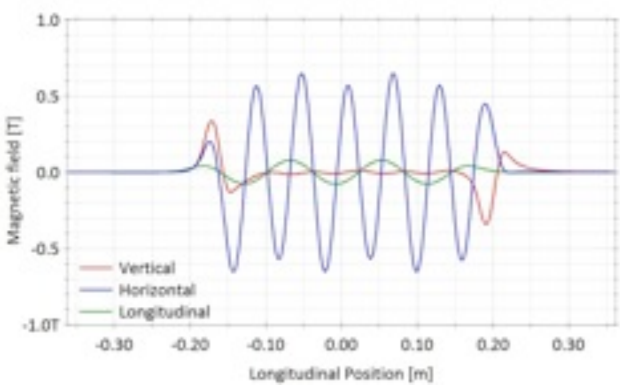

Fig. 1 : Magnetic fields at minimal gap and λ/2 mm shift

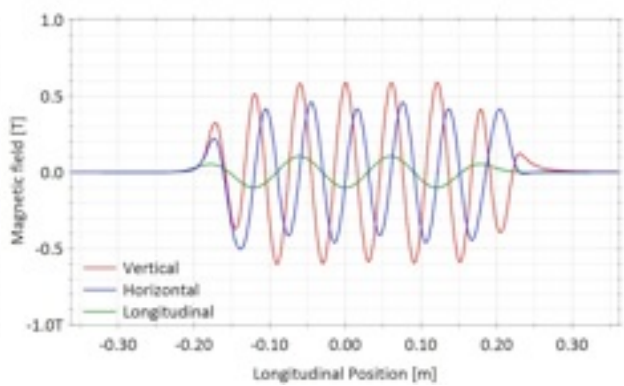

Fig. 1 : Magnetic fields at minimal gap and 3λ/4 mm shift

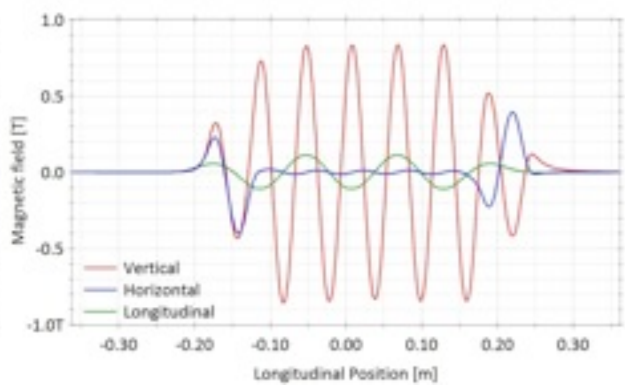

Fig. 1 : Magnetic fields at minimal gap and λ mm shift

ElectroMagnetic Permanent magnet Helical Wiggler

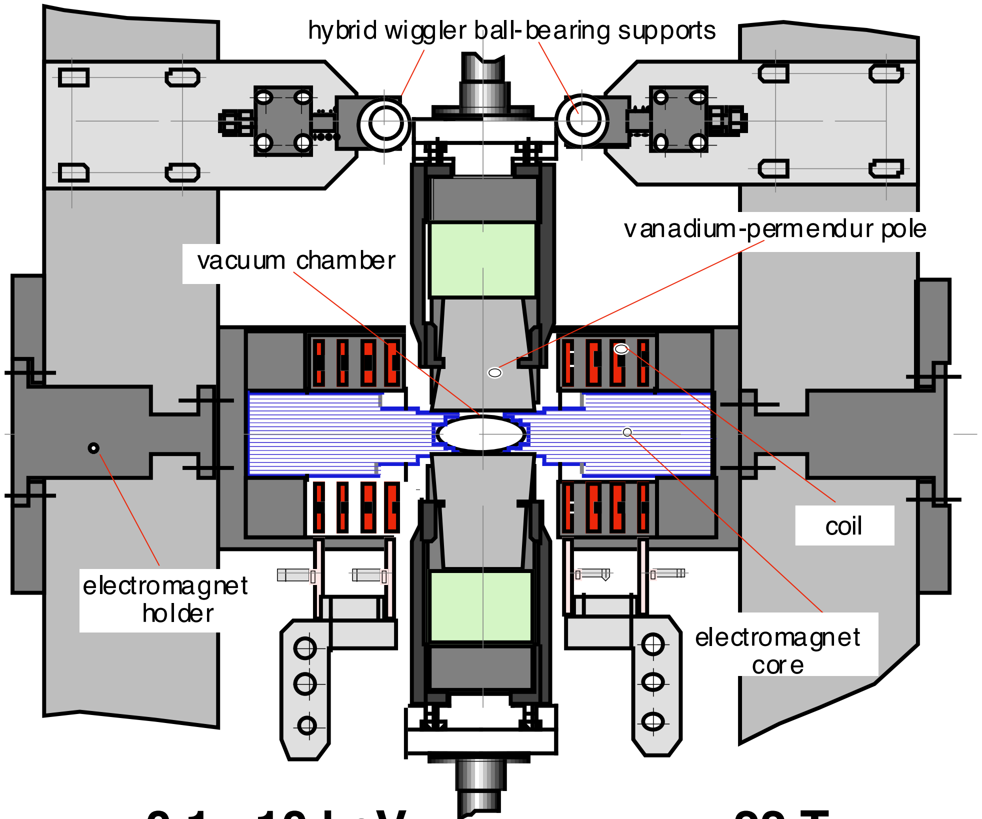

Modification of the polarisation at 100 Hz

Gluskin et al.

0.1 - 10 keV
(2.6 keV)

.22 T
B_V = 0.8 T
λ_0 = 16 cm

Light Source Context

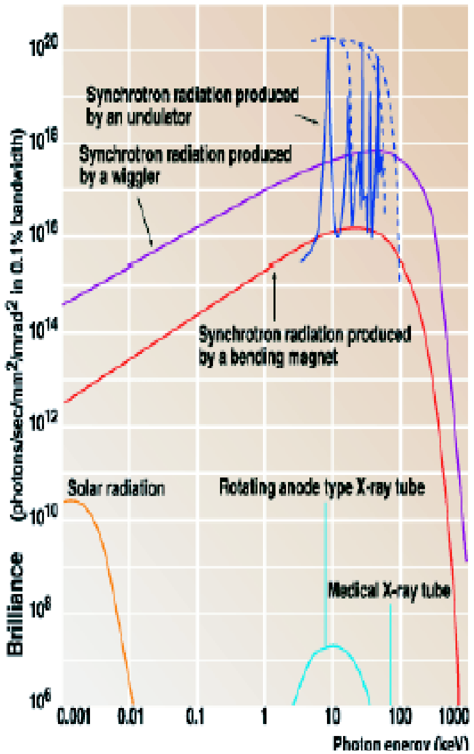

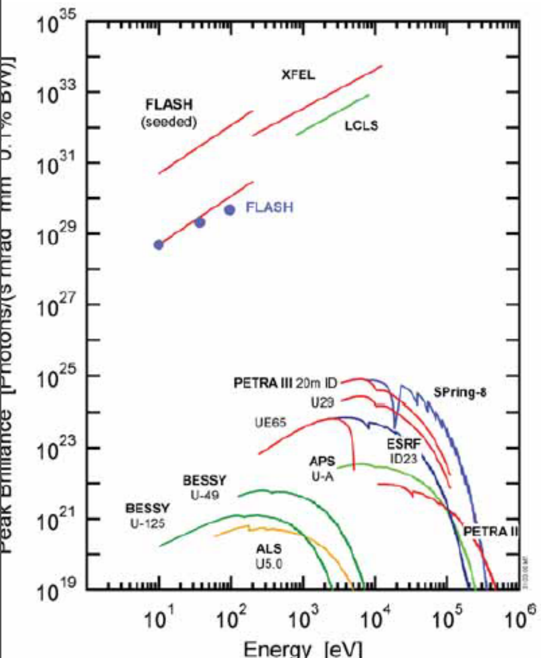

B: Nber of photons / phase space cell

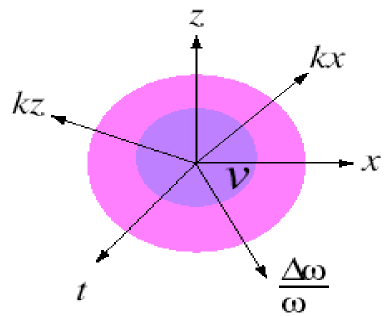

$$\nu = \Delta x \ \Delta x' \ \Delta z \ \Delta z' \ \Delta t \quad \Delta\omega / \omega$$

diffraction limit:
$\Delta x. \Delta x' \sim \lambda/2\pi$

Fourier limit : $\Delta\omega. \Delta\tau \sim 1$
Gaussian beams case :
$c \ \Delta t.\Delta\lambda/\lambda^2=0.44$

Synchrotron radiation used as spontaneous emission for the production of coherent intense radiation (emittors in phase)
Higher harmonics

generation	accelerator	
1	storage ring	parasitic use of synchrotron radiation
2	storage ring	few undulators, ε~few 10nm.rad
3	storage ring	Long straight sections for ID, ε~few nm.rad Ultimate storage ring
4	Linac ERL	fs pulses, ε~εn/E longitudinal coherence for FEL
5	LWFA	LWFA based FEL

❖ Horizontal (natural) Emittance:

$$\varepsilon_x = \frac{C_q \gamma^2 \langle H \rangle_{dipole}}{J_x \rho_x}$$

J_x= Horizontal damping partition number

❖ Horizontal emittance is determined by the equilibrium between the quantum excitation due to the emission of photons and the damping due to the RF acceleration field used to compensate the energy loss of the synchrotron radiation.

❖ J_x is related to the damping partition ***D*** by : $J_x = 1 - D$

where
$$D = \frac{\frac{1}{2\pi}\oint \frac{\eta_x(s)}{\rho_x}\left[\frac{1}{\rho_x^2} + 2K(s)\right]ds}{\oint \frac{ds}{\rho_x^2}}$$

(the integral is to be evaluated only in dipoles).

- For an isomagnetic storage ring with separate function magnets, where K(s) = 0 in dipoles,

$$D = \frac{1}{2\pi\rho}\oint \frac{\eta(s)}{\rho_x} ds = \frac{\alpha R}{\rho_x}$$

- Since the momentum compaction α **<< 1** then ***D* << 1** for separate function machines.

- And since $J_x = 1 - D$

- Then, for an isomagnetic storage ring with separate function magnets, $\boldsymbol{J_x = 1}$

Such as : $J_x + J_z + J_s = 4$ where $J_z = 1$ and $J_s = 2$

❖ Looking at the general expression of the damping partition ***D***, $\boldsymbol{J_x}$ ***and*** $\boldsymbol{\varepsilon_x}$:

$$D = \frac{\frac{1}{2\pi}\oint \frac{\eta_x(s)}{\rho_x}\left[\frac{1}{\rho_x^2} + 2K\ (s)\right]ds}{\oint \frac{ds}{\rho_x^{\ 2}}} \qquad J_x = 1 - D \qquad \varepsilon_x = \frac{C_q\gamma^2\langle H\rangle_{dipole}}{J_x\rho_x}$$

❖ If we can make ***D = -1*** $\Rightarrow$ $\boldsymbol{J_x = 2}$

And the horizontal emittance can be divided by a factor 2!

Such as: $J_x + J_z + J_s = 4$ where $J_z = 1$ and $\boldsymbol{J_s = 1}$

❖ Note that ***D*** depends on the dispersion function η(s) and the quadrupole strength K(s)

$$D = \frac{\frac{1}{2\pi}\oint \frac{\eta_x(s)}{\rho_x}\left[\frac{1}{\rho_x^2} + 2K(s)\right] ds}{\oint \frac{ds}{\rho_x{}^2}}$$

❖ And can be re-written:

$$D = \frac{\frac{1}{2\pi}\left(\oint \frac{\eta_x}{\rho_x^3}\, ds + \frac{2}{B^2 \rho_x^2}\oint \eta_x B \frac{dB}{dx}\, ds\right)}{\oint \frac{ds}{\rho_x{}^2}}$$

A magnetic element introducing the product ***B*dB/dx*** in a straight section where the dispersion η_x is non zero contributes to the modification of ***D***.

SOLEIL energy acceptance

The energy acceptance of the bare machine is large : +/- 4%

Off-momentum (dp/p, x) map

Calculated

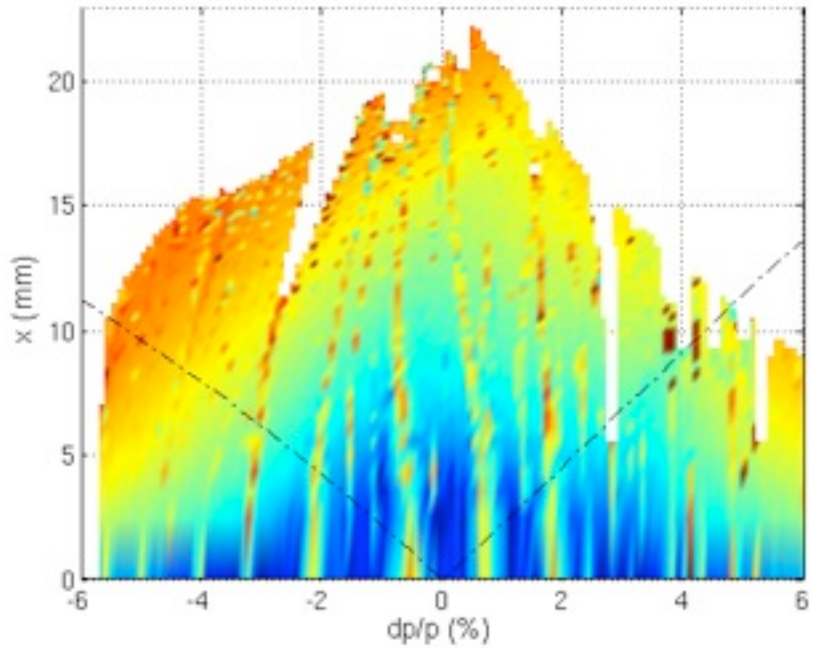

Measured

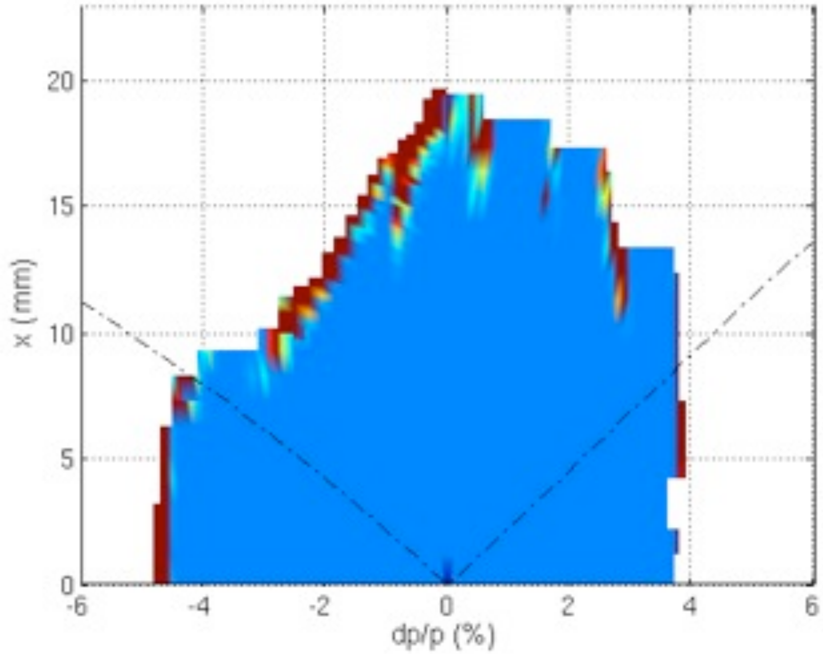

Vacuum chamber at 12 mm

Effect on injection efficency

Reduction of the on-momentum dynamic aperture and the energy acceptance in the presence of IDs => reduction of the injection rate

Measured on-momentum (x, z) map

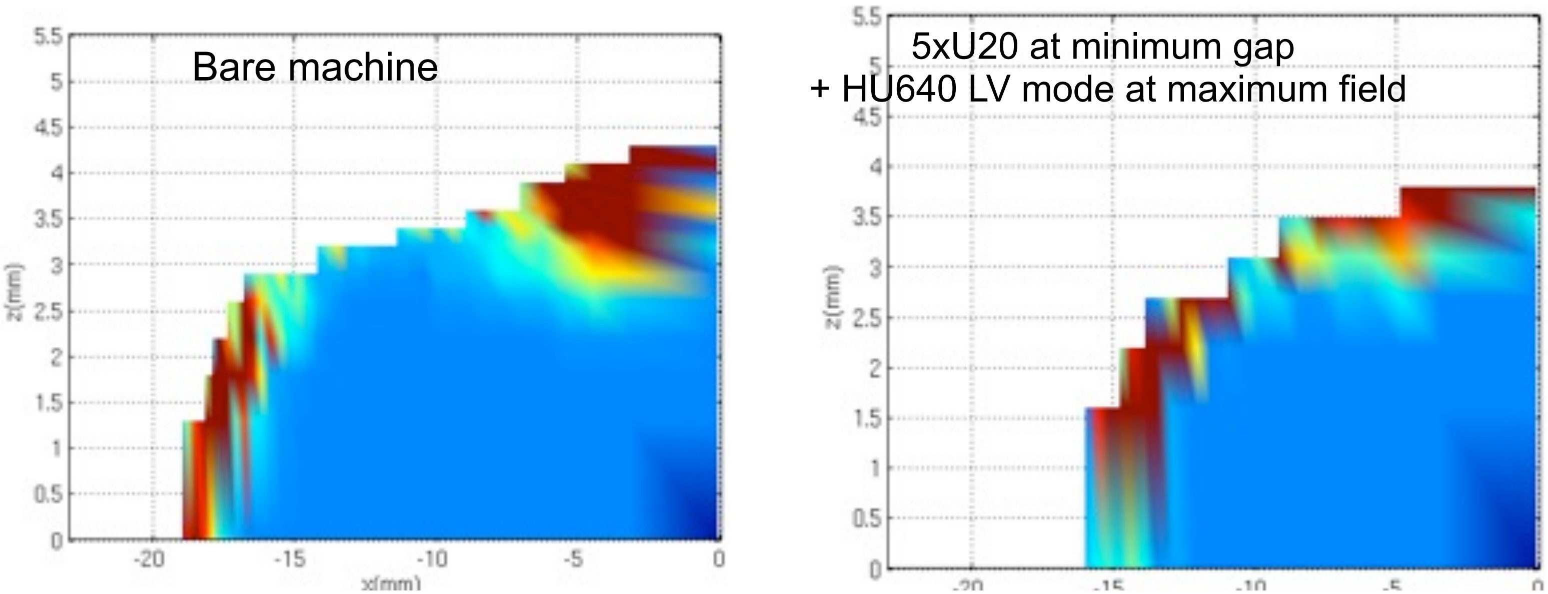

Measured off-momentum (dp/p, x) map

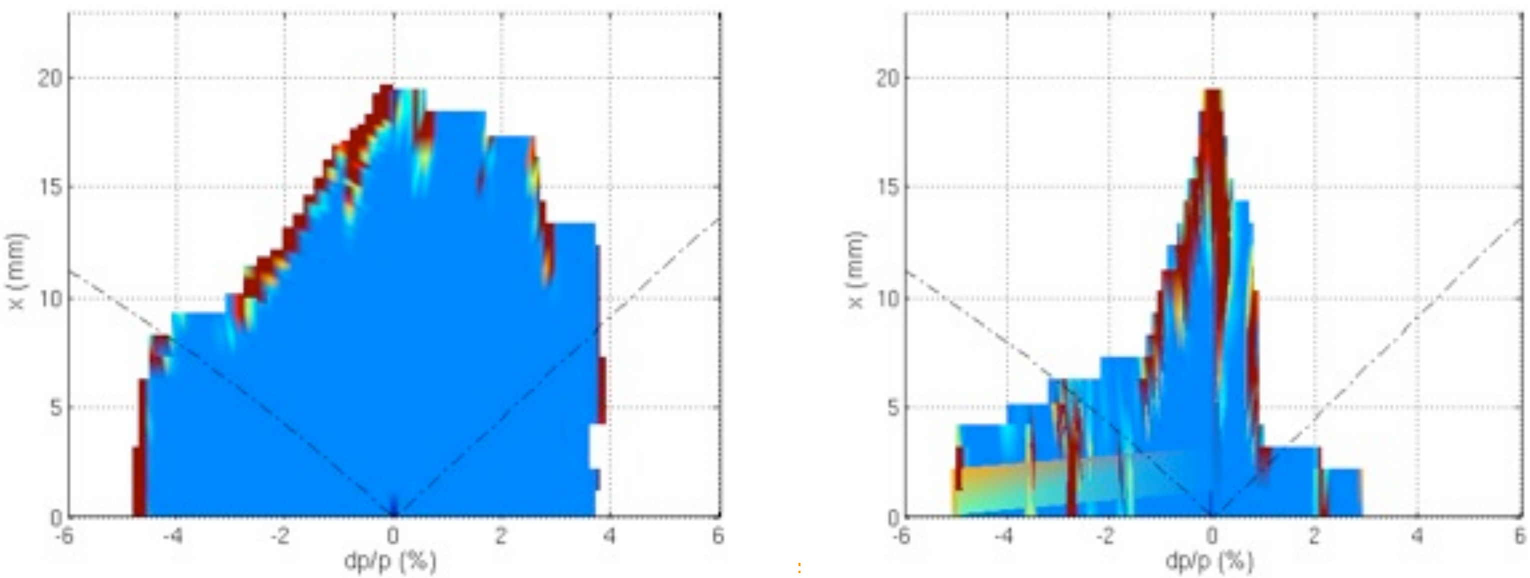

Rare Earth Magnet behaviour versus temperature

M. Sagawa et al. J. Magn. Magn. Mater. 70, 316 (1987)
T. Hara et al. APAC2004, Gyeongju, Korea, 216

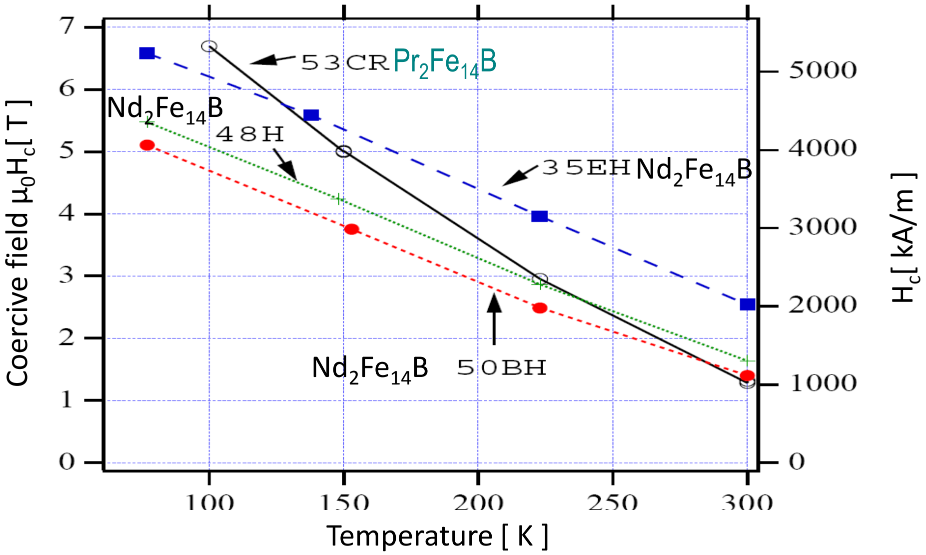

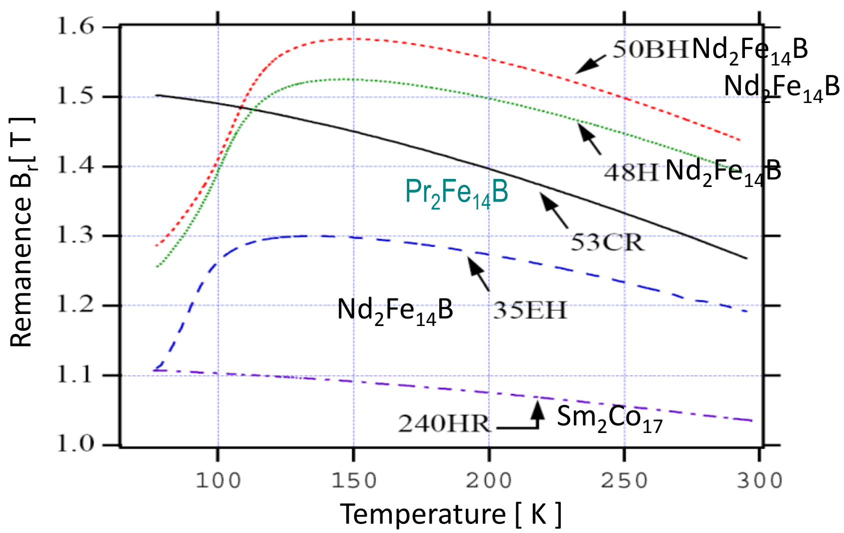

Spin Transition Reorientation
NdFeB strong Magneto-Crystalline Anisotropy (MCA) => orientation along [001]
Magneto-cristalline orientation given by the energy : $E(T) = K_1 \sin^2(\theta) + K_2 \sin^4(\theta)$, θ angle between the magnetisation and [001]
at room temperature : magnetisation // c
Fe MCA independant of T, Nd : K_1 // [001] dominant at room T and K_2//[110] at low T

D. Givord et al. Solid State Comm. 51 (1984) 857
L. M. garcia et al. Phys. Rev. Lett. 85 (2) 429

Examples of CPMU

Lab.	Tech.	Period (mm)	Magnet	Br (T)	Hcj (kA/m)	Installation	Length (m)	Reference
SPring-8	PPM	15	$Nd_2Fe_{14}B$,	1.41	1114	Lab	0.6	*T. Hara, et al., . Phys. Rev. Spec. Topics 7, 050702 (2004)*
NSLSII	Hybrid	14.5	$Nd_2Fe_{14}B$	1.37		Lab	0.11	*T. Tanabe, et. al., Proceedings, Vol. 1234, p.29 (2010). 4.85 mm gap*
SLS/SPring-8	Hybrid	14	$Nd_2Fe_{14}B$	1.33	1670	3G	1.7	*T. Tanaka, et al., . Phys. Rev. Spec. Topics 12, 120702 (2009)*
ESRF n°1	Hybrid	18	$Nd_2Fe_{14}B$	1.16	2400	3G	2	*J. Chavanne et al., PAC09,*
ESRF n°2	Hybrid	18	$Nd_2Fe_{14}B$	1.16	2400	3G	2	*J. Chavanne et al., IPAC 2008, 2011, 3245*
DIAMOND/ Danfysik	Hybrid	17.7	$Nd_2Fe_{14}B$	1.31	1670	3G	2	*C. Benabderrahmane et al. NIMA A 669 (2012) 1-6*
SOLEIL	Hybrid	20	$Nd_2Fe_{14}B$	1.41	1114		0.08	*C. Benabderrahmane et al. NIMA A 669 (2012) 1-6*
SOLEIL	Hybrid	18	$Pr_2Fe_{14}B$	1.35	1355		0.072	
SOLEIL	Hybrid	18	$Pr_2Fe_{14}B$	1.35	1355	3G	2	*C. Benabderrahmane et al. IPAC 2011*
BESSY/UCLA	Hybrid	9	$Pr_2Fe_{14}B$			5G	2	*J. Bahrdt et al. IPAC10, 3111* fixed gap=2.5 mm
NSLSII/ADC	Hybrid	18	$Nd_2Fe_{14}B$			3G	2	*T. Tanabe, et al.*
NSLSII	Hybrid	17				3G	2.7	*T. Tanabe, et. al., PAC 2011, 2090*
SOLEIL/ LUNEX5	Hybrid	12-15	$Nd_{2,x}Pr_{2,1-x}Fe_{14}B$			*4-5G*	3-5	

High Tc Tanaka PRST et New Journal of Physics

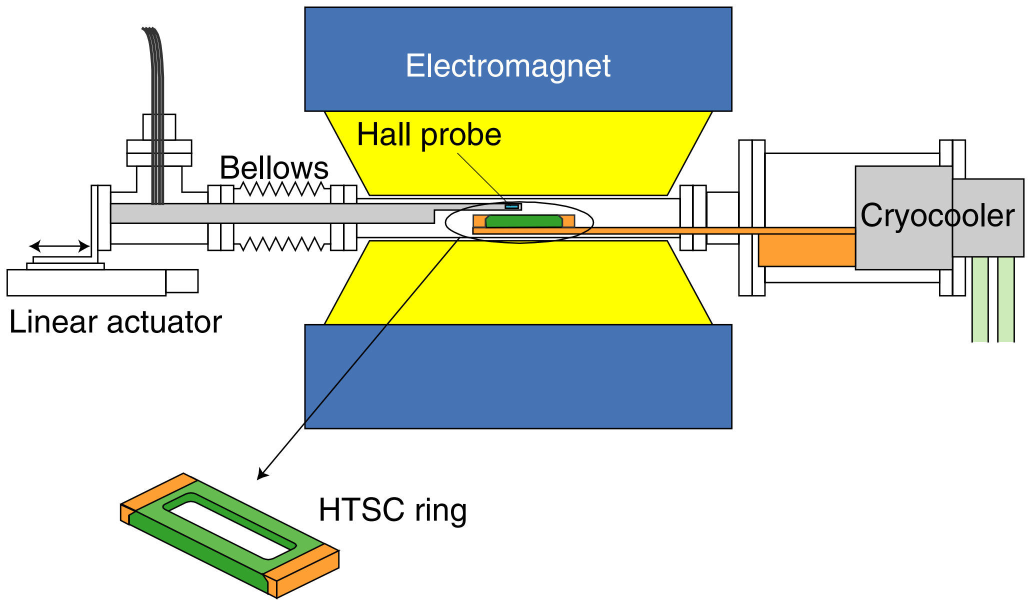

3- EPU and fast polarisation switching

Permanent magnets EPU

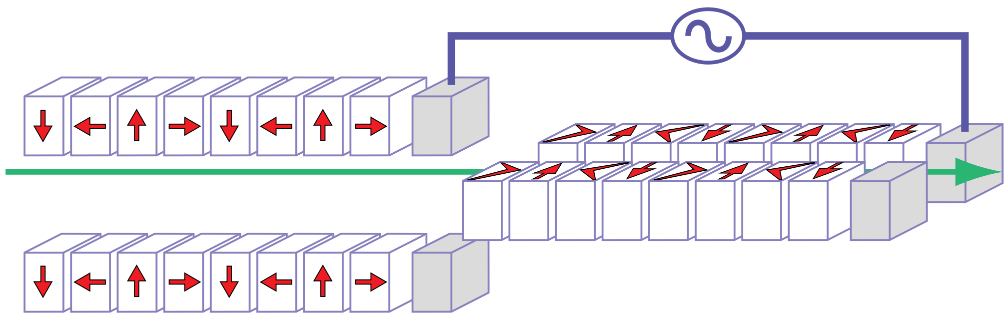

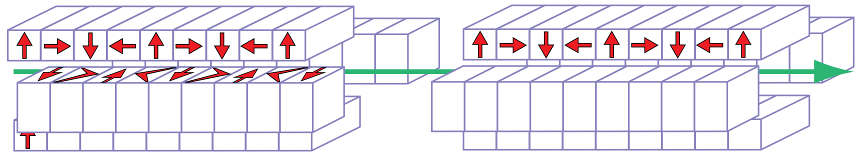

Cross undulators :

M. Moissev et al. Sov. Phys. J. 21, 332, 1978
K. J. Kim NIMA219, 426 (1986)

Onuki et al.

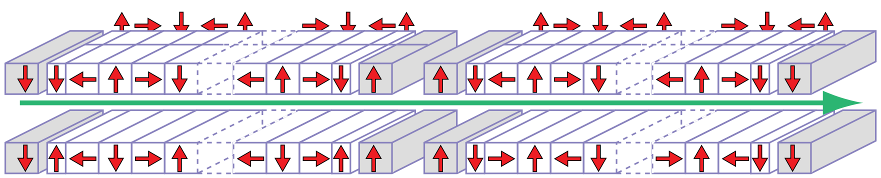

Helios et al.

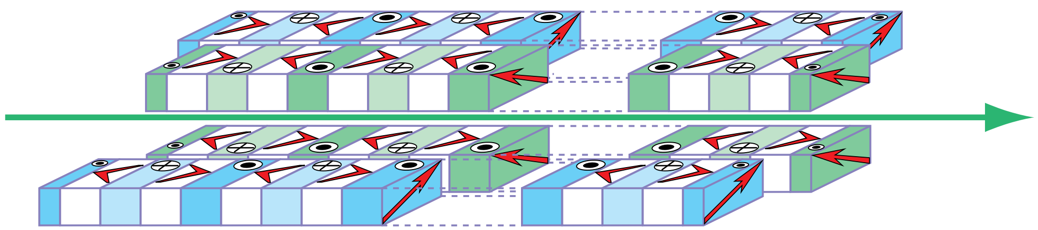

Sasaki et al.

Dynamic field integral compensation

Compensation of the dynamic integral by magic fingers

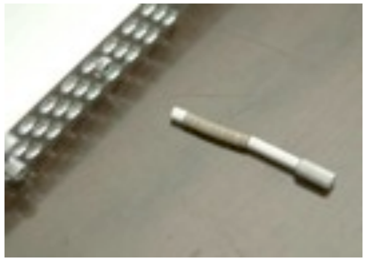

J. Safranek et al, Phys. Rev. Special Topics (2002), Vol. 5, 010701, pp. 1-7
O. Marcoullé et al, IPAC 2011, 3236

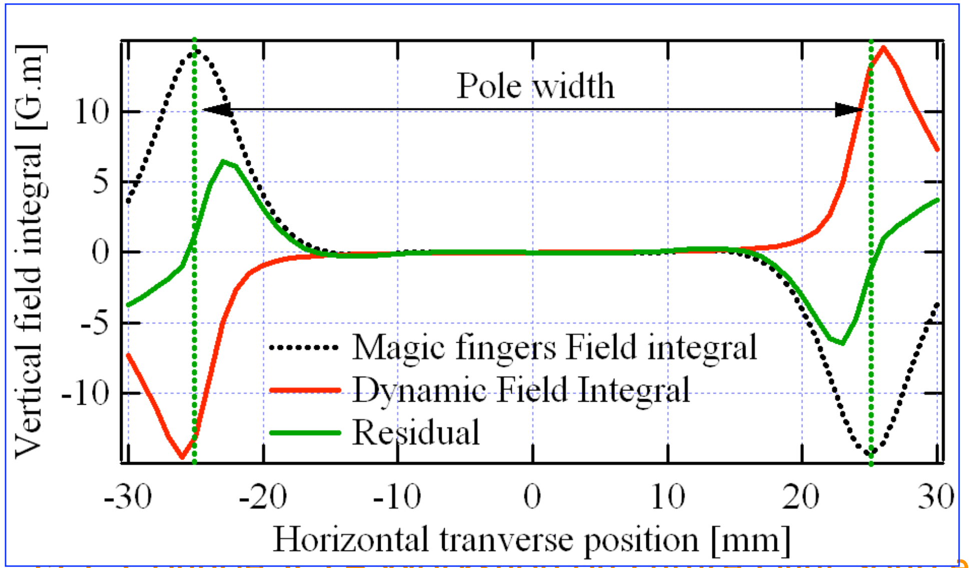

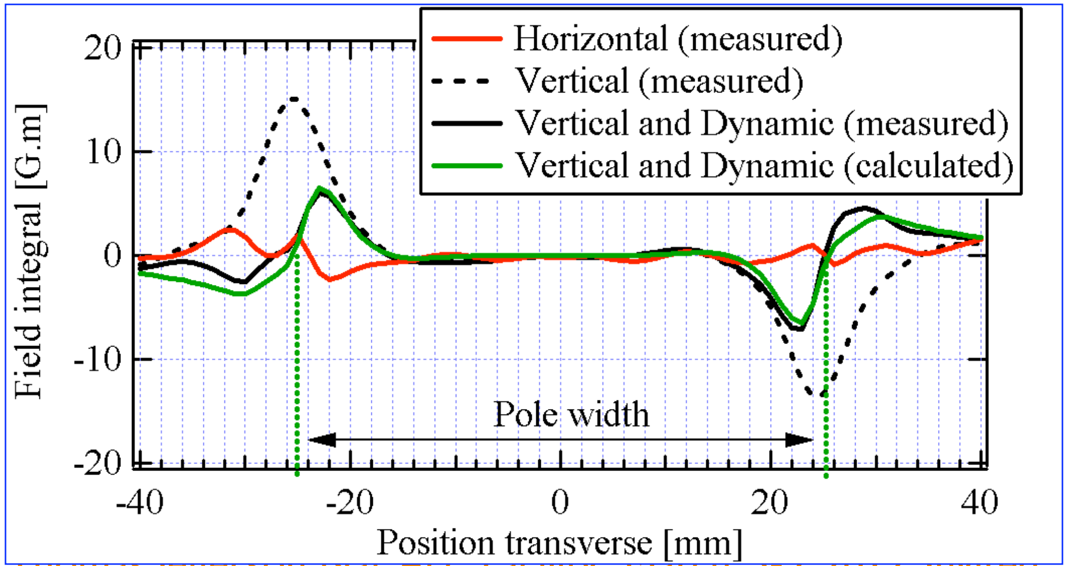

Desired ID effects: damping wiggler

$$\epsilon_{xw} = C_a \frac{E^2}{J_x} \frac{\langle \mathscr{H}/\rho^3 \rangle_0 + \langle \mathscr{H}/\rho^3 \rangle_w}{\langle 1/\rho^2 \rangle_0 + \langle 1/\rho^2 \rangle_w}$$

emittance : equilibrium between quantum excitation and radiation damping (loss of transverse momentum)
J_x : horizontal partition number

$$\left\langle \frac{\mathscr{H}}{\rho^3} \right\rangle_w = \frac{1}{C} \oint_w \frac{\mathscr{H}}{\rho^3} ds = \frac{1}{\rho_w^3} \langle \mathscr{H} \rangle_w$$

$$\left\langle \frac{\mathscr{H}}{\rho^3} \right\rangle_0 = \frac{1}{C} \oint_0 \frac{\mathscr{H}}{\rho^3} ds = \frac{1}{\rho_0^3} \langle \mathscr{H} \rangle_0,$$

$$\left\langle \frac{1}{\rho^2} \right\rangle_w = \frac{1}{C} \oint_w \frac{1}{\rho^2} ds = \frac{L_w}{C} \frac{1}{\rho_w^2},$$

$$\left\langle \frac{1}{\rho^2} \right\rangle_0 = \frac{1}{C} \oint_0 \frac{1}{\rho^2} ds = \frac{1}{\rho_0 R}.$$

$$\mathscr{H} = \frac{1}{\beta} \left\{ \eta^2 + \left(\beta \eta' - \tfrac{1}{2} \beta' \eta \right)^2 \right\}$$

$$C_a = c C_q / (2 C_D)$$

$$C_q = \frac{55}{48\sqrt{3}} \frac{r_e \hbar c}{(mc^2)^6}$$

$$C_D = \frac{c}{3} \frac{r_e}{(mc^2)^3}$$

More damping with additional synchrotron radiation through installation of strong wiggler magnets places in a dispersion free location (for the equilibrium orbit to be independant of the particle energy)

$$\frac{\epsilon_{xw}}{\epsilon_{x0}} = \frac{1 + \left(\frac{\rho_0}{\rho_w} \right)^3 \frac{\langle \mathscr{H} \rangle_w}{\langle \mathscr{H} \rangle_0}}{1 + \frac{L_w}{2\pi\rho_0} \left(\frac{\rho_0}{\rho_w} \right)^2}$$

$$\frac{\sigma_{Ew}^2}{\sigma_{E0}^2} = \frac{1 + \frac{L_w}{2\pi\rho_0} \left(\frac{\rho_0}{\rho_w} \right)^3}{1 + \frac{L_w}{2\pi\rho_0} \left(\frac{\rho_0}{\rho_w} \right)^2}.$$

+ corrections due to the own dispersion created by the wiggler

H. Wiedemann, An ultra-low emittance mode for PEP using damping wigglers, Nucl. Instr. Meth. A266 (1988) 24-31.
K. Robinson, Radiation effects in Circular electron accelerators, Phys. Rev. 111 (2), 1958, 373

3- Effect of the ID on the light source operation

Modelisation with field maps

HU36 undulator : Measured <u>horizontal</u> field integrals at 11.5 mm minimum gap

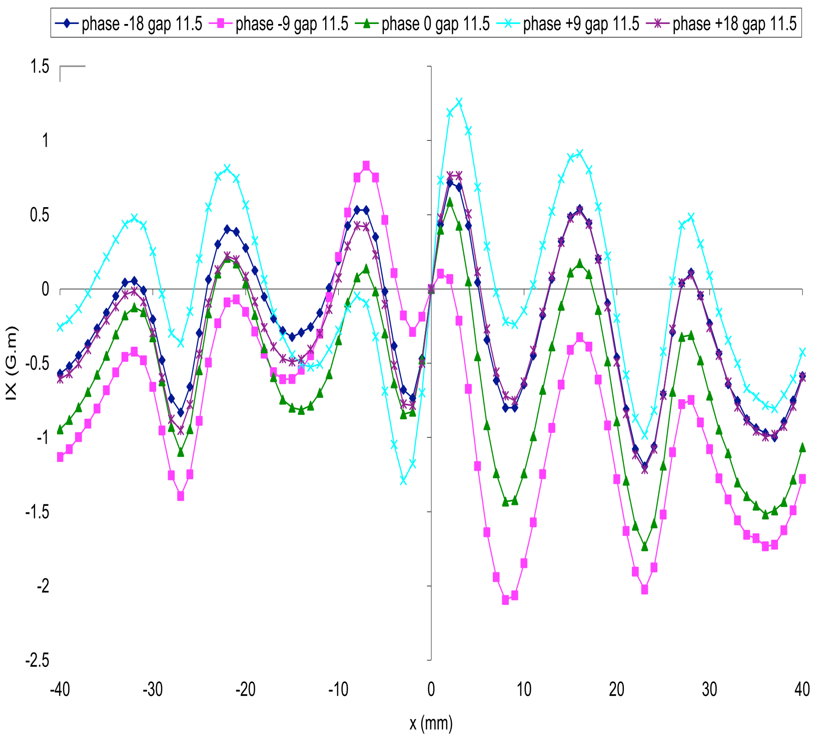

HU36 undulator : Measured <u>vertical</u> field integrals at 11.5 mm minimum gap

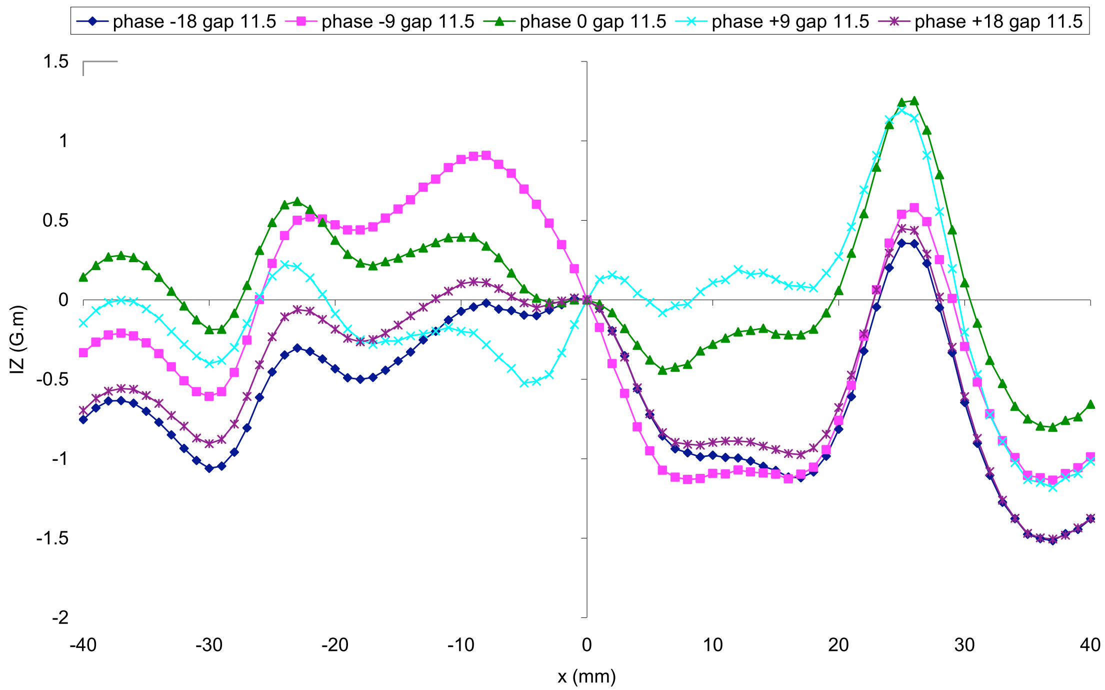

Figure8 or bi-periodic undulator

T. Tanaka, H. Kitamura, Nucl. Instrum. Methods A 346, 368-373

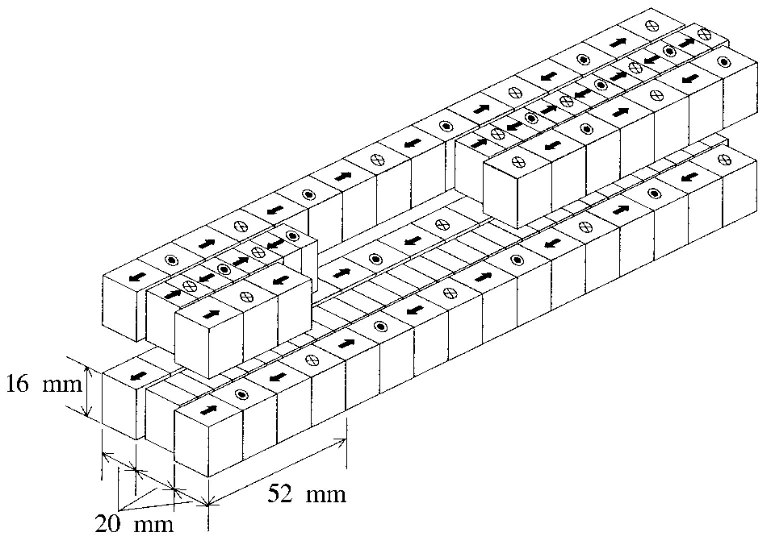

Figure 8
V. und. period = 2X H und. period

- Linear polarised soft X ray: on axis power density lower than for an ordinary undulator
- odd (LH), integer (LH), and half integer harmonics (LV)

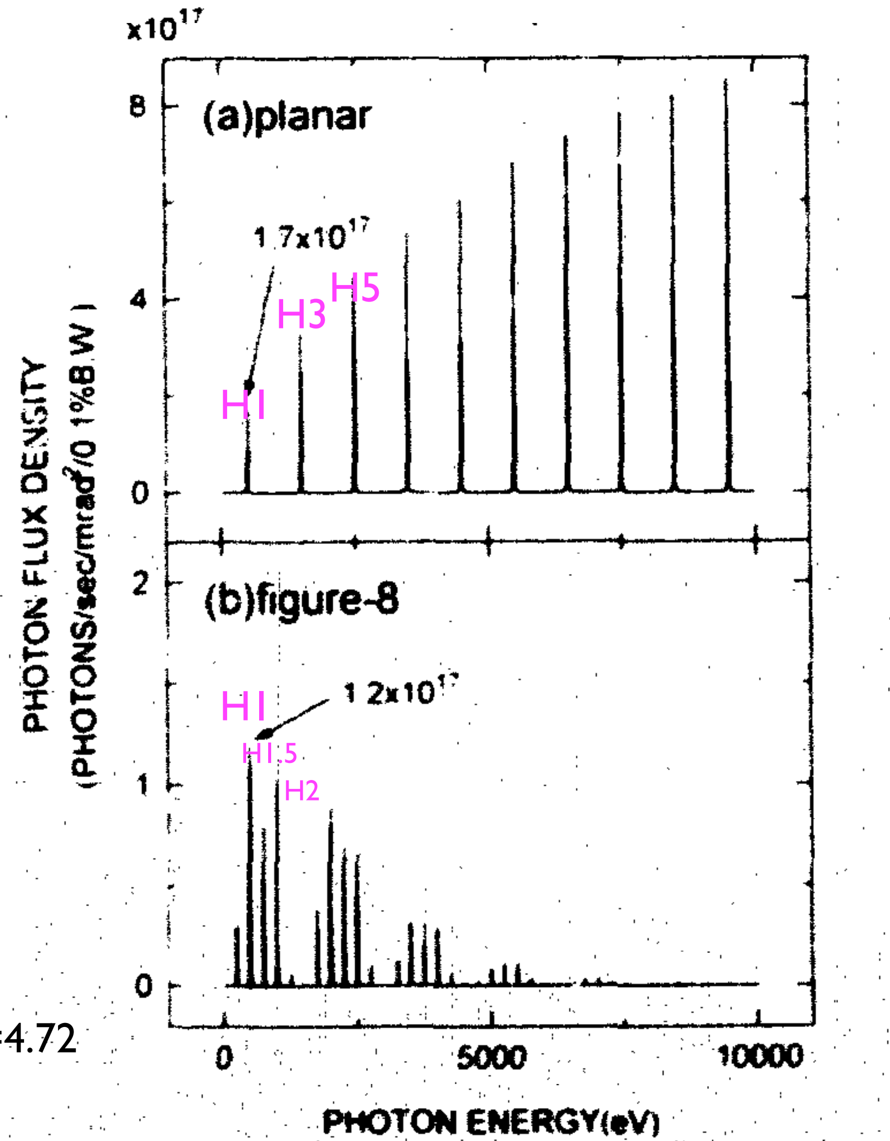

On axis radiation, 8 GeV K=4.72
planar, Fig.8 K_x=K_z=3.34

3- EPU and fast polarisation switching

EMPHU @ SOLEIL

Static measurements

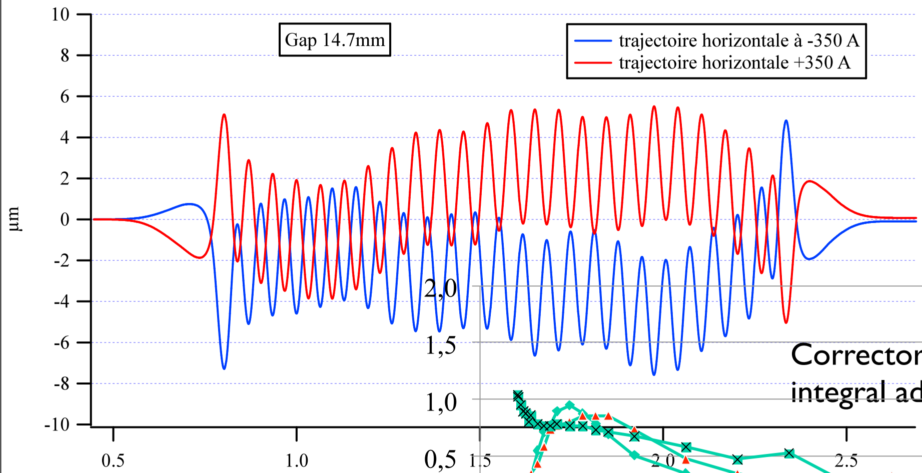

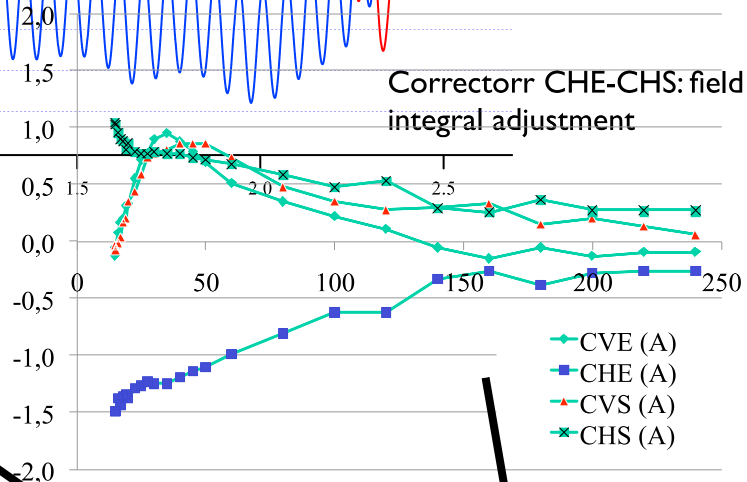

Correctorr CHE-CHS: field integral adjustment

Correctorr IP50 : adjustment of the exit position

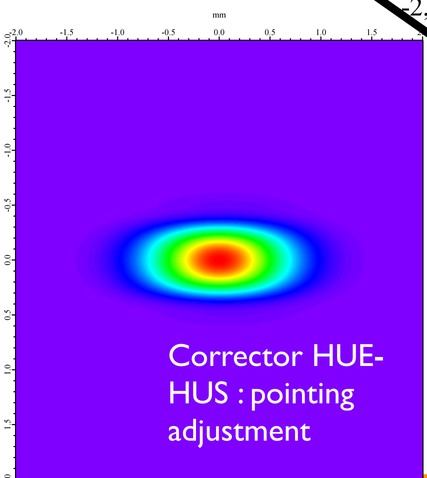

Corrector HUE-HUS : pointing adjustment

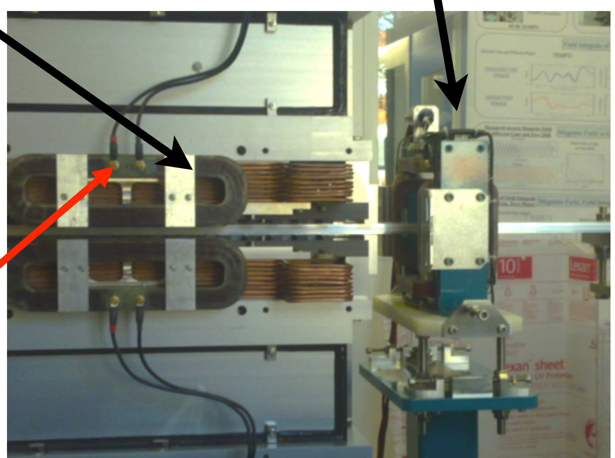

Dynamic measurements

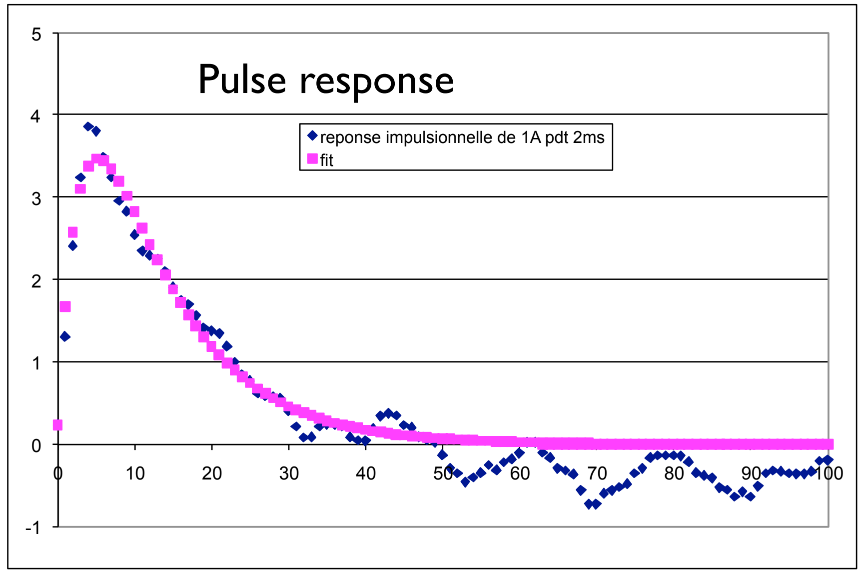

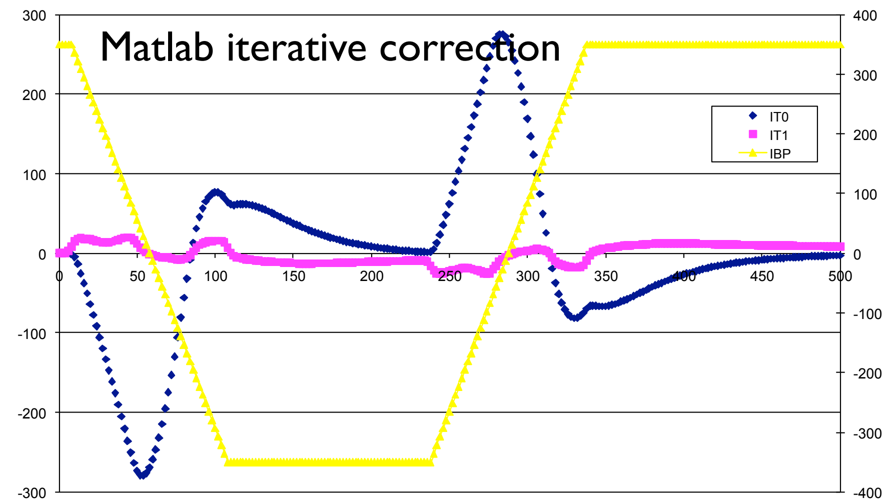

Desired ID effects: Robinson wiggler

Application to SOLEIL

horizontal emittance : 3.7 nmrad⇒1.85 nmrad

Short straight section : η_x **= 0.28 m**

=>

D=-1 =>

Type	B(T)	g (mm)	dB/dx (T/
out of vacuum	1.4	11	140
In vacuum	1.0	5.5	182

Questions : - Js=1 damping in longitudinal plane
- high gradients?
- field homogeneity (injection, lifetime)
- radiation properties

Desired ID effects: Robinson wiggler

Application to SOLEIL

horizontal emittance : 3.7 nmrad⇒1.85 nmrad

$$\boxed{D = \frac{\rho_0 \eta_x}{\pi (\rho_0 B_0)^2} \left\langle B_w \frac{dB_{w,z}}{dx} \right\rangle L_w}$$

Short straight section : η_x **= 0.28 m**

=>

D=-1 =>

Type	B(T)	g (mm)	dB/dx (T/
out of vacuum	1.4	11	140
In vacuum	1.0	5.5	182

Questions : - Js=1 damping in longitudinal plane
- high gradients?
- field homogeneity (injection, lifetime)
- radiation properties

Desired ID effects: Robinson wiggler

Application to SOLEIL

horizontal emittance : 3.7 nmrad⇒1.85 nmrad

$$D = \frac{\rho_0 \eta_x}{\pi (\rho_0 B_0)^2} \left\langle B_w \frac{dB_{w,z}}{dx} \right\rangle L_w$$

Short straight section : η_x **= 0.28 m**

=>

D=-1 =>

Type	B(T)	g (mm)	dB/dx (T/
out of vacuum	1.4	11	140
In vacuum	1.0	5.5	182

Questions : - Js=1 damping in longitudinal plane
- high gradients?
- field homogeneity (injection, lifetime)
- radiation properties

Desired ID effects: Robinson wiggler

Application to SOLEIL

horizontal emittance : 3.7 nmrad ⇒ 1.85 nmrad

$$\boxed{D = \frac{\rho_0 \eta_x}{\pi (\rho_0 B_0)^2} \left\langle B_w \frac{dB_{w,z}}{dx} \right\rangle L_w}$$

($\rho_0 B_0$ = 9.138 Tm for SOLEIL)

Short straight section : η_x **= 0.28 m**

=>

D=-1 =>

Type	B(T)	g (mm)	dB/dx (T/
out of vacuum	1.4	11	140
In vacuum	1.0	5.5	182

Questions : - Js=1 damping in longitudinal plane
- high gradients?
- field homogeneity (injection, lifetime)
- radiation properties

Desired ID effects: Robinson wiggler

Application to SOLEIL

horizontal emittance : 3.7 nmrad⇒1.85 nmrad

$$D = \frac{\rho_0 \eta_x}{\pi (\rho_0 B_0)^2} \left\langle B_w \frac{dB_{w,z}}{dx} \right\rangle L_w$$

B_w = wiggler peak field, L_w = wiggler length (2m) , g= wiggler gap

($\rho_0 B_0$ = 9.138 Tm for SOLEIL)

Short straight section : η_x **= 0.28 m**

=>

D=-1 =>

Type	B(T)	g (mm)	dB/dx (T/
out of vacuum	1.4	11	140
In vacuum	1.0	5.5	182

Questions : - Js=1 damping in longitudinal plane
- high gradients?
- field homogeneity (injection, lifetime)
- radiation properties

Desired ID effects: Robinson wiggler

Application to SOLEIL

horizontal emittance : 3.7 nmrad ⇒ 1.85 nmrad

$$\boxed{D = \frac{\rho_0 \eta_x}{\pi (\rho_0 B_0)^2} \left\langle B_w \frac{dB_{w,z}}{dx} \right\rangle L_w}$$

B_w = wiggler peak field, L_w = wiggler length (2m) , g= wiggler gap

($\rho_0 B_0$ = 9.138 Tm for SOLEIL)

Short straight section : η_x **= 0.28 m**

$$D \approx 5.6\times 10^{-3} \left\langle B_w \frac{dB_{w,z}}{dx} \right\rangle L_w$$

$$\frac{dB_{w,z}}{dx} \approx \frac{\hat{B}_{w,z}}{g} \quad => \quad \left\langle B_{w,z} \frac{dB_{w,z}}{dx} \right\rangle \approx \frac{\hat{B}_{w,z}^2}{2g}$$

D=-1 =>

Type	B(T)	g (mm)	dB/dx (T/
out of vacuum	1.4	11	140
In vacuum	1.0	5.5	182

Questions : - Js=1 damping in longitudinal plane
- high gradients?
- field homogeneity (injection, lifetime)
- radiation properties

Desired ID effects: Robinson wiggler

Application to SOLEIL

horizontal emittance : 3.7 nmrad⇒1.85 nmrad

$$\boxed{D = \frac{\rho_0 \eta_x}{\pi (\rho_0 B_0)^2} \left\langle B_w \frac{dB_{w,z}}{dx} \right\rangle L_w}$$

B_w = wiggler peak field, L_w = wiggler length (2m) , g= wiggler gap

($\rho_0 B_0$ = 9.138 Tm for SOLEIL)

Short straight section : η_x **= 0.28 m**

$$D \approx 5.6\times 10^{-3} \left\langle B_w \frac{dB_{w,z}}{dx} \right\rangle L_w \qquad \frac{dB_{w,z}}{dx} \approx \frac{\hat{B}_{w,z}}{g} \quad => \quad \left\langle B_{w,z} \frac{dB_{w,z}}{dx} \right\rangle \approx \frac{\hat{B}_{w,z}^{2}}{2g}$$

D=-1 => $\boxed{\frac{\hat{B}_{w,z}^{2}}{2g} \approx 89 \text{ T}^2/\text{m}}$

Type	B(T)	g (mm)	dB/dx (T/
out of vacuum	1.4	11	140
In vacuum	1.0	5.5	182

Questions : - Js=1 damping in longitudinal plane
- high gradients?
- field homogeneity (injection, lifetime)
- radiation properties